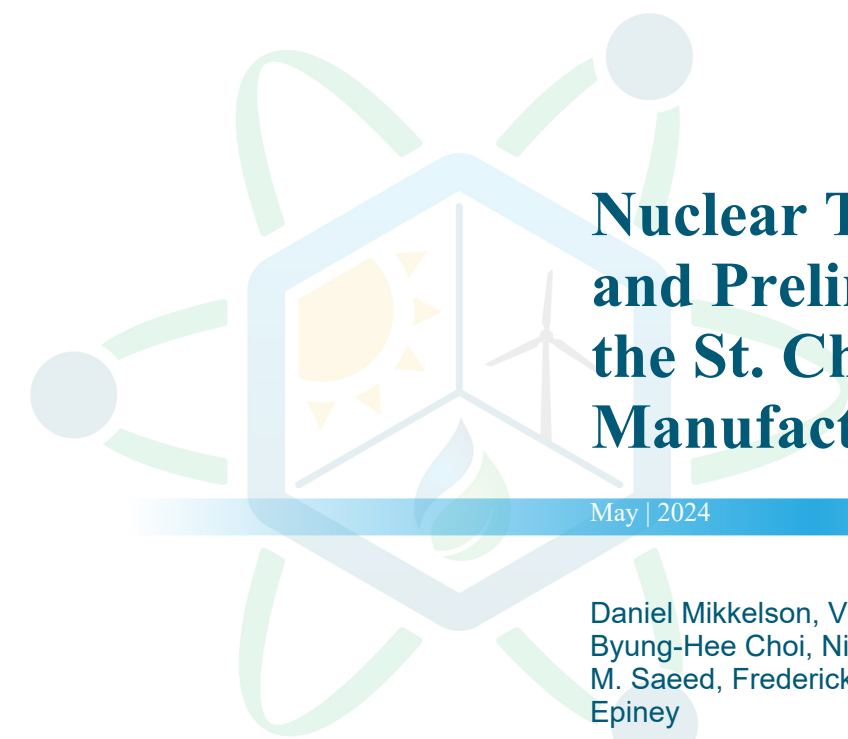


DISCLAIMER

This report was prepared as an account of work sponsored by an agency of the United States Government. Neither the United States Government nor any agency thereof, nor any of their employees, makes any warranty, express or implied, or assumes any legal liability or responsibility for the accuracy, completeness, or usefulness of any information, apparatus, product, or process disclosed, or represents that its use would not infringe privately owned rights. Reference herein to any specific commercial product, process, or service by trade name, trademark, manufacturer, or otherwise does not necessarily constitute or imply its endorsement, recommendation, or favoring by the United States Government or any agency thereof. The views and opinions of authors expressed herein do not necessarily state or reflect those of the United States Government or any agency thereof. Reference herein to any social initiative (including but not limited to Diversity, Equity, and Inclusion (DEI); Community Benefits Plans (CBP); Justice 40; etc.) is made by the Author independent of any current requirement by the United States Government and does not constitute or imply endorsement, recommendation, or support by the United States Government or any agency thereof.



Nuclear Technology Selection and Preliminary Integration at the St. Charles and Carrollton Manufacturing Sites

May | 2024

Daniel Mikkelsen, Vaclav Novotny, Logan Williams, Junyung Kim, Byung-Hee Choi, Nipun Popli, Sarah Creasman, Iza Lantgios, Rami M. Saeed, Frederick Joseck, Paul Talbot, Aidan Rigby, and Aaron Epiney

Idaho National Laboratory

Scott Bury, Michael Curtis, and Gretchen Baier

The Dow Chemical Company



DISCLAIMER

This information was prepared as an account of work sponsored by an agency of the U.S. Government. Neither the U.S. Government nor any agency thereof, nor any of their employees, makes any warranty, expressed or implied, or assumes any legal liability or responsibility for the accuracy, completeness, or usefulness, of any information, apparatus, product, or process disclosed, or represents that its use would not infringe privately owned rights. References herein to any specific commercial product, process, or service by trade name, trademark, manufacturer, or otherwise, does not necessarily constitute or imply its endorsement, recommendation, or favoring by the U.S. Government or any agency thereof. The views and opinions of authors expressed herein do not necessarily state or reflect those of the U.S. Government or any agency thereof.

Nuclear Technology Selection and Preliminary Integration at the St. Charles and Carrollton Manufacturing Sites

Daniel Mikkelsen, Vaclav Novotny, Logan Williams, Junyung Kim, Byung-Hee Choi, Nipun Popli, Sarah Creasman, Iza Lantgios, Rami M. Saeed, Frederick Joseck, Paul Talbot, Aidan Rigby, and Aaron Epiney
Idaho National Laboratory
Scott Bury, Michael Curtis, and Gretchen Baier
The Dow Chemical Company

May | 2024

**Idaho National Laboratory
Integrated Energy Systems
Idaho Falls, Idaho 83415**

<http://www.ies.inl.gov>

**Prepared for the
U.S. Department of Energy
Office of Nuclear Energy
Under DOE Idaho Operations Office
Contract DE-AC07-05ID14517**

Page intentionally left blank

EXECUTIVE SUMMARY

Key Research Question

As a zero-CO₂ emitting baseload energy source capable of dispatching energy as needed for integrated facilities, nuclear energy is a viable candidate for the decarbonization of industrial facilities. Because each industrial facility is unique, analyzing which nuclear technology represents the best option should be evaluated on a case-by-case basis. For two identified facilities run by two wholly-owned subsidiaries of The Dow Chemical Company, an ideal mix of nuclear energy resources was calculated, and integration strategies proposed.

Research Overview

This research was funded through a Gateway for Accelerated Innovation in Nuclear (GAIN) nuclear energy voucher specifically aimed toward near-term engineering solutions for introducing nuclear-generated energy into the Dow chemical facilities. The research is split into four main phases: background on reactors and chemical facilities, preliminary engineering analysis for determining how reactor technologies can be integrated into specific facilities, site characterization and discrete hazards analysis, and optimization of reactor/facility selection by using Framework for Optimization of ResourCes and Economics (FORCE) tools.

The reactor technology overview is based on open-source information that was gathered and curated. The goal is to concisely explain distinctions between nuclear technologies, and to provide readers who may not have much knowledge of the various advanced reactor technologies currently under development an overview of the companies that offering designs and their progress in the licensing process, their planned deployments, and relevant planned operational conditions. Dow provided historical operational data, the site-specific utility relationship information, the engineering priorities, and the plant timeline data, thus defining the boundary conditions for the solutions proposed throughout this report.

With the site characterization data and potential reactor technologies, preliminary engineering analysis begins by developing various reactor configurations capable of delivering heat, combined heat and power (CHP), or generated electricity (the nominal configuration for advanced reactors) to the Dow facilities. Thermodynamic balances are presented, showing the configurations and calculations integrating the nuclear systems into the Dow facilities' steam systems. These balances are also leveraged to generate quantity transfer functions, detailing how energy could potentially be networked within the facility.

As a brownfield solution proposal, the area around the current sites is also investigated to determine the limitations of introducing nuclear reactors at the Dow facilities. With the anticipated selection of small modular reactors (SMRs) and microreactors (μ Rxs) for these solutions, anticipated regulatory shifts are included in the reactor siting analysis. Some site-specific hazards are also analyzed in anticipation of requirements pertaining to selecting a nuclear site that is as physically close to the Dow facilities as possible (so as to decrease thermal lag by reducing the system size, thus allowing for faster responses to changes in demand, lowered costs as a result of less equipment, and decreased energy losses due to reduced surface area).

The thermodynamics and siting information are collected to set up a combined thermodynamic and economic analysis, leveraging the Holistic Energy Resource Optimization Network (HERON) tool to determine the optimal sets of nuclear technologies and storage systems that would provide consistent heat and power to the selected Dow facilities. Economic data were sourced from comprehensive open-source reviews of projected advanced nuclear reactor costs. The methods in this study are repeatable, but the conclusions and results are dependent on these values, and this study should be repeated as advanced reactor vendors firm up their technology sales prices. Multiple optimization runs were executed in series: first to identify an optimal set of reactors by technology type, next to leverage discrete options in reactor technologies to identify purchasable solutions, then to determine statistically ideal configurations, and lastly to evaluate the economic value of integrating thermal energy storage (TES).

Key Findings

Dow provided the study data for two sites operated by the wholly-owned subsidiaries, the Union Carbide Corporation (UCC) and the Dow Silicones Corporation (DSC): the St. Charles Operations (SCO) facility in Louisiana, located adjacent to the Mississippi River and operated by UCC, and the Carrollton facility in Kentucky, adjacent to the Ohio River and operated by DSC.

At the SCO site, it was determined that sets of only HTGRs, 800 MWth, or only LWRs, 1250 MWth, were statistically indistinguishable from an economic standpoint using current literature cost estimates. Other viable solutions with comparable project costs combine these reactor types, but the CAPEX reduction from having multiple SMR types located on a single site was not introduced into the calculations, so the practical recommendation is to determine a single vendor with whom to contract and interface. The solution indicates that, per the current cost projections for advanced reactors sized appropriately for integration with the SCO facility, no technology has proven to be clearly economically superior at this point. Furthermore, there does not appear to be a significant reason why SMRs could not be introduced in the immediate area surrounding the Dow facility. An LWR is already sited just over a mile upstream on the Mississippi river, and the local utility Entergy is already a nuclear operator. Colocation at that facility, or siting a new location even closer to the Dow facility, should be possible to provide CHP.

Integration of the SMRs with the SCO site would phase out baseload generation from fossil-fuel-based boilers and CHP units, replacing CO₂ emitting assets with zero-carbon steam and power. In 2021, CO₂ emissions from stationary combustion systems at the SCO site totaled ~2.1 million tons per year, per U.S. government data. These emissions are primarily associated with fossil fuel combustion to generate steam, power, and heat for the ethylene cracking furnaces. The combustion CO₂ emissions from the site could be reduced by ~615,000 tons per year (~30%) by installing and integrating SMRs to supply clean steam and power, as shown in Figure ES 1.

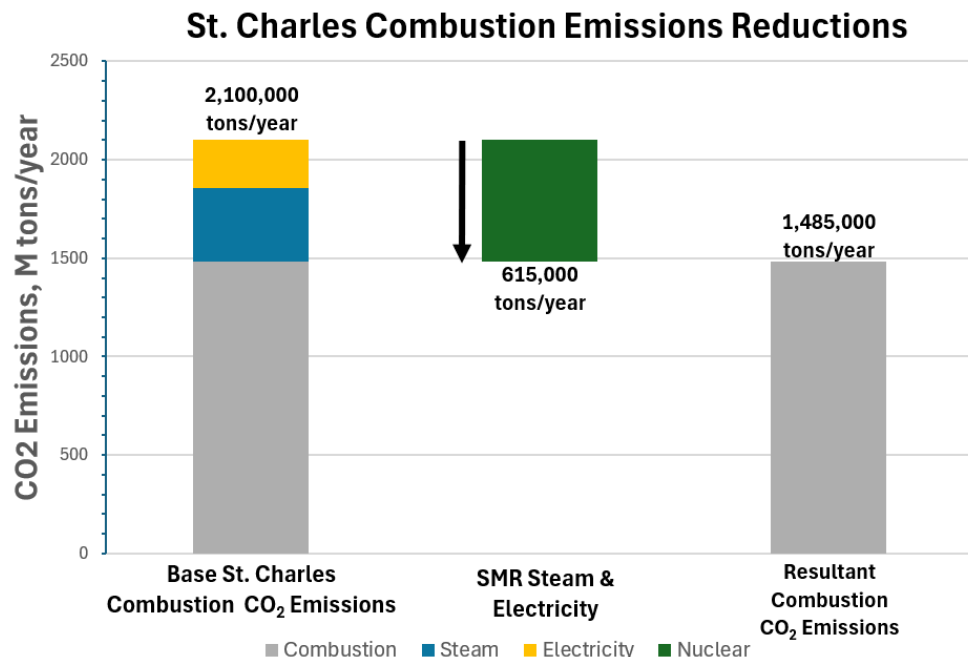


Figure ES i. SCO facility CO₂ emissions, and the reductions achieved via SMR integration.

At the Carrollton site, the thermal and electrical demands were considered too small to be efficiently met by SMRs, due to reliability considerations (as maintenance, unplanned, or refueling outages would effectively shut down the entire plant). Due to the nature of currently proposed μ Rx designs, the high

economic uncertainty between designs, and the thermal conditions required at the Carrollton facility, different μ Rx designs were considered to be relatively interchangeable. As companies begin to provide firm prices and more detailed deployment configurations, this evaluation will be updated. The optimal nuclear size was determined to be 167.3 MWth, with 183.2 MWh-th of TES. Dow owns sufficient land at the Carrollton site to deploy μ Rxs within their facility.

Kentucky does not have any existing or closed nuclear power plants and has an unstructured electric market; nuclear power is not regulated as a possible distributed energy generation source in Kentucky. However, a 2023 report by the Kentucky Office of Energy Policy concluded that there are no insurmountable barriers to nuclear energy development in Kentucky, but challenges require serious attention and coordination among stakeholders [1]. For Dow, this means further engagement and development of their relationship with the local utility, Kentucky Utilities Corporation(KCU), to develop a strategy to address the expected barriers. The proposed suite of μ Rxs represents a significant addition to KUC's energy resource portfolio.

In 2021, CO₂ combustion emissions from the Carrollton site totaled ~174,000 tons per year, according to U.S. government data. These emissions are primarily associated with fossil fuel combustion to generate steam, and this combustion would be phased out by introducing μ Rxs onsite. The CO₂ emissions from the site could be eliminated with installation and integration of μ Rxs to supply clean steam, as shown in Figure ES 2.

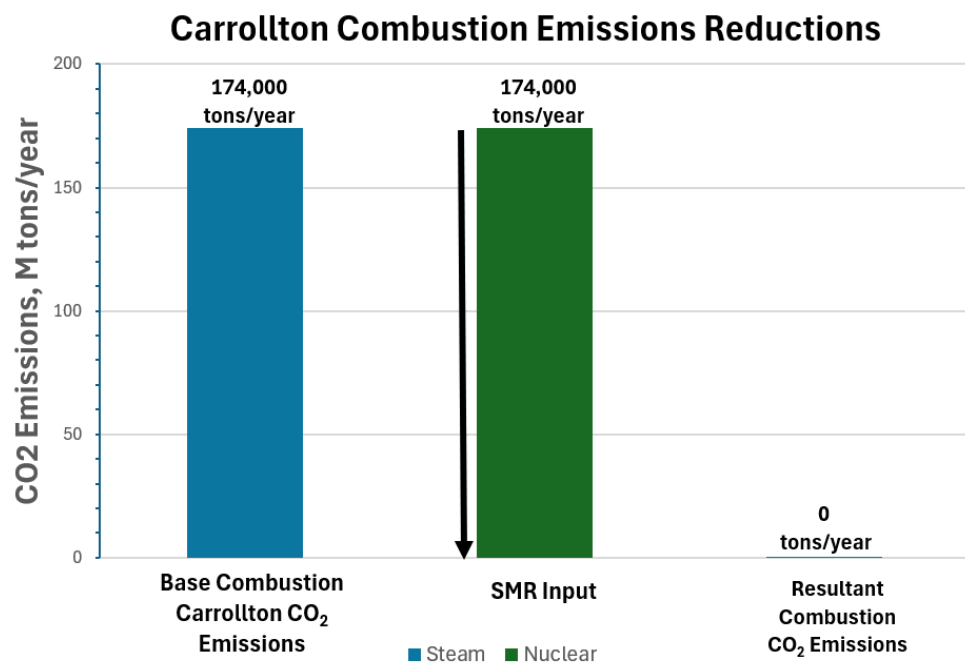


Figure ES ii. Carrollton-site combustion CO₂ emissions, and the reduction via μ Rxs integration.

Why This Matters

This study shows the methodology of and results for thermally interconnecting advanced reactor technologies with chemical facilities. The complexity of this challenge should not be underestimated, but this study shows how specific sites can integrate nuclear heat and electricity within steam systems. The Dow Chemical Company has announced a 2030 decarbonization target to reduce net annual carbon emissions by 5 million metric tons versus the 2020 baseline (~15% reduction). Nuclear power represents a clean, dispatchable, and reliable method for realizing that goal. Companies seeking to decarbonize heavy thermal loads should analyze these results as a basis for determining how clean energy—likely nuclear—can be leveraged to create a cleaner future economy.

How to Apply Results

Nuclear technology developers can use this analysis to demonstrate to potential industrial energy clients how they might be able to meet their heat and electricity demands. At the same time, these solutions require deployment of nuclear technology beyond the current licensed electricity generation configurations. Engaging with licensing entities is key, and showing how large CHP applications can be implemented without altering nuclear-sensitive design points may be valuable.

Industrial energy users can leverage this analysis to help meet their own net-zero goals. Specific facility requirements may introduce unique results, but the overall analysis path presented herein can likely be leveraged across many diverse kinds of locations.

CONTENTS

EXECUTIVE SUMMARY.....	v
ACRONYMS.....	xvi
1. INTRODUCTION.....	1
2. ADVANCED NUCLEAR REACTORS.....	2
2.1 Small Modular Reactors.....	2
2.1.1 Light-Water Reactors.....	2
2.1.2 High-Temperature Gas Reactors.....	4
2.1.3 Liquid-Metal Fast Reactors.....	5
2.1.4 Molten-Salt Reactors.....	6
2.2 Microreactors.....	7
2.2.1 High-Temperature Gas Reactors.....	8
2.2.2 Liquid-Metal Fast Reactors.....	9
2.2.3 Heat Pipe Reactors.....	9
3. DOW SITES.....	9
3.1 St. Charles Site.....	9
3.1.1 Primary Chemical Processes and Operation.....	9
3.1.2 Geography.....	10
3.1.3 Energy Systems and Demand Profiles.....	10
3.1.4 Utility Relationship.....	12
3.2 Carrollton Site.....	14
3.2.1 Primary Chemical Processes and Operation.....	14
3.2.2 Geography.....	14
3.2.3 Energy Systems and Demand Profiles.....	14
3.2.4 Utility Relationship.....	15
4. METHODS.....	16
4.1 Preliminary Demand-Fitting Analysis.....	17
4.1.1 Thermodynamic Model for the HTGR SMR.....	17
4.1.2 Thermodynamic Model for an LWR SMR.....	20
4.1.3 Thermodynamic Models for Microreactors.....	23
4.1.4 Thermal Energy Storage.....	24
4.1.5 Thermal Transport Considerations.....	30
4.2 Synthetic Data Generation.....	31
4.3 Holistic Energy Resource Optimization Network.....	32
4.3.1 Transfer Functions.....	35
4.3.2 Cost Information.....	36
4.4 Siting and Safety Calculations.....	37
4.5 Thermal and Electrical Reliability.....	40
5. RESULTS.....	41

5.1	Preliminary Energy Balance Investigation – SCO.....	41
5.1.1	Xe-100 Reactors with PCCs.....	42
5.1.2	Xe-100 Reactors with PCCs and TES.....	44
5.1.3	NuScale Power Modules with PCCs.....	48
5.2	Preliminary Energy Balance Investigation – Carrollton.....	50
5.2.1	Microreactors with PCCs.....	51
5.2.2	Microreactors with PCCs and TES.....	54
5.3	System Capacities Analysis with HERON.....	58
5.3.1	St. Charles Operations.....	58
5.3.2	Carrollton Site.....	69
5.4	Carbon Emission Reduction.....	72
5.4.1	St. Charles Operations.....	72
5.4.2	Carrollton Site.....	73
5.5	Siting Hazard Analysis.....	73
5.5.1	Seismic Possibility.....	74
5.5.2	Flooding.....	74
5.5.3	Road Traffic and Railroad Information.....	75
5.5.4	Population.....	76
5.5.5	Utility and Chemical Facility.....	78
5.5.6	Land Ownership.....	79
5.5.7	Combined Hazards Map.....	79
6.	CONCLUSIONS.....	81
7.	ACKNOWLEDGEMENTS.....	81
8.	REFERENCES.....	81

FIGURES

Figure 1. Map of electricity generation in Louisiana, as taken from [64]. The SCO site is represented by the red square.....	10
Figure 2. SCO process steam system.....	11
Figure 3. Synthetic heat and electricity demand profiles of SCO for 2022. These profiles are generated using actual plant data and an ARMA model.....	12
Figure 4. Entergy service map of the SCO area [66].....	12
Figure 5. Summary of the three electricity tiers within the industrial contract from Entergy LLC.	13
Figure 6. Synthetic heat production and electricity consumption profiles for DSC Carrollton site in 2022. These profiles were generated using actual plant data and an ARMA model.	15
Figure 7. Map of Kentucky utilities [72]. The Carrollton site is indicated by the added red square.	15

Figure 8. Energy balance model, HTGR-POWER, of the standard electrical-power-generation steam cycle for the HTGR system, which provides a net output of 81 MWe.....	17
Figure 9. Energy balance model of a HTGR-CHP system with an extraction-condensing turbine.....	18
Figure 10. Output and efficiencies of an HTGR-CHP system with an extraction-condensing turbine. (a) Thermal and electric output and (b) efficiency changes, both with a varying steam extraction fraction.....	19
Figure 11. Energy balance model of an HTGR-HEAT system with a backpressure turbine.....	19
Figure 12. Extraction steam pressure boosting configuration, LWR-CHP, for the NPM. LWR-POWER is a near-identical configuration, just without the Pressure Boosting or Process Heat sections.....	21
Figure 13. Energy balance model, LWR-HEAT, of heat upgrade from a NPM for baseload heat delivery.....	22
Figure 14. Characteristics of an LWR-CHP, becoming an LWR-HEAT, system with an extraction- condensing turbine and boosting power output. (a) Thermal and electric output and (b) efficiency changes, both with varying steam extraction fraction.....	22
Figure 15. Energy balance model, μ Rx-CHP, of a conversion system that leverages a backpressure steam turbine CHP μ Rx applications.....	24
Figure 16. Various configurations for integrating TES. (a) Type A: ideal configuration of TES coupled to the nuclear reactor primary loop. (b) Type B: configuration of TES charged by main steam. (c) Type C: layout of TES integration within the heat extraction branch.....	25
Figure 17. Process flow diagram of the proposed separated high- and low-temperature TES system for HTGR integration [84].....	26
Figure 18. HTGR-CHP-TES coupling approach combining the HTGR-CHP and Type A TES configurations. Thermodynamic balance of the system is achieved using two TES systems to establish low-and high-temperature TES.....	26
Figure 19. Q-T diagrams of TES (a) charging and (b) discharging.....	27
Figure 20. HTGR-CHP-TES coupling approach using HTGR-CHP and the Type B TES.....	28
Figure 21. Q-T diagrams of TES (a) charging and (b) discharging.....	28
Figure 22. HTGR-CHP coupling approach integrating Type C TES.....	29
Figure 23. Q-T diagrams of TES (a) charging and (b) discharging.....	30
Figure 24. Proposed configuration of the heat transfer station (process steam generation node) interfacing extracted nuclear plant steam and process steam going to the site.....	31
Figure 25. Two ARMA samples compared for a single 5-day cluster. Note that the trends are nearly identical but the specific demand paths are unique.....	32
Figure 26. HERON initial resource map at the beginning of the optimization activities.....	33
Figure 27. HERON block diagram of heat generation.....	34
Figure 28. HERON block diagram of heat storage.....	34
Figure 29. HERON block diagram of heat utilization.....	35

Figure 30. Vibratory hazards resulting from explosions, with different levels of damage caused by different over-pressurization levels [94].....	38
Figure 31. Switchyard component fragility to over-pressurization stemming from vibratory hazards [96].....	39
Figure 32. General illustration of nuclear-sourced process steam integration for SCO. The sections with dashed lines could become obsolete after introducing the nuclear-CHP system.....	41
Figure 33. System configuration of the HTGRs with CHPs for SCO, where η is the energy conversion (thermal to electric) efficiency.....	42
Figure 34. Illustrative representation of the system configuration featuring a common steam bus.	43
Figure 35. Overall electricity balance, measured against one synthetic data set from SCO, using HTGRs with PCC configurations (detailed in Figure 33).....	43
Figure 36. Total heat supply and demand at SCO for 1 year, from a set of four HTGRs.....	44
Figure 37. Total electricity supply and demand at SCO for 1 year, from a set of four HTGRs.....	44
Figure 38. Illustration of the system configuration for the HTGRs with CHPs and TES (Type B) for SCO, where η is the subsystem thermal-to-electric conversion efficiency.....	45
Figure 39. Difference in net electricity balance between cases involving a TES system (red) and cases not involving one (blue).....	45
Figure 40. State of TES system charge throughout the year, same data set as Figure 39.....	46
Figure 41. Illustration of the system configuration of the HTGRs with CHPs and TES (Type A) for SCO.....	46
Figure 42. Net electricity generation both with and without TES when the TES is operating in a power-steadying mode, intending to generate 30 MWe.....	47
Figure 43. State of TES charge throughout the year when in power-steadying mode at 30 MWe.	47
Figure 44. Graph of system parameters as a function of storage capacity.....	48
Figure 45. Illustration of the LWR CHP system configuration for SCO.....	48
Figure 46. Heat supply and demand from LWRs to SCO.....	49
Figure 47. Electricity supply and demand from LWRs to SCO.....	49
Figure 48. Overall electricity balance of SCO after integrating the proposed NuScale-PCCs system.....	50
Figure 49. Nuclear integration layout integrating into the Carrollton site process steam system..	50
Figure 50. Conceptual nuclear IES configuration for the DSC Carrollton site, considering dedicated power-only and heat-only reactor units.....	51
Figure 51. Conceptual nuclear IES configuration for the DSC Carrollton site, considering backpressure PCC systems for each reactor unit.....	52
Figure 52. Thermal and electrical net balances for the DSC Carrollton site, leveraging five μ Rxs in a baseload backpressure configuration.....	52
Figure 53. Thermal and electrical net balances for the DSC Carrollton site, leveraging six μ Rxs in a baseload backpressure configuration.....	53

Figure 54. Thermal energy dispatch from the auxiliary boilers required to meet the thermal demands at the DSC Carrollton site via a five- μ Rx configuration.....	53
Figure 55. Resulting net demand electricity fluctuations from the backpressure turbine bypass in one μ Rx.....	54
Figure 56. Conceptual nuclear IES configuration for the Carrollton site, considering backpressure CHP systems for each reactor unit and a TES system coupled to one of the units.....	54
Figure 57. One year of thermal dispatch from the proposed DSC's IES, with TES integrated into one module.....	55
Figure 58. One year of electricity generation from the proposed Carrollton IES, with TES integrated into one module.....	55
Figure 59. Thermal and electrical energy balance of the site with 100MWh _{th} storage is installed.	56
Figure 60. State of charge across operation for a 4-hour (100 MWh _{th}) TES system.....	56
Figure 61. Energy balance of the site and state of charge of the storage system in time for a 24-hour (600 MWh _{th}) TES system.....	57
Figure 62. State of charge for a 24-hour (600 MWh _{th}) TES system.....	57
Figure 63. Reduction of annual external energy demand, electricity export, and heat curtailment—based on TES capacity—along with the annual number of TES cycles.	58
Figure 64. Heat map and projection of the project NPV in regard to different reactor sizes.....	60
Figure 65. Reactor heat dispatch across five-day cluster for LWR-only case.....	62
Figure 66. HP steam demand and production across five-day cluster for LWR-only case.....	63
Figure 67. Total IP steam demand and production across five-day cluster for LWR-only case....	63
Figure 68. LP steam demand and production across five-day cluster for LWR-only case.....	63
Figure 69. HERON dispatch of reactor heat across a 5-day dispatch cluster for SCO, with two Type 2 and two Type 3 PCCs.....	66
Figure 70. Sources and applications of HP steam in the SCO case, per HERON dispatch. Positive values indicate HP steam sources, negative values indicate HP steam applications.....	67
Figure 71. Sources and applications of LP steam in the SCO case, per HERON dispatch. Positive values indicate IP steam sources, negative values indicate IP steam applications.....	67
Figure 72. Sources and applications of LP steam in the SCO case, per HERON dispatch. Positive values indicate LP steam sources, negative values indicate LP steam applications.....	68
Figure 73. Sources and applications of electricity in the SCO case, per HERON dispatch. Positive values indicate electricity generation sources, negative values indicate electricity consumption.....	68
Figure 74. NPV (a) heat map and (b) projection measured against reactor TES sizes.....	70
Figure 75. Measured impact of installed storage capacity at Carrollton.....	70
Figure 76. HERON dispatch of reactor heat across a five-day dispatch cluster for Carrollton.....	71
Figure 77. TES storage level across a five-day dispatch cluster for Carrollton.....	71

Figure 78. Sources and applications of steam in Carrollton case per HERON dispatch. Positive values indicate steam sources, negative values indicate steam applications.....	72
Figure 79. Sources and applications of electricity in DSC case per HERON dispatch. Positive values indicate electricity generation sources, negative values electricity consumption.....	72
Figure 80. SCO combustion CO ₂ emissions and the reduction achieved through SMRs.....	72
Figure 81. DSC's Carrollton site combustion CO ₂ emissions, and the reduction by introducing μ Rxs.....	73
Figure 82. Flood Insurance Rate Map near the SCO site [102]. The red area indicates the general location of the SCO facility.....	74
Figure 83. Annually averaged road traffic near the SCO plant site. The red area indicates the general location of the SCO facility.....	75
Figure 84. Map of railroads located near the SCO site. The red area indicates the approximate location of the SCO facility.....	76
Figure 85. Population density during the (a) daytime and (b) nighttime in the area surrounding the SCO facility. The red area indicates the approximate location of the SCO facility.....	77
Figure 86. Population density results from from Siting Tool for Advanced Nuclear Deployment [106]; the shaded regions represent areas with a population density over 500 people per square mile.....	77
Figure 87. Utility map of the area near the SCO site. The red area indicates the approximate location of the SCO facility.....	78
Figure 88. Map of land ownership for the immediate area surrounding the SCO facility.....	79
Figure 89. Multi-layered map presenting potential consideration for NPP site selection at SCO area. Dow facility is within boxed area.....	80

TABLES

Table 1. Summary of PCC options afforded by the Xe-100.....	20
Table 2. Key NuScale VOYGR design values.....	20
Table 3. Summary of PCC options with NPM.....	23
Table 4. Summary of PCC options for a generic μ Rx.....	24
Table 5. Nuclear CAPEX and OPEX costs input to the HERON simulations.....	36
Table 6. All components, capacities, transfer functions, CAPEX and OPEX values, and generation or consumption prices used in the discrete reactor sweep in HERON.....	59
Table 7. Economic evaluations of various nuclear integration scenarios, showing systems that were able to meet dynamic load demands and those unable.....	60
Table 8. New HERON input parameters for the LWR-only case used to obtain dispatch.....	61
Table 9. System components included in second HERON optimization run for SCO.....	64
Table 10. Delta NPVs for different configurations of PCCs.....	65
Table 11. Delta NPVs for different configurations of PCCs without TES.....	65
Table 12. HERON components, links, transfer functions, and values input for the Carrollton facility case.....	69

Table 13 Earthquakes reported near St. Charles Parish since 1950.....	74
Table 14. Power plants near the SCO site.....	78

ACRONYMS

ALOHA	Areal Locations of Hazardous Atmospheres
ARDP	Advanced Reactor Demonstration Program
ARMA	auto-regressive moving average
BANR	BWXT AT Advanced Nuclear Reactor
BP	backpressure [turbine]
BWXT AT	BWXT Advanced Technologies
BWR	boiling-water reactors
CAPEX	capital expenditure
CHP	combined heat and power
COP	coefficient of performance
CSTG	condensing steam turbine generator
DOD	Department of Defense
DOE	Department of Energy
DSC	Dow Silicones Corporation
FHR	fluoride salt-cooled high temperature reactor
FMR	Fast Modular Reactor
FORCE	Framework for Optimization of Resources and Economics
GA-EMS	General Atomics Electromagnetic Systems
GAIN	Gateway for Accelerated Innovation in Nuclear
HALEU	high-assay low enriched uranium
HERON	Holistic Energy Resource Optimization Network
HP	high-pressure [steam]
HRSG	heat recovery steam generator
HTGR	high-temperature gas-cooled reactor
IES	integrated energy system
INL	Idaho National Laboratory
IP	intermediate pressure
KUC	Kentucky Utilities Company
LEU	low-enriched uranium
LFR	lead fast reactors
LMFR	liquid-metal fast reactors
LP	low-pressure [steam]
LPT	low-pressure turbine
LWR	light-water reactor

MMR	Micro Modular Reactor
MSR	molten-salt reactors
NPM	NuScale power module
NPP	nuclear power plant
NPV	net present value
NRC	Nuclear Regulatory Commission
OPEX	operational expenditures
PCC	power conversion cycle
PCM	phase change material
PWR	pressurized-water reactors
REC	Renewable Energy Certificates
RFG	refinery fuel gas
RPV	reactor pressure vessel
SCO	St. Charles Operations
SDA	standard design approval
SFR	sodium fast reactors
SMR	small modular reactor
sCO ₂	supercritical CO ₂
TES	thermal energy storage
UCC	Union Carbide Corporation
μRx	microreactor
USNC	Ultra Safe Nuclear Corporation

Nuclear Technology Selection and Preliminary Integration at the St. Charles and Carrollton Manufacturing Sites

1. INTRODUCTION

The Dow Chemical Company has committed that by the year 2030, they will reduce net annual carbon emissions by 5 million metric tons compared to their 2020 baseline (~15% reduction) and by 2050 they intend to be carbon neutral including for Scope 1, 2, and 3 emissions plus product benefits. Dow maintains a broad chemical and materials manufacturing portfolio encompassing ~100 manufacturing sites globally. The present collaboration between Idaho National Laboratory (INL) and The Dow Chemical Company is being executed via a Gateway for Accelerated Innovation in Nuclear (GAIN) nuclear energy voucher aimed at determining what kinds of nuclear power may be readily applicable to chemical plant sites identified by Dow, as well as conducting a high-level thermodynamic assessment specifically pertaining to how nuclear-generated heat may be integrated within Dow plants, both thermally or electrically. The U.S. Department of Energy (DOE)'s Integrated Energy Systems (IES) program agreed to provide a concise analysis of the leading and most mature small modular reactor (SMR) and microreactor (μ Rx) technologies that would be able to meet operational requirements at Dow facilities. This analysis will include dynamic capabilities, specific steam manifold integration tactics, characterization of thermal and electric reliability, capacity factors, needed heat augmentation, desired energy storage, and plant impacts.

For the analysis, Dow provided data for two sites operated by the wholly-owned subsidiaries, the Union Carbide Corporation (UCC) and the Dow Silicones Corporation (DCS): the St. Charles Operations (SCO) site in Louisiana, located adjacent to the Mississippi River and operated by UCC, and the Carrollton site in Kentucky, adjacent to the Ohio River and operated by DCS. SCO is an ethylene cracking and ethylene derivatives site, and Carrollton is a siloxane production facility. These two facilities are highly dissimilar in terms of overall energy requirements, internal processes, and thermal-to-electric energy consumption ratios. Dow has provided site information, including historical steam and electricity consumption data.

This report begins with an overview of advanced nuclear reactor technologies being developed that may be appropriate for the timelines Dow is seeking (with deployment occurring sometime in the early 2030s). This summary covers both SMRs and μ Rxs, since they are suitable for different locations, namely St. Charles and Carrollton, respectively. The analysis of the Dow facilities includes the relevant local geography, onsite hazards, and the relationship with the utility regarding locating nuclear plants near those sites. Using the provided historical steam and electricity usage data, different configurations that integrate nuclear heat and power were proposed, then selected via economic optimization of thermodynamic integrations of both sites. Thermal energy storage (TES) integration is considered as well.

The IES analysis leverages the Framework for Optimization of Resources and Economics (FORCE) toolset, developed at INL. The primary FORCE tools used are modeling techniques consistent with the HYBRID modeling repository and Holistic Energy Resource Optimization Network (HERON) for thermodynamic analysis and optimal nuclear technology selection, respectively. Section 4 discusses the various methods in detail.

2. ADVANCED NUCLEAR REACTORS

DOE broadly defines an advanced reactor as being a “nuclear fission reactor, including a prototype plant, with significant improvements compared to reactors operating on December 27, 2020.” [1] At this point, nearly all reactors available for construction—or in the design phase—can be considered advanced reactors featuring sufficient levels of safety—beyond the “traditional” reactors deployed across the globe primarily during the period of 1960–2000. As with most power plants, nuclear system capacities are measured in electrical output, and most advanced systems fall under the traditional 1 GWe threshold. These smaller reactors are categorized as either SMRs or μ Rxs [3]. The threshold for a μ Rx is about 100 MWth.

The present report includes an overview of many different advanced reactor types, with a particular focus on SMRs and μ Rxs. Note that certain vendor design details are not final, nor is this list comprehensive, as some advertised designs were not included, due to the level of published information. Some of the most comprehensive information on advanced reactors is stored on the International Atomic Energy Agency’s Advanced Reactors Information System [4].

2.1 Small Modular Reactors

Per DOE’s definition, all SMR designs should be considered advanced reactors as they include improved safety features over currently operating nuclear plants [5]. The marketable intended difference between SMRs and traditional nuclear reactors is the manner of their construction. Traditional nuclear construction requires extensive site-specific designs (in the past, designs were often not yet finished when site preparation began) entailing great difficulty in fabricating the equipment used throughout the plant. The building of traditional nuclear reactors, which in total produce 1–4 GWe, is considered a mega-project. SMR construction should alleviate some of the site individualism, potentially reducing construction times.

Nearly all SMR designs are currently advertising Rankine-cycle-based power conversion systems. A Rankine cycle approach is advantageous for combined heat and power (CHP) systems, especially ones that interact with existing process steam systems. Advanced reactor systems such as high-temperature gas-cooled reactors (HTGRs), liquid-metal fast reactors (LMFRs), and molten-salt reactors (MSRs) can, broadly speaking, generate sufficiently energetic steam to be integrated into most or all steam systems at a given chemical facility. For advanced light-water reactors (LWRs), the produced steam may be insufficiently energetic for integration into existing steam networks, thus requiring additional energy input (e.g., steam compression or electrical heating) prior to process steam system injection [6].

2.1.1 Light-Water Reactors

Multiple light-water SMR designs are under development, often building and improving on the vast global LWR operating experience. LWR designs largely use traditional zirconium-based or the newer, more accident-tolerant types that lack zirconium, cladded uranium dioxide fuel enriched to around 5%, leveraging the techniques and supply chain already established within the nuclear industry. LWRs are generally divided into two categories: pressurized-water reactors (PWRs), which are more widely deployed, and boiling-water reactors (BWRs). PWRs are two-loop systems in which the primary core coolant and secondary-side turbine steam are separated via a heat exchanger. In BWRs, the primary coolant boils significantly within the core, is separated in dryers and moisture-separating sections, and is then run directly through the turbine without exchanging heat to additional thermal loops.

NuScale US-600 and VOYGR

The NuScale US-600 is the only SMR design to have been granted full U.S. Nuclear Regulatory Commission (NRC) design approval—a landmark achievement for the company [7]. The US-600 design is a 180 MWth, 50 MWe design that NuScale is seeking to power uprate to 250 MWth, 77 MWe—named VOYGR—without significantly altering the design. NuScale’s vision has always been to construct a safe-by-design system that is both operationally simple and walk-away safe. A key feature of the NuScale design is that the primary coolant is driven solely via natural circulation during all operational modes. A tall “chimney” at the core outlet allows hotter, less-dense water to rise before exchanging heat to the power distribution system via the reactor pressure vessel (RPV)-embedded heat exchangers. The cooler water then flows along the outside of an internal core barrel as a colder, higher-density liquid, driving circulation flow. Following the power uprate, the NuScale VOYGR module will generate steam that enters the power conversion system at 283°C (541.4°F) and 32.8 bar (476 psia). NuScale has already engaged with steam compressor vendors, and company analysis indicates that steam compression can be leveraged to provide steam at 500°C or even 650°C, potentially increasing the industrial integration viability for VOYGR plants [8].

NuScale’s website advertises 10 active projects in various stages of VOYGR reactor deployment. NuScale previously had a Memorandum of Understanding with Utah Area Municipal Power Systems as part of the Carbon Free Power Project, which was dissolved in late 2023 [9]. The cancellation was attributed to rising costs, including significant producer price index hikes for steel, wiring, and electrical equipment. The costs of these materials greatly outpaced inflation, likely as a result of changes stemming from the COVID-19 global pandemic. There were also per-MW cost increases due to reducing the overall size of the project as a result of low guaranteed power subscription, which did not even reach the level of the smaller facility’s size [10] [11]. Together, these factors caused the projected capital cost of delivering the contracted energy via a six-module suite to exceed \$20,000/kW—significantly higher than the nominal projected cost of the system, which is closer to \$4,000/kW. It remains unclear how much of this cost increase will also translate to future projects, how much of this cost increase will translate across all advanced nuclear technologies, and whether this project was an indicator of how much energy prices may increase regardless of what dispatchable sources are used in the near future.

Holtec SMR-300

Holtec International is developing its SMR-300 design as a 300 MWe, (around) 1050 MWth LWR that leverages natural circulation coolant flow during operation and walk-away passive safety systems during accident scenarios. The SMR-300 is a PWR that produces steam within a secondary loop that transfers heat through the primary heat exchanger. Specific design information on the SMR-300 is hard to come by (the design was uprated from 160 to 300 MWe in August or September 2023), but the anticipated nominal steam conditions are around 45–55 bar (652–797 psia) and 300°C–320°C (572°F–608°F), as is typical for LWRs. The SMR-300 was intentionally designed to be capable of low water use, with possible atmospheric final heat rejection, thus increasing the number of potential installation sites.

The company reached an agreement with Michigan to site two SMR-300 reactors at the Palisades Nuclear Power Plant, with a target date of mid-2030, in order to help repower the Palisades site. Holtec is beginning the process of engaging the NRC regarding the necessary site licenses, and they do not anticipate that submitting documentation in 2026 or so will impact their 2030 deployment timeframe [12]. Holtec, in its divisions and subsidiaries, has acquired the most significant portion of its nuclear experience from owning several decommissioning nuclear plants within the United States, as well as through their onsite spent fuel storage technology and projects. The SMR-300 will be the first nuclear design constructed by Holtec.

General Electric BWRX-300

The BWRX-300 from General Electric and its subsidiaries leverages the company's wealth of experience in global nuclear operations and deployment. The BWRX-300 is a natural-circulation BWR that produces 300 MWe and around 1000 MWth. GE-Hitachi believes the BWRX-300 will be able to distribute its thermal energy to applications beyond simple electricity generation, and to do so at lower cost [13]. BWRX-300 steam will be produced at 72 bar and 285°C [14]. GE-Hitachi is currently engaged in pre-application activities with the NRC, and have multiple anticipated deployments, including with Ontario Power Generation and Tennessee Valley Authority [15] [16]. These two utilities, along with Synthos Green Energy, are helping develop and license the BWRX-300 design. Reactor deployment is anticipated to occur in around 2028.

Westinghouse AP300

The Westinghouse AP1000 reactor is currently one of the most widely deployed traditional-sized systems in the world. AP1000 systems are rated at over 3000 MWth and operate at between 1000 and 1150 MWe, depending on the specifics of the deployment area. Westinghouse is leveraging "tens of millions of man-hours" from the AP1000 design to create a smaller 990 MWth, 300 MWe system: the AP300, which is a Generation III+, one-loop PWR. As such, it can be assumed that the steam conditions match the AP1000, at 57.6 bar (821 psig) and 273°C (523°F) [17]. Westinghouse announced plans for the AP300 in May 2023 and plan to start construction in 2030, with the AP300 reactor to begin running within 3 years. Westinghouse is engaged in pre-application activities with the NRC and believes that since much of the configuration and the passive safety systems have already been licensed for the AP1000, the license approval process will be smooth [18]. Westinghouse's publication materials indicate they are intending to design the AP300 for CHP applications, with graphics showing various potential applications [19].

2.1.2 High-Temperature Gas Reactors

For HTGRs, limited operating experience has been accrued globally, but they are anticipated to offer the highest level of compatibility with non-electric applications. This is due to the high temperatures—up to 750°C (1382°F)—expected in the near term, as well as the eventual operating temperatures of 950°C (1,742°F) and above. HTGRs use helium as a coolant, as it is inert and features desirable neutron interaction properties. Two fuel structures have been mainly used/proposed for HTGRs: prismatic and pebble. Prismatic fuel is similar to LWR fuel rods, with dedicated vertical coolant channels for cooling each individual, vertically stacked rod. The structure is set within a graphite network. The other type is a pebble-bed system in which fuel kernels are set into graphite pebbles, each around 5 cm in diameter, that are constantly cycled through the core via an online refueling system. The pebble movement is uncontrolled, but design features ensure that all pebbles cycle through and that blockages do not occur.

X-Energy Xe-100

The Xe-100, which is X-energy's flagship design, produces around 200 MWth or 80 MWe via a Rankine cycle that leverages steam at 565°C (1049°F) and 16.5 MPa (2393 psia) [20] [21]. The pebble-bed core will use high-assay low-enriched uranium (HALEU) enriched to 15.5%, and will operate with long cycles attributable to online refueling. X-energy is an Advanced Reactor Demonstration Program (ARDP) awardee, having received as much as \$1.2B in funding to license and construct their first reactor [22]. X-energy and Dow have selected a location at Seadrift, TX, for the first four-pack of reactors that is intended to begin operation in the early 2030's.

X-Energy owns a subsidiary company, TRISO-X, that is constructing a fuel fabrication facility near Oak Ridge, TN. This facility will be able to produce 714,000 pebbles per year—enough for around 3.25 Xe-100 initial core loads. TRISO-X is still undergoing licensing of the facility but has already broken ground in anticipation of success.

General Atomics Fast Modular Reactor and EM²

General Atomics Electromagnetic Systems (GA-EMS) is developing two HTGR designs. Its fast modular reactor is a 112 MWth, 50 MWe system that uses a direct Brayton cycle to produce electricity [23] [24]. Helium conditions within the core are anticipated to be 7 MPa, with an inlet temperature of 509°C and an outlet temperature of 800°C. Due to the Brayton cycle configuration, it is unlikely that any CHP opportunity would arise except by leveraging the intercooler water that serves as the heat rejection stage of the system. GA-EMS is intending to demonstrate the system by 2030 and is engaged in pre-application activities with the NRC [25] [26].

The other GA-EMS design is the EM² HTGR, which is a modular helium-cooled fast reactor with a 500 MWth design featuring a net power output of 265 MWe per unit. The core lifetime is 30 years, and the fuel works by converting fertile material to fissile material, which they refer to as a “convert and burn” core design [27]. A direct closed-cycle gas turbine Brayton cycle is used as the power conversion unit, with the same integration assumptions as applied to the fast modular reactor design. In March 2024, General Atomics signed a Memorandum of Understanding with the Emirates Nuclear Energy Corporation to investigate collaborative project opportunities [28]. GA-EMS is engaged in pre-application activities with the NRC on the EM² design, as well [29].

2.1.3 Liquid-Metal Fast Reactors

LMFRs use atomically heavier metals in a liquid state to cool the core without moderating neutrons into the thermal region. Fast reactors use a more highly energetic neutron spectrum, which changes some of the physics of fission within the system and enables different fuel types to be used. Broadly speaking, thermal and epithermal fission reactors require more highly enriched (meaning a higher atomistic content of U-235 to U-238) fuel to operate. Fast spectrum reactors can generate fuel through converting (mainly) U-238 atoms into Pu-239 atoms and splitting Pu-239 as an additional fuel source. The two most common LMFR designs are sodium fast reactors (SFRs) and lead fast reactors (LFRs). Coolant temperatures are significantly higher in SFRs and LFRs than in existing LWRs, reaching up to the 500°C–650°C range (932°F–1202°F). A key advantage of these reactors is that they allow for atmospheric or minimally pressurized systems, as the liquid coolant operates far below the boiling point. LMFRs are also sub-categorized by the flow path used for the primary coolant. The loop-type design operates similarly to traditional PWRs and designed HTGRs, with forced coolant flowing through a separately located heat exchanger. Pool-type designs have large amounts of hot coolant at the top of the reactor vessel to take advantage of buoyancy effects. Embedded heat exchangers in the primary vessel circulate secondary-loop coolants in the top pool of the system, aiding in natural circulation of the system. Pool-type reactors also have relatively low flow velocities.

TerraPower Natrium

TerraPower's Natrium reactor is an 840 MWth, approximately 345 MWe SFR design. By some definitions, this excludes Natrium from being classified as an SMR. The Natrium core leverages metallic fuel and is a pool-type design. As mentioned above, use of liquid-metal coolants allows the system to operate at atmospheric pressure. It is a relatively unique design among SMRs, in that the system has a two-tank molten-salt thermal storage system, with a hot-tank temperature of up to 621°C, accepting reactor heat and discharging heat to the power conversion system [16]. This temperature, and considering the projected thermal-to-electric efficiency, indicate that steam conditions will be similar to those of the Xe-100 system at 565°C (1049°F) and 16.5 MPa (2393 psia). While the system's nominal output is 345 MWe, TerraPower posits that the system can produce 500 MWe for over 5.5 hours at a time, which equates to a little over 850 MWh-e of storage in the loop with the oversized discharge system.

Like X-energy, TerraPower is an ARDP awardee. A demonstration plant is scheduled to come online in Kemmerer, WY, in around 2030, though possibly as late as 2032. This location is the site of a retiring coal plant, and TerraPower recently submitted materials for their construction permit for the Kemmerer location and has been engaged in licensing activities with the NRC since 2022 [30]. TerraPower has also engaged Uranium Energy Corp and Global Nuclear Fuel to secure their fuel supply chain [31] [32]. TerraPower as a company has significant financial backing.

Westinghouse LFR

The Westinghouse LFR is a 950 MWth reactor design capable of a 450 MWe net average electrical output. Westinghouse is investigating a unique method of flexibly generating electricity via integrated TES that discharges to provide supplemental feedwater heating, enabling intra-turbine extraction lines to be closed so as to increase steam flow through the turbine system. Westinghouse is also investigating charging the storage system by using a parabolic solar collectors. The exact design remains a work in progress, but steam conditions are anticipated to be 500°C–630°C [33].

Westinghouse is building 10 test facilities to support the development of its LFR design, focusing on demonstrating key phenomena, materials, and components [34]. Three of these test facilities are being installed at the Westinghouse Springfields facility in the United Kingdom. The test facilities will investigate lead freezing and under-lead viewing, primary heat exchanger failure, and material corrosion/erosion. An additional testing rig at the Westinghouse facility in Churchill, Pennsylvania, will be utilized to conduct tensile tests in molten-lead environments so as to research liquid-metal embrittlement [34]. Much of the initial testing has been completed for the LFR design, and at present, the anticipated date for a demonstration reactor is around 2030 [35].

ARC Clean Technology ARC-100

The ARC-100 reactor is a 100 MWe, 286 MWth SFR with a 20-year refueling cycle that utilizes HALEU with an average enrichment of 13.1%. The sodium temperature at the core outlet is 510°C [36]. Projected steam conditions are unknown, but turbine selection indicates generated superheated steam at pressures of up to 14.0 MPa (2030 psia). The ARC-100 is a commercial scale version of the Experimental Breeder Reactor-II design, which achieved criticality in 1965 at INL's National Reactor Testing Station [36]. In partnership with New Brunswick Power, ARC Clean Technology is planning to deploy the ARC-100 at the Point Lepreau Nuclear Generating Station in New Brunswick, Canada [37]. They are currently engaged in pre-application activities with the NRC [38].

2.1.4 Molten-Salt Reactors

There are two different MSR types: salt-cooled and salt-fueled. Salt-cooled MSRs use molten salt as the coolant only, and employ solid fuel. In a molten-salt-fueled reactor, the fuel itself is a molten-salt fluid. One type of MSR is a fluoride-salt-cooled high-temperature reactor (FHR). Two molten-salt-fueled research reactors have previously been built and operated at Oak Ridge National Laboratory: the Aircraft Reactor Experiment and the Molten Salt Reactor Experiment.

MSRs operate at high temperatures (up to 750°C) and near-atmospheric pressure, eliminating the need for large reactor vessels and thick containment buildings. The design space for MSRs is vast. The fuel salt can be comprised of fluorides, chlorides, or even nitrates, and the neutron spectrum can be thermal, epithermal, or fast. The reactor can be a breeder or a burner. There are also a plethora of fuel options including low-enriched uranium, HALEU, thorium, plutonium, and spent nuclear fuel.

Kairos KP-FHR

Kairos Power's KP-FHR design is a FHR with a thermal power of 280 MWth and an electrical output of 140 MWe. Kairos Power has been engaged in pre-application activities with the NRC ever since November 2018 [39]. Design steam conditions for KP-FHR are 19 MPa (2755 psia) and 585°C (1085°F) [40]. The fuel is a TRISO-coated particle fuel laid out in a pebble bed configuration and enriched to 19.75%. This design should allow for online refueling.

An application for a permit to construct an advanced test reactor to support development of both the KP-FHR and Hermes (see the next sentence) was submitted to the NRC by Kairos Power LLC on September 29, 2021; the construction permit decision was approved on December 12, 2023 [41]. Hermes is a low-power test reactor—35 MWth and no electricity generation—being built to support the KP-FHR technology and development. A second test reactor, Hermes 2, will incorporate two low-power test reactors, each with a thermal power of 35 MWth—the same as for the Hermes reactor—but will introduce a Rankine cycle to produce electricity. The application for this construction permit was submitted on July 14, 2023 [42].

Terrestrial Integral Small Modular Reactor

Terrestrial Energy has been developing their Integral Small Modular Reactor, a 442 MWth, 195 MWe MSR that employs a three-loop salt system in which the tertiary loop contains salt that produces steam at 585°C [43]. Terrestrial Energy has engaged with the NRC in pre-licensing activities, and the Canadian Nuclear Safety Commission has concluded that no fundamental barriers exist to its licensing [44]. The intended operation is to fully factory-fabricate a core unit and then completely replace the reactor vessel after a 7-year operating life. Terrestrial Energy is targeting 2030 as the deployment date for their systems [45].

2.2 Microreactors

μRxs are very small nuclear systems all under 100 MWth. Their main features include transportability, fast initiation, and a small footprint. Many designs are also looking to enact remote operations to reduce eventual operating costs. As a rule, these systems tend to be more expensive on a per-unit-energy basis, as the economies of scale are lost and never sufficiently recovered as they might otherwise be in SMR systems.

2.2.1 High-Temperature Gas Reactors

BWXT Advanced Technologies (BWXT AT) Advanced Nuclear Reactor (BANR)

The BANR system generates 50 MWth within its core and is designed to allow for cogeneration. The BANR design received an ARDP award in 2020 to support deployment. The BANR reactor is an HTGR technology that can be transported by truck, rail, or ship [46]. BWXT AT can construct the system using existing facilities and can produce enough of their own fuel for a 5-year refueling cycle. BWXT AT already maintains fuel fabrication licenses from the NRC, and intends to leverage those licenses to accelerate their final licensing activities [47]. The BANR system is currently designed to use a Rankine cycle to generate steam and integrate with cogeneration cycles. Specific conditions are not published, but as the system is an HTGR, it can be assumed that the system will operate with superheated steam at pressures in excess of 8.0 MPa (1160 psia).

BWXT AT has partnered with a Wyoming industrial machinery company called L&H Industrial and a trona mining company to deploy BANR for cogeneration of electricity and process heat [48] [49]. This project may serve to deploy the first BANR system by as early as 2028, and is leveraging both ARDP awards and the Wyoming Governor's Energy Matching Funds program. BWXT was also the first awardee of Project Pele, a Department of Defense (DOD) initiative to construct a μ Rxs. The Pele design may come online as early as 2025 [50].

Ultra Safe Nuclear Corporation (USNC) Micro Modular Reactor (MMR)

The USNC MMR is an HTGR design capable of 3.5–15 MWe or 10–45 MWth [51]. USNC advertises it as a “fission battery” with 300 MW-yr of energy. The design does not use water, and the two-unit MMR Energy System has a footprint of less than 5 acres. Demonstration units are scheduled for 2026, and USNC is currently engaged in licensing activities [51]. The MMR is designed to produce steam at 660°C (1220°F) at pressures between 30–60 bar (435–870 psia).

The MMR uses Fully Ceramic Micro-encapsulated (FCM) fuel, meaning TRISO particles within layered ceramic coatings and encased within a fully dense silicon carbide matrix. USNC’s proprietary manufacturing method improves the packing factor of their fuel and thus increases the energy density within the core. MMR deployments are intended to be temporary, with deployment sites being easily returned to their natural conditions following termination of the project. USNC has multiple demonstrations underway, including one at the University of Illinois Urbana-Champaign and one with Ontario Power Generation [52]. A manufacturing facility that is scheduled to break ground in Alabama in 2024 is expected to produce up to 10 MMR units per year, starting in 2027 [53].

X-energy Xe-Mobile Microreactor

The Xe-Mobile design is a 20 MWth core that uses TRISO-X, producing 5 MWe and building on the design experience pertaining to the Xe-100 system [54]. Some of the Xe-Mobile design is also based on work that occurred under project Pele, with the DOD as the second project awardee. Based on the available materials, Xe-Mobile appears to employ a closed Brayton cycle for electricity production with atmospheric heat rejection. Xe-Mobile also won a 2023–2024 DOE Office of Nuclear Energy industry funding opportunity announcement to help continue the design process. Among the other participants supporting this design are Bosal, Calnetix, INL, and Oak Ridge National Laboratory [54]. X-energy is currently engaged in pre-licensing activities with the NRC on this design.

2.2.2 Liquid-Metal Fast Reactors

Oklo Aurora Powerhouse

The Oklo Aurora Powerhouse is a stationary, metal-fueled/-cooled fast reactor design. As the operator, Oklo uses long-term power purchase agreements to sell heat and power. The Aurora Powerhouse is scalable from 15 to 50 MWe and can be used for cogeneration applications, with refueling timelines of 10 or more years for any particular module. Oklo is anticipating a supercritical CO₂ power cycle, although they are also open to integrating their technology with a Rankine cycle. Oklo is in the process of deploying a demonstration reactor in Idaho, using recycled fuel from DOE. Three other projects are also underway, including two at Centrus Energy's enrichment plant in Ohio [55]. The Idaho project is targeting an online date of 2026 or 2027, but could be pushed to close to 2030 depending on licensing [56]. Oklo is engaged in pre-application activities with the NRC [57].

2.2.3 Heat Pipe Reactors

Westinghouse eVinci Microreactor

The eVinci μRx uses proprietary heat pipe specifications to remove core heat via 12-foot nuclear-grade heat pipes. Westinghouse is targeting a highly transportable and mobile design that affords rapid onsite deployment. The most recent data from Westinghouse indicates that the eVinci design will operate a 13 MWth core for a 5 MWe system [58]. The core is designed with an 8+ year refueling cycle in mind. Westinghouse won funding through the U.S. DOE ARDP program, as well as funding from the Government of Saskatchewan, Canada to produce the first unit [59] [60]. Heat rejection from the heat pipes occurs via heat exchange to air, which nominally powers an open Brayton cycle. Westinghouse anticipates very fast load-following capabilities from eVinci units, along with heat output of up to 150°C from the open Brayton cycle. Westinghouse has engaged in pre-application activities with the NRC [61].

3. DOW SITES

Dow selected chemical process plants in St. Charles, Louisiana, and Carrollton, Kentucky, for analysis. This section of the report summarizes both plants' operating details, geographies, energy profiles, and relationships with the relevant utility. In this report, we define steam conditions as being low pressure (LP) when below 100 psig (7.9 bar), intermediate pressure (IP) at 100–600 psig (7.9–42.3 bar), high pressure (HP) at 600–1000 psig (42.3–70.0 bar), and very high pressure when above 1000 psig (70.0 bar).

3.1 St. Charles Site

3.1.1 Primary Chemical Processes and Operation

The SCO site spans 2,000 acres and sits 14 miles upstream from New Orleans along the Mississippi River, adjacent to a nuclear power plant. The chemical facility produces a range of products, including ethylene, polyethylene, polyethylene glycol, acrylic acid, latex, and acetylene. These materials serve as the building blocks for various goods such as plastics, insecticides, antifreeze, brake fluid, detergents, and paints. Originally comprising Union Carbide Taft and the Star Petrochemical Plant, the site underwent integration and rebranding as Dow SCO following Dow's acquisition of Union Carbide in 2001.

In 2021, CO₂ emissions from the St. Charles site totaled ~2.1 million tons per year [62]. These emissions primarily stem from fossil fuel combustion to generate steam, power, and heat for the ethylene cracking furnaces.

3.1.2 Geography

The SCO site is one of many process sites located in a prominent industrial zone that runs along the Mississippi River between Baton Rouge and New Orleans. The northern plant boundary is the Mississippi River, to the west is a partner chemical process facility, to the east is undeveloped land followed by a small residential area, and to the south is mostly swampland.

SCO is just over a mile from the Waterford Nuclear Generating Station, an existing LWR plant whose nameplate capacity is 1152 MWe. While there is no guarantee that such a site could be expanded, it is encouraging to note that nuclear licensing and operation is already approved for the surrounding area.

Decarbonization options outside the utilization of nuclear energy are significantly limited in Louisiana. The grid's electricity, generated at facilities mapped in Figure 1, mostly stems from natural gas and coal generation. Renewable electricity net generation is low within the state, with renewable energy sources (mostly biomass) representing only about 3.5% of the total electricity net generation [63]. Despite high offshore wind potential, no offshore wind capacity is currently installed. The onshore wind potential is limited, with no current statutory authority for siting onshore wind [64]. The utility-scale solar energy generation is low within the state, and the potential for future hydroelectric capacity expansion is low as well [63].

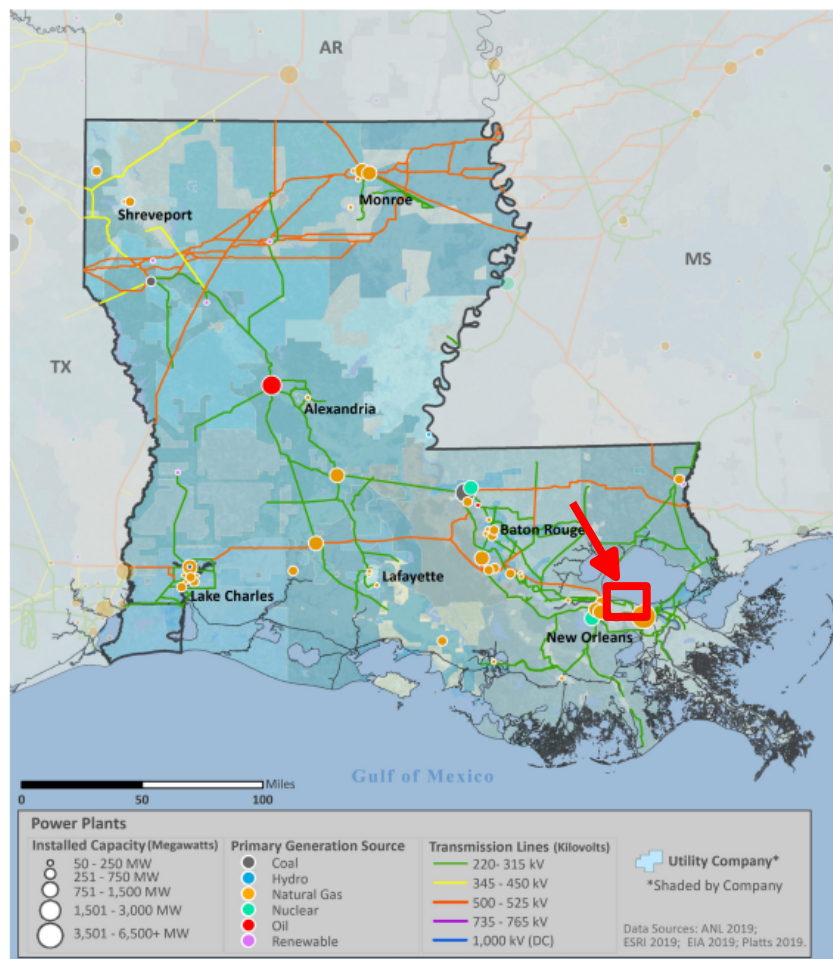


Figure 1. Map of electricity generation in Louisiana, as taken from [65]. The SCO site is represented by the red square. **Energy Systems and Demand Profiles**

Thermal energy distribution at SCO entails three main steam manifolds. One network is a HP line that operates at 600 psig (4.2 MPa), another is an IP line that operates at 200 psig (1.5 MPa), and the last is a LP system that operates at 75 psig (0.62 MPa) [66]. Processes interconnect with these manifolds to source steam as needed. The HP network is presently fueled via natural gas boilers and heat recovery steam generators that also produce electricity from the steam prior to its insertion into the HP network.

The current CHP system combines two heat recovery steam generators (HRSGs) and natural-gas boilers to generate the requisite steam in a natural-gas combined cycle system. The very high-pressure steam is either let down through expansion valves or, mostly, passed through a backpressure turbine to the facility HP process steam line. Steam in the HP line is distributed to meet specific demands, to the IP steam line via letdown valves and turbopump turbines, and to a condensing steam turbine generator (CSTG) that also has extraction to the LP steam header. The IP steam line also has steam injection from lower-pressure production in the HRSGs. The CSTG operates at 20%–100% of its normal exhaust flow rate. Steam is also generated via several processes within the plant and is treated as part of the net steam demand profile. The nuclear integration work will focus on meeting the HP, IP, and LP demands, as electricity generation will no longer be a priority of the onsite steam system, since it will be met by the nuclear source. A simplified overall layout is shown in Figure 2.

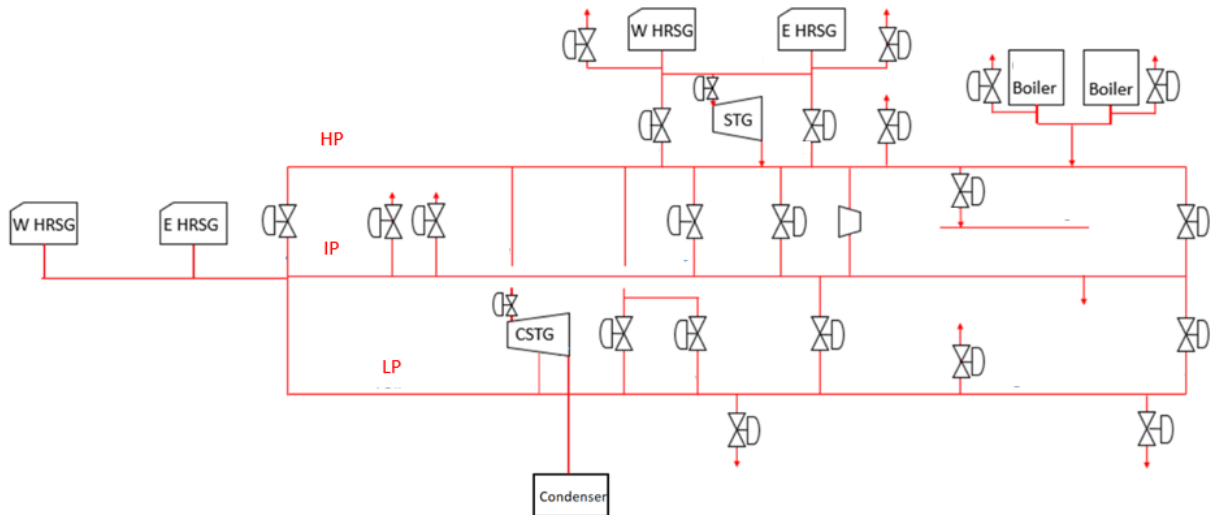


Figure 2. SCO process steam system. Overall heat demand and power production/consumption profiles were provided by Dow and are shown in Figure 3. The total heat demand is obtained by summing the HP, IP, and LP demands.

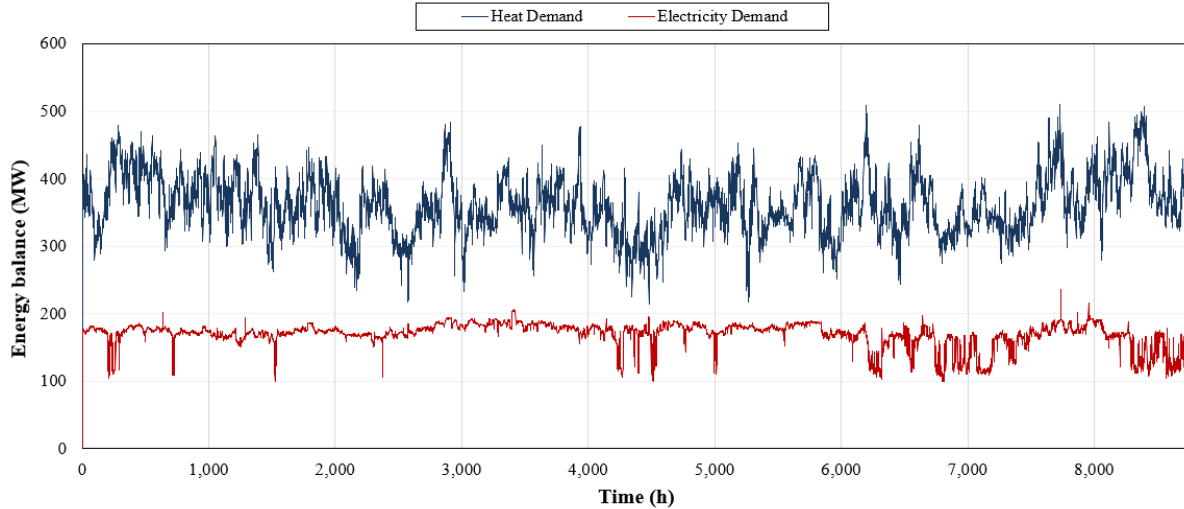


Figure 3. Synthetic heat and electricity demand profiles of SCO for 2022. These profiles are generated using actual plant data and an ARMA model.

3.1.4 Utility Relationship

Utility agreements are made complex by the reliability requirements placed on chemical plants, the overall plant size, and the status as a distributed generator. The local electrical utility for SCO is Entergy LLC, a regulated utility responsible for balancing the grid across most of Louisiana as well as parts of the surrounding states (see Figure 4).



Figure 4. Entergy service map of the SCO area [67].

With the industrial nature of SCO operations, bilateral contractual obligations and terms are set governing energy provisions for the operating site. Contracts are typically set for multiple years to ensure that the customer has a guaranteed energy supply while still allowing the utility to plan for infrastructure, rate schedules, and portfolio requirements. Contractual limitations will frequently include maximum customer power draw and demand variation thresholds to ensure grid stability, a power factor ratio that balances real power and reactive power to maintain equipment safety and transmission efficiency, and, potentially, demand-side response terms that either require reduced loads during peak demand periods or the requesting of power from the industrial plant as needed. The SCO plant operates under a significant baseload electricity rate, as seen in Figure 3, but variations beyond that level can reach as high as 33% beyond baseload. While SCO presently generates all necessary electricity internally and has internal backup, the utility relationship may shift in response to a proposed dedicated nuclear solution with Entergy LLC, depending on the owner-operator relationship. The assumption in this work is that Dow will own the nuclear assets but Entergy will operate them and provide Dow with required energy in a manner similar to a power purchase agreement. Entergy is already a nuclear operator, with four nuclear generation sites in its portfolio. It is recommended that during the next contractual renewal process, the idea of Dow purchasing nuclear assets for dedicated clean energy to the SCO plant be bridged with Entergy so that both parties can properly anticipate future changes to the operating paradigm.

In a power purchase agreement scenario, the operating assets for an industrial customer may still prove insufficient for power generation. Entergy provides three tiers of contracted service so as to ensure reliability in such cases. These are summarized in Figure 5 and cover most potential incidents.



Figure 5. Summary of the three electricity tiers within the industrial contract from Entergy LLC.

On-peak hours for this area are, with a few holiday exceptions, 2:00–8:00 PM Monday through Friday from April 1 through October 31, and 6:00–10:00 AM and 5:00–9:00 PM Monday through Friday from November 1 through March 31.

3.2 Carrollton Site

3.2.1 Primary Chemical Processes and Operation

Dow Silicones Corporation (DSC) develops, manufactures, and markets a broad range of silicone-based products. Ground metallurgical silicon power is converted into dimethyl-dichlorosilane via the Muller-Rochow process, and dimethyl-dichlorosilane is turned into different kinds of siloxane through hydrolysis. Their product portfolio includes sealants, elastomers, emulsions, and other silicone-based materials utilized across diverse applications.

In 2021, CO₂ emissions from the Carrollton site totaled ~174,000 tons per year [68]. These emissions primarily stem from fossil fuel combustion to generate steam for the site.

3.2.2 Geography

The DSC chemical plant referenced in this study is located in Carrollton, KY, east of the main town and adjacent to the Ohio River. Carrollton is located about halfway between Louisville, KY, and Cincinnati, OH, with Carrollton itself located across the Ohio River from Indiana. The local county has a population density of around 80 persons/mi². The area is relatively flat, with local development intermixed with forests. As shown in subsequent sections, the demands of the Carrollton facility are more readily met by a set of μ Rxs than by SMRs. DSC owns around 40 acres of undeveloped land in and around the Carrollton facility. Nuclear μ Rxs and SMRs produce, on an order of magnitude, around 10 MWe/acre, which is more than sufficient to meet the facility demands.

The DSC facility is located about 4.8 miles from the Ghent Generating Station, which is the largest coal plant in the Kentucky Utilities and Louisville Gas and Electric Company portfolio and can generate nearly 2000 MWe, though one of the four units at the Ghent Generating Station is being proposed for retirement by 2027 [69][70]. INL is the lead entity that has provided in-depth analysis on transforming coal generating sites into nuclear sites, showing that nuclear overnight costs could decrease between 15–35% relative to a nominal greenfield project, potentially lending this kind of site to a coordinated effort to reduce local carbon emissions by introducing nuclear power [71].

3.2.3 Energy Systems and Demand Profiles

The energy system at Carrollton is much smaller and less complex than at the SCO location. The average amount of electricity being purchased from the grid is around 20 MWe. The Dow-provided electricity data in Figure 6 is only tracked monthly at the facility. Natural gas boilers generate an average 120 MWth of total process heat demand into a single IP steam header. The steam demand shows frequent oscillations due to cyclical operations as well as some intermittent onsite generation within certain subprocesses. One of the most significant differences between SCO and Carrollton is the difference in the thermal:electric energy ratios required at the plant. At SCO, the ratio of heat to electricity was about 1.5:1, while at Carrollton the ratio is around 6:1.

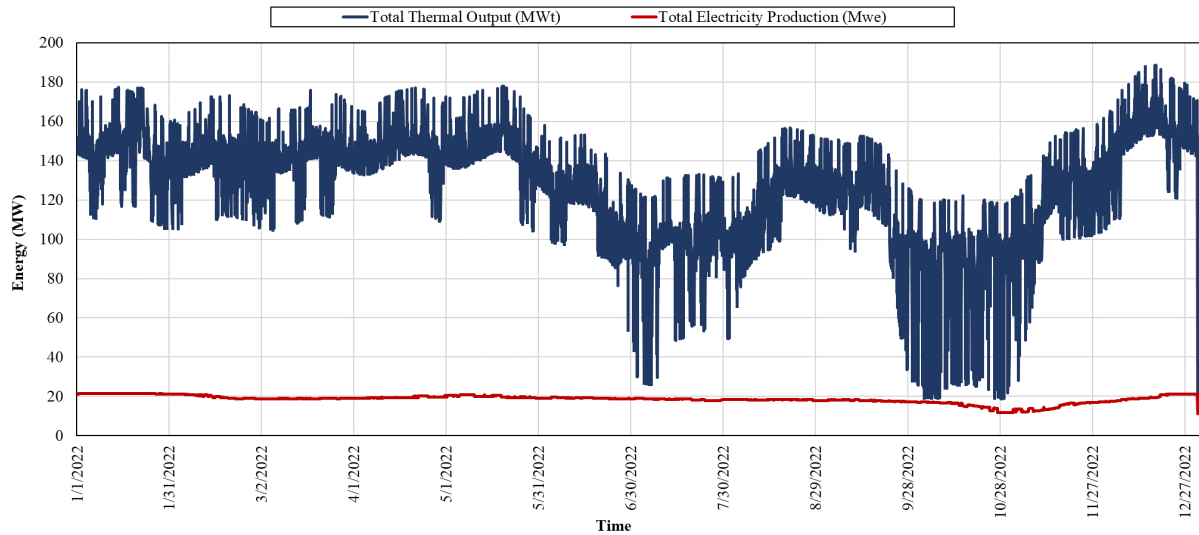


Figure 6. Synthetic heat production and electricity consumption profiles for DSC Carrollton site in 2022. These profiles were generated using actual plant data and an ARMA model.

3.2.4 Utility Relationship

The local utility for the Carrollton site is the Kentucky Utilities Company (KUC). A map of the Kentucky utilities is included in Figure 7. A majority of KUC's generating assets are coal and natural gas, with some hydroelectric and solar facilities supplementing that generation. It is important to note that KUC is not currently a nuclear operator, and no commercial nuclear plants exist in Kentucky or Indiana. Kentucky very recently voted to establish the Kentucky Nuclear Energy Development Authority, so the state may be willing to both programmatically and financially support new nuclear projects [72].

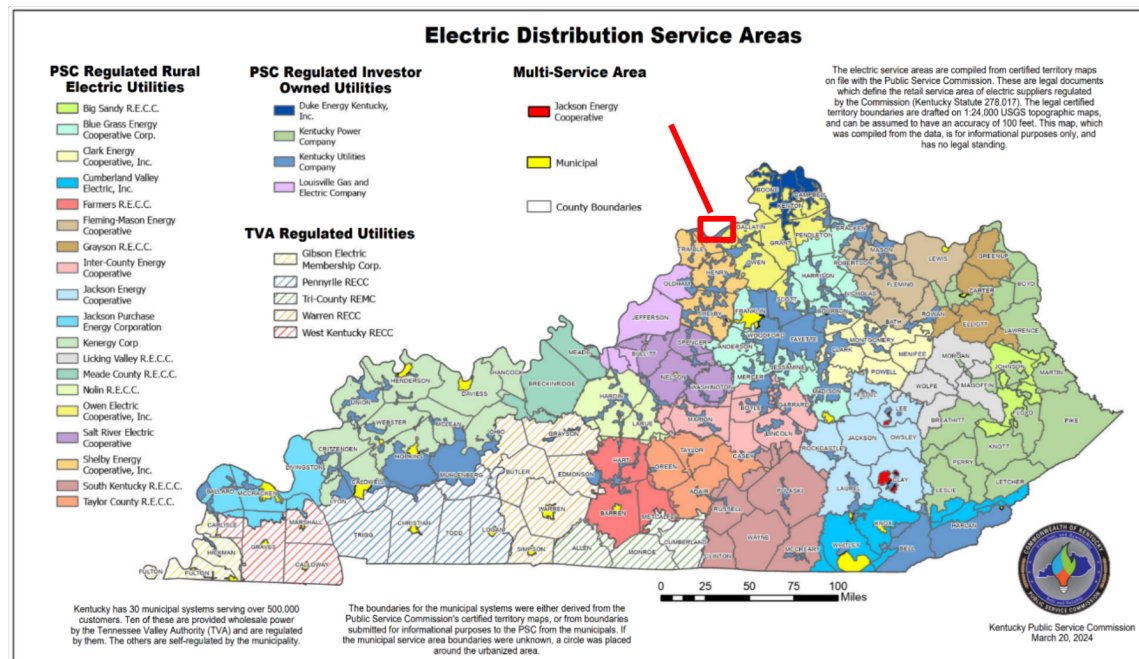


Figure 7. Map of Kentucky utilities [73]. The Carrollton site is indicated by the added red square.

State-wide and utility-specific rules apply to distributed generation, which any proposed solution for the DSC facility would likely entail. KUC operates a Green Energy Program that enables residential and industrial customers to purchase Renewable Energy Certificates (RECs). Using 20 MWe as the baseline, the Carrollton facility would need to purchase around 3230 “blocks” per month [74]. In 2023, the highest number of RECs purchased in a single month by KUC was 30,973 in October, with the monthly average being 22,885 RECs; thus, Dow, to claim RECs for Carrollton, would likely need to verify that there is sufficient capacity in KUC’s purchasing avenues to accommodate an approximate 14% increase in monthly REC purchases [75].

In 2008, the Kentucky General Assembly passed Senate Bill 83, establishing updated net metering requirements for distributed generating facilities. This document declares that (emphasis added):

“An eligible customer-generator shall mean a retail electric customer of the Utility with a generating facility that:

Generates electricity using solar energy, wind energy, biomass or biogas energy, or hydro energy;

Has a rated capacity of not greater than thirty (30) kilowatts;

Is located on the customer’s premises;

Is owned and operated by the customer;

Is connected in parallel with the Utility’s electric distribution system; and

Has the primary purpose of supplying all or part of the customer’s own electricity requirements.

At its sole discretion, the Utility may provide Net Metering to other customer-generators not meeting all the conditions listed above on a case-by-case basis.” [76]

A nuclear facility on the Carrollton facility property would not meet all the listed criteria and thus may require a special exception, as noted in the quote above. KUC’s net metering policy, as stated on their website, indicates these requirements are still in place, but with a higher rated capacity of 45 kW [77]. However, due to the reliability of nuclear plants relative to renewable systems, it may be that net metering constraints identified in Senate Bill 83 may be lifted.

In a separate document, KUC’s (as well as Louisville Gas and Electric’s) Interconnection Requirements document indicates there may be policies more conducive to industrial-scale customer interactions [78]. This document details the technical requirements for distributed generating facilities. For MW-scale (differentiating between greater or less than 10 MW) facilities, several grid support functionalities are required for connectivity, including ramping, the ability to cease power delivery, power curtailment, and other grid-stabilizing abilities. Direct communication with KUC is recommended to understand how state-wide statutes and company policies would interact at the DSC facility.

4. METHODS

This section reviews steam manifold integration strategies, the resource capacity optimization tool, siting and safety concerns, engineering analysis, and thermal and electricity reliability. Some preliminary results are included if they were leveraged within other steps to obtain further solutions.

4.1 Preliminary Demand-Fitting Analysis

An initial thermal analysis was conducted of the SCO and Carrollton steam systems to pinpoint operational trends, load capacities, and the production quality necessary for seamlessly integrating a nuclear plant with existing facilities. This analysis includes an engineering evaluation of feasible systems for CHP generation that enable meeting onsite requirements. The preliminary analysis for SCO focuses on two DOE-supported reactors: the Xe-100 HTGR and the NuScale VOYGR LWR, with reference data being found in the literature [79] [80]. The Carrollton facility analysis utilizes a generic high-temperature μ Rx-sized system that is assumed to be able to generate steam at 12 MPa and 520°C, with a feedwater temperature requirement at or below 135°C, as is consistent with the details available on the Oklo Aurora Powerhouse. During this stage of analysis, control of the TES system takes the form of a simple algorithm that determines what is required to match the system supply and demand under the limitation of minimum and maximum charge states.

4.1.1 Thermodynamic Model for the HTGR SMR

Figure 8 presents the thermodynamic model of the standard power conversion cycle (PCC) for the HTGR system. The power output, after accounting for a 3.9 MWe parasitic load, is 81.3 MWe, matching X-energy's advertised efficiency of 40% at the current design point of the Xe-100 reactor (203 MWth). The system is assumed to use an industrial turbine from a standardized manufacturing product line portfolio (e.g. SST-600 from Siemens Energy [81]). These turbines are well suited for CHP applications, having the ability to accommodate multiple controlled and uncontrolled extractions.

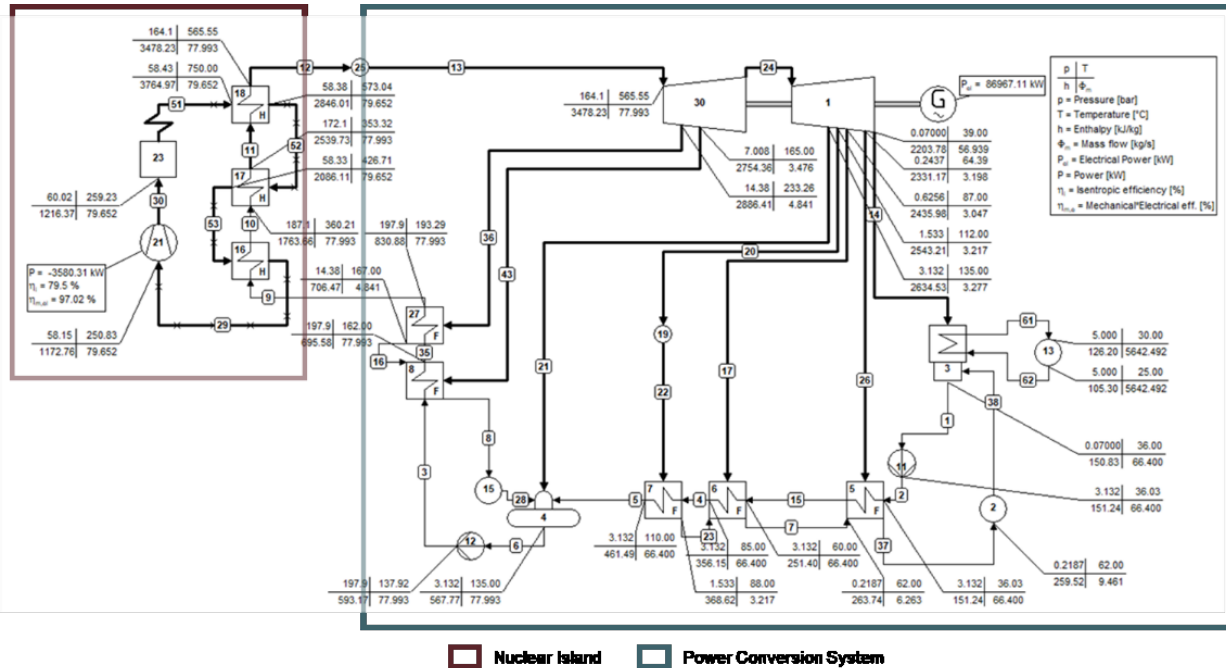


Figure 8. Energy balance model, HTGR-POWER, of the standard electrical-power-generation steam cycle for the HTGR system, which provides a net output of 81 MWe.

To account for energy loss in long-distance steam delivery, and to maintain sufficient temperature differentials across heat exchangers between the nuclear and industrial plant, an industrial heat extraction line was added to the nominal electricity configuration to extract steam at 50 bar. This added line is highlighted in red in Figure 9. This approach is optimal when the heat demand conditions are lower in pressure and temperature than the heat content in the supply steam. Heat output should be readily

regulated across a wide range of conditions, using this extraction method. The initial extraction line is limited to 85% of the nominal inlet steam flowrate to ensure that the condensing section of the turbine maintains adequate cooling of the turbine blades.

Note that the process steam temperature can reach about 360°C (excluding heat transport losses), which is about 45 K below the nominal temperature of the HP steam line. This is achieved with an already optimistic minimal temperature difference of 30 K between the power-plant-extracted superheated steam and the process steam (superheated). While the saturation temperature (i.e. pressure) is the primary parameter of the process steam for heating, were higher superheat necessary, additional superheated could be implemented. The most efficient source would be branching the main steam of the power plant before the turbine, with supplemental heat provided by electric heaters. The total combined power needed to match current superheat levels at SCO are 4% of delivered thermal power.

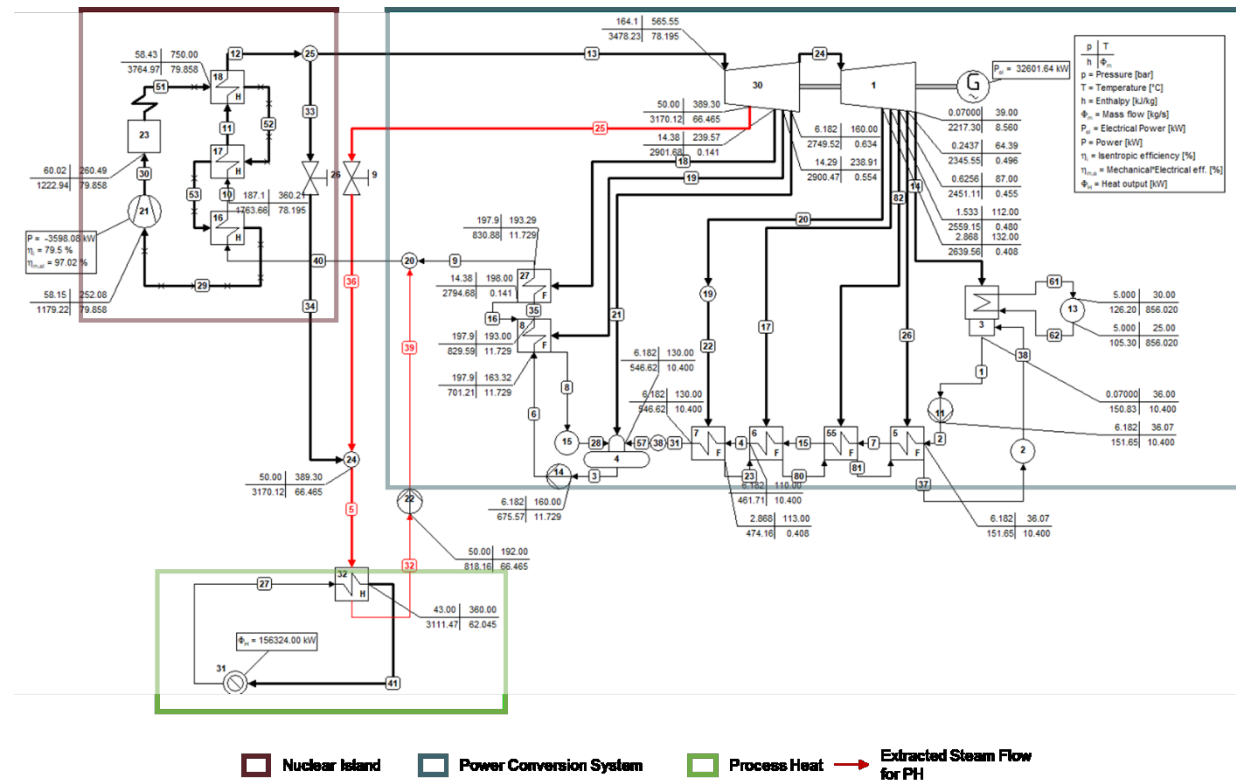


Figure 9. Energy balance model of a HTGR-CHP system with an extraction-condensing turbine.

The operating flexibility enabled by this configuration would likely be advantageous, especially in cyclical or predictably changing load scenarios. Figure 10 shows the efficiency and performance characterization of the extraction HTGR-CHP system, assuming no decrease in the condensing turbine section's performance during partial load. Thus, Figure 10 shows the theoretical maximum performance, which would be somewhat reduced during extraction. If a continuous baseload extraction is intended, a smaller turbine could be purchased to achieve maximum performance by changing the nominal configuration. e⁺

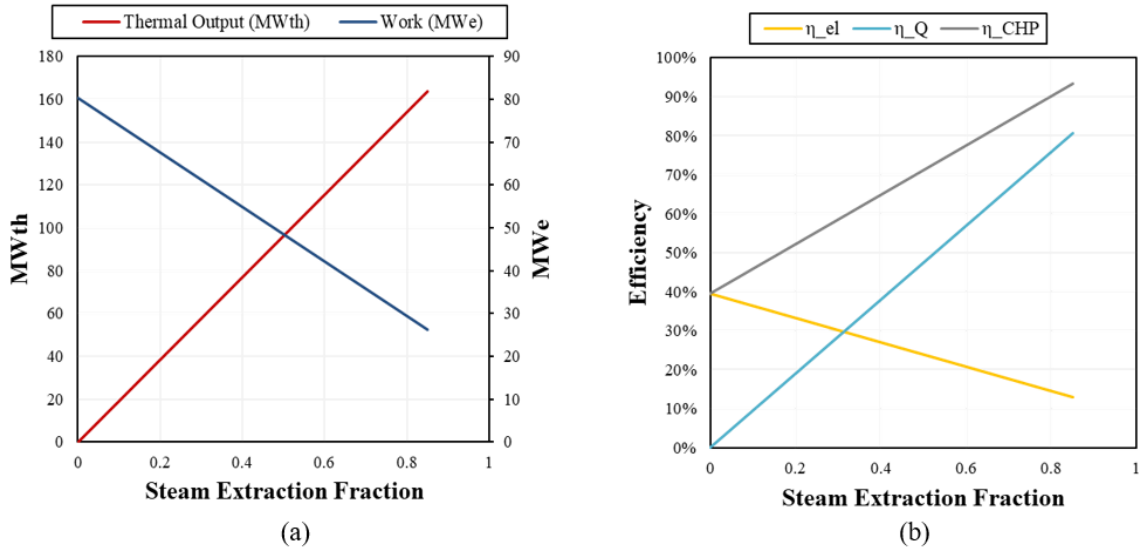


Figure 10. Output and efficiencies of an HTGR-CHP system with an extraction-condensing turbine. (a) Thermal and electric output and (b) efficiency changes, both with a varying steam extraction fraction.

For scenarios with sufficiently large baseload heat demand, a backpressure turbine may be employed. Figure 11 shows this alternative HTGR-HEAT system. While this configuration offers limited control of heat output without maneuvering reactor power, it yields exceptional CHP efficiency (around 99%) and maximizes nuclear heat utilization. Additionally, by eliminating the condensing section and auxiliary systems (e.g., deaerators, feedwater heaters, and condenser vacuum systems), the backpressure configuration significantly reduces costs as compared to a condensing turbine system.

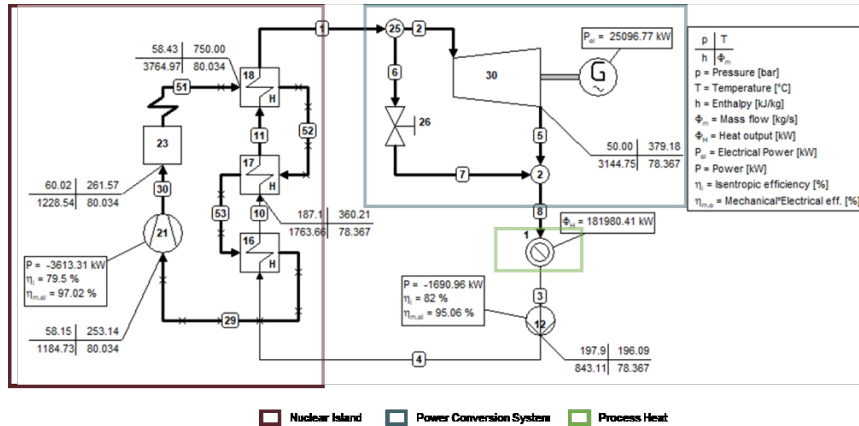


Figure 11. Energy balance model of an HTGR-HEAT system with a backpressure turbine.

Table 1 summarizes the output of all three PCC configurations for the reference HTGR system.

Table 1. Summary of PCC options afforded by the Xe-100.

Power Conversion Cycle		Work (MWe)	Electrical Efficiency (%)	Heat Production Efficiency (%)	CHP Efficiency (%)
Type	Features				
HTGR-POWER	Elec. Power Gen.	80	40.0	0	40.0
HTGR-CHP	Elec. Power Gen. + Process Heat w/ Extracted Steam	80.3 ~ 26.2	39.5 ~ 12.9	0 ~ 80.6	39.5 ~ 93.5
HTGR-HEAT	Elec. Power Gen. + Process Heat w/ Steam after Backpressure Turb.	19.8	9.7	89.6	99.9

4.1.2 Thermodynamic Model for an LWR SMR

The NuScale VOYGR system was chosen as a representative LWR SMR. Each NuScale Power Module (NPM) is designed to generate superheated steam at lower steam pressures, as opposed to traditional LWR systems that produce higher-pressure saturated steam. The nominal conditions are summarized in Table 2.

Table 2. Key NuScale VOYGR design values.

Process Parameters	Values
NPM steam outlet temperature:	283°C (541°F)
NPM feedwater inlet temperature:	120°C (248°F)
NPM steam outlet pressure	32.8 bar (475.7 psig)
Thermal/electrical output	250 MWth / 77 MWe

Based on these values, the NPM will produce steam that is below the integration requirements at SCO. Steam compression is suggested to reach the required pressure. Figure 12 shows a configuration that employs this strategy. The steam required at the industrial site is produced via turbine bypass to leverage the most energetic state in the power cycle. The steam is then transported to the industrial site, and it flows through a compressor, raising the steam temperature and pressure. Existing commercial steam compressors can produce the results shown in Figure 12 [82]. Assuming the steam use at SCO is intended primarily for heating purposes, where the pressure (saturation temperature) needs to be maintained and specific superheat has low importance, which is held in the analyses in this report, this approach should allow for straightforward integration. The compressor outlet temperature is about 100°C (160°F) below current HP steam header temperatures.

If maintaining current HP temperature is also necessary, an option would be additional electrical heating of the steam using nuclear generated electricity. Adding electrical heating results in 2.5x more power consumption than just the included compressor load.

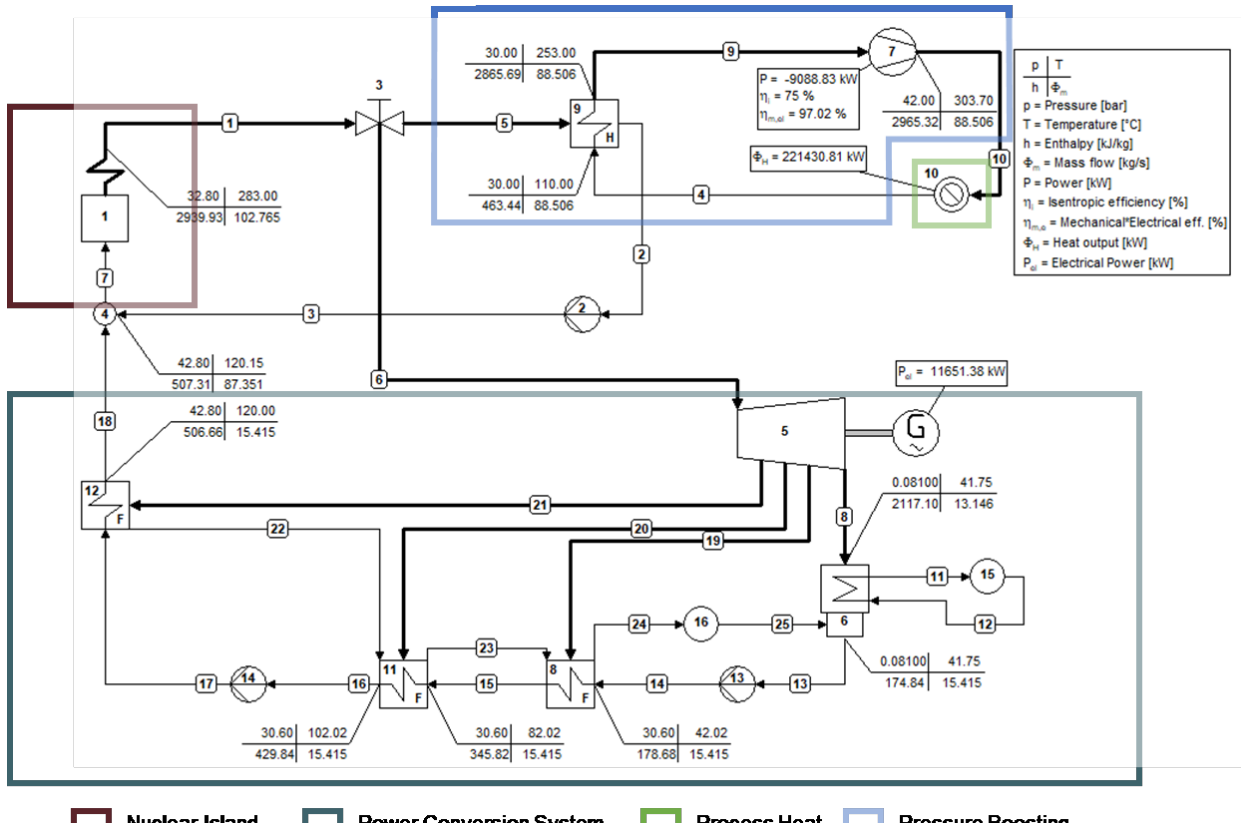


Figure 12. Extraction steam pressure boosting configuration, LWR-CHP, for the NPM. LWR-POWER is a near-identical configuration, just without the Pressure Boosting or Process Heat sections.

Within the main condensing steam turbine, a limitation must be upheld—just as with the HTGR system—in which a minimal nominal steam flow rate must be maintained for turbine operational safety. While it is nominally assumed that the turbogenerator system would be sized to accommodate full reactor power, this system could be reduced in size if a baseload thermal extraction is anticipated. Reducing equipment size may improve the economics if a primarily thermal CHP application is anticipated. Figure 13 shows a baseload heat configuration that generates steam at 30 bar (435 psia) and compresses it to 42 bar (609 psia), and in which the electricity generating system is entirely omitted. The coefficient of performance of the LWR-HEAT system, operating as a heat pump, is 24.6.

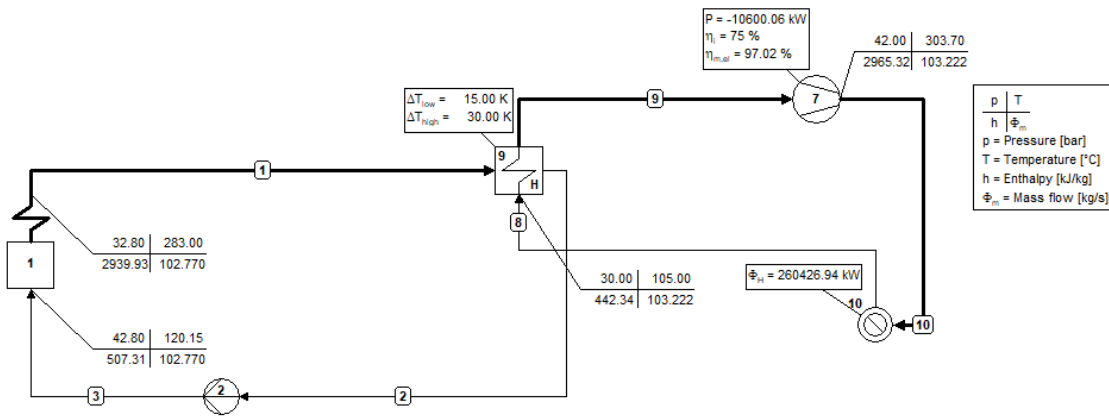


Figure 13. Energy balance model, LWR-HEAT, of heat upgrade from a NPM for baseload heat delivery.

The LWR-HEAT and LWR-CHP configurations (shown) use industrial-side condensate temperatures of 105°C and 110°C. These values are required to ensure that the steam generator inlet temperature in the NPM is maintained at 120°C, imposed by using the nominal feedwater heating configuration in the turbine, in combination with a matching return temperature from the industrial process heat exchanger. At SCO, this presents a dilemma, as the system condensate temperature is around 140°C. A few options for resolving this situation present themselves. The first is to use additional heat rejection to reduce either the industrial condensate temperature or the returning reactor condensate temperature. This option is undesirable, as it reduces efficiency yet simultaneously increases system complexity. Feedwater heater temperatures can be actively controlled, but this reduces steam extraction capabilities and increases system complexity. Ideally, an alternative use at SCO can be identified that can help cool condensate to 110°C or less.

Figure 14 shows the LWR heat delivery characteristics of the LWR-CHP and LWR-HEAT systems.

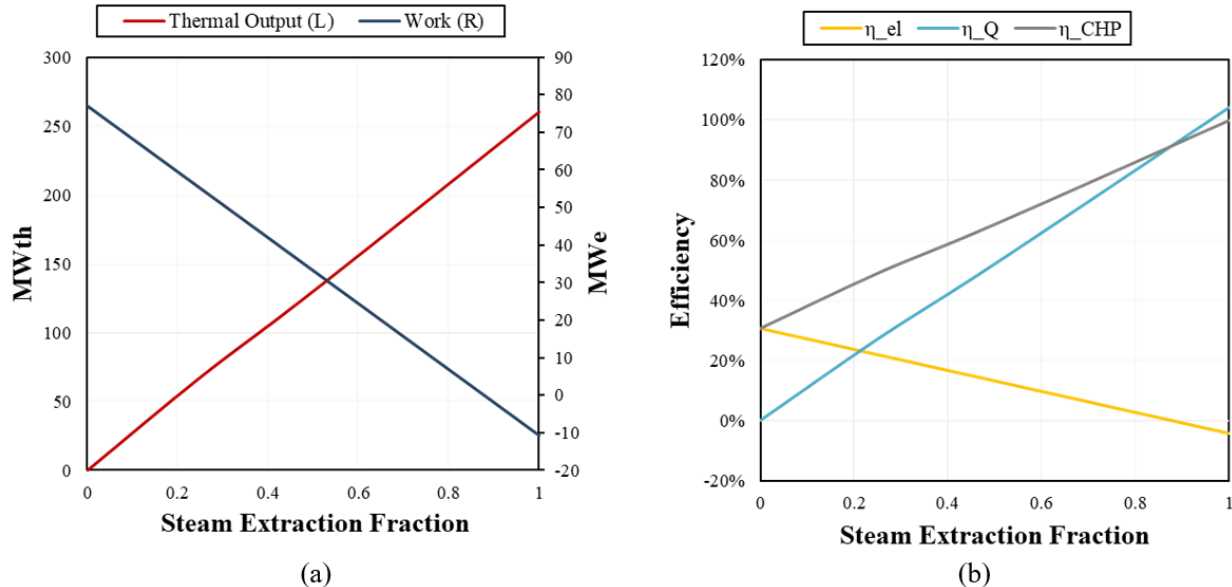


Figure 14. Characteristics of an LWR-CHP, becoming an LWR-HEAT, system with an extraction-condensing turbine and boosting power output. (a) Thermal and electric output and (b) efficiency changes, both with varying steam extraction fraction.

Table 3 summarizes the three considered configurations. The LWR-CHP maximum heat output assumes that a minimum nominal steam flow rate of 15% still passes through the turbine.

Table 3. Summary of PCC options with NPM.

Power Conversion Cycle		Work (MWe)	Electrical Efficiency (%)	Heat Production Efficiency (%)	CHP Efficiency (%)
Type	Features				
LWR-POWER	Elec. power gen.	77	30.8	0	30.8
LWR-CHP	Elec. power gen. + process heat w/ upgraded main steam	77 ~ 2.4	30.8 ~ 0.9	0 ~ 88.6	30.8 ~ 89.5
LWR-HEAT	Process heat only by upgrading all main steam	-10.6	-4.2	104.1	99.8

4.1.3 Thermodynamic Models for Microreactors

μ Rx vendors tend to advertise either Brayton or supercritical CO₂ (sCO₂) cycles for power production, implying an emphasis on standalone power production. These cycles are likely preferable for various reasons, including a smaller configuration footprint, smaller turbomachinery (though some high-speed small turbines are available for steam cycles), and the leveraging of recuperation configurations to attain relatively high efficiencies. To achieve high temperatures for industrial process heat, direct heat integration from the reactor appears to be the preferred method at this point. Consequently, CHP applications using μ Rxs will likely involve separate units for heat and power, meaning that these systems will forego the thermodynamic benefits of cogeneration. For example, Oklo employs an sCO₂ cycle in a readily available manner. Their system uses a recuperated re-compression cycle with heat rejection temperatures below 200°C. This configuration is unsuitable for industrial CHP applications with the combination of a low rejection temperature and the inability to extract high-temperature heat. Brayton cycle applications, used by Westinghouse and BWXT, face similar CHP limitations.

For industrial steam applications, particularly those between 10 and 50 bar (145 to 725 psia), the steam cycle offers desirable CHP performance. Nuclear utilization can be very high in these systems, thus generating net cost savings, even with the lower electrical efficiency seen in small Rankine units. The efficiency characteristics are shown in Section 5.2.1. The rise in efficiency is particularly evident in backpressure configurations, in which CHP efficiency approaches 100% while maintaining a compact footprint and low capital expenditures (CAPEX). Small steam turbogenerator systems are readily available commercially, including Siemen's condensing turbines, which are as small as 2 MWe with extraction and backpressure options [81]. Steam turbines for backpressure and letdown systems are even feasible starting from around 20 KWe [83] [84]. With a realized application for industrial CHP systems, μ Rx vendors may revert to a steam cycle to improve efficiencies and thus reactor economics.

The reference μ Rx was selected to have a thermal output of 30 MWth and to operate at a sufficiently high core outlet temperature (i.e., 550°C) to support a reasonably efficient Brayton cycle. A 35% nominal efficiency is assumed for configurations that leverage a Brayton or sCO₂ cycle. For a steam cycle system, a backpressure configuration is assumed due to its compact size and alignment with the heat-to-power ratio (6:1) at the Carrollton site. Figure 15 shows the thermodynamic balance of this system. Steam is produced at 12 MPa (1740 psia) and 520°C (968°F), and passes through a turbine with an isentropic efficiency of 87%. The system can produce 4.5 MWe and 25.2 MWth, for a CHP efficiency of 99%.

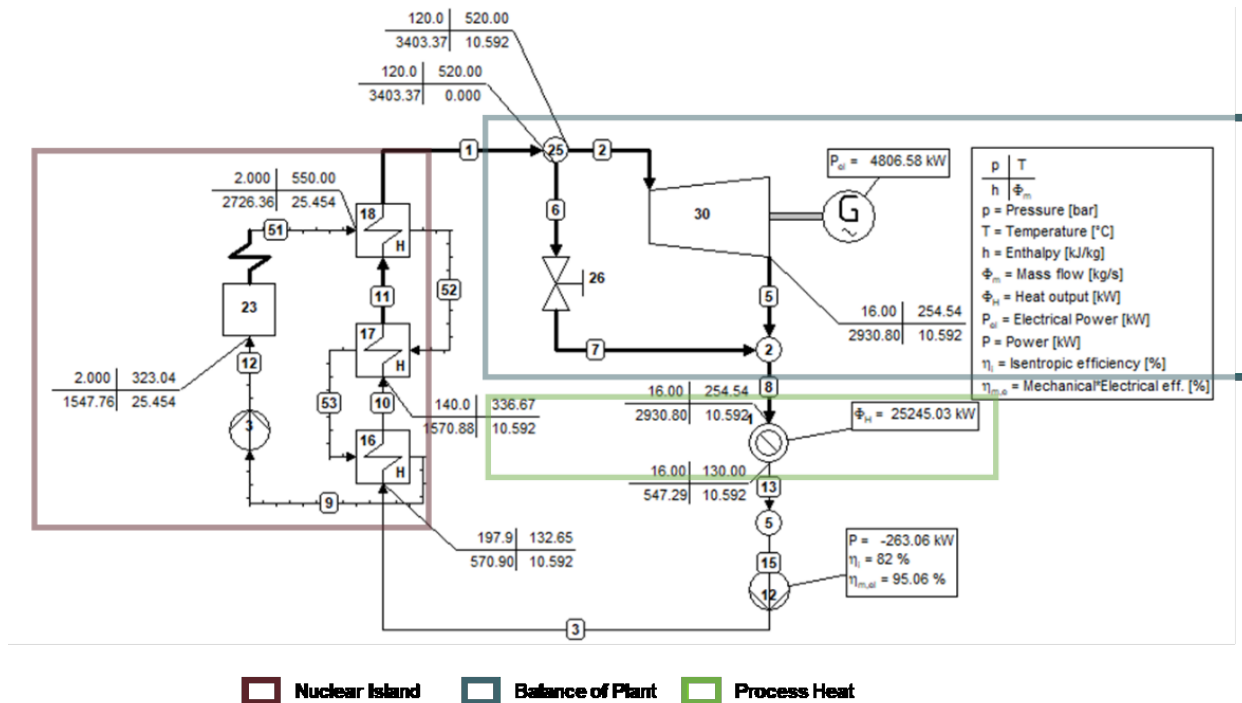


Figure 15. Energy balance model, μ Rx-CHP, of a conversion system that leverages a backpressure steam turbine CHP μ Rx applications.

Table 4 presents the PCC options for the generic μ Rx system.

Table 4. Summary of PCC options for a generic μ Rx.

Power Conversion Cycle		Work (MWe)	Electrical Efficiency (%)	Heat Production efficiency (%)	CHP Efficiency (%)
Type	Features				
μ Rx-POWER	Brayton cycle elec. power gen.	10.5	35	0	35
μ Rx-CHP	Backpressure steam turbine system	4.5	15	84	99
μ Rx-HEAT	Process heat only (neglected parasitic loads)	0	0	100	100

4.1.4 Thermal Energy Storage

TES may be an option for nuclear systems, offering flexibility and potentially even efficiency enhancements. In this study, we assume that the TES will be a molten-salt-based two-tank sensible heat storage system, as this system has already been demonstrated at industrial sizes and is known to operate in the appropriate temperature ranges. Some of the commentary on storage integration and capabilities would shift if other methods such as thermochemical energy storage or latent heat energy storage sufficiently mature for high-temperature applications.

Figure 16 summarizes three potential TES configurations explored by the IES program. The first and most efficient system, Type A (see Figure 16a), functions as the entire reactor heat sink and then dispatches heat to the turbine system at its own discretion. This configuration is currently used in the TerraPower Natrium and USNC MMR designs. Type B (see Figure 16b) is charged using steam bypassed directly off of the steam generator. This choice should involve the least amount of reconfiguring to existing vendor designs, but notable inefficiencies arise as the hot tank temperature is effectively limited by the nuclear-generated steam pressure (setting saturation temperature), and the cold tank must be hot enough to produce steam at a useful pressure for its own Rankine cycle. There are significant tradeoffs in efficiency and TES footprint. Figure 16c shows a third configuration, Type C, in which the storage is charged using reactor bypass or HP extraction and is discharged to augment heat extraction from a further downstream mid-turbine extraction point.

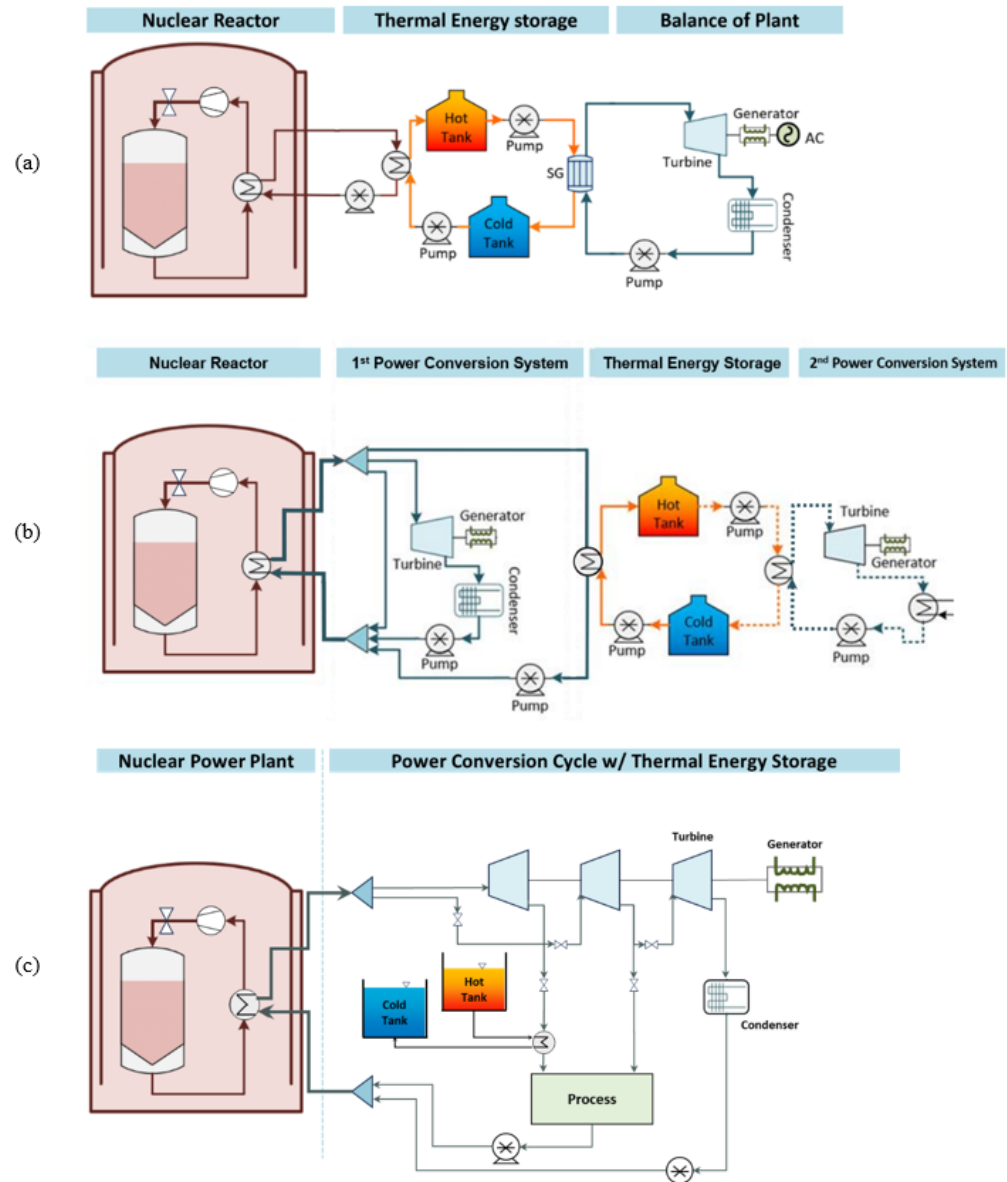


Figure 16. Various configurations for integrating TES. (a) Type A: ideal configuration of TES coupled to the nuclear reactor primary loop. (b) Type B: configuration of TES charged by main steam. (c) Type C: layout of TES integration within the heat extraction branch.

Figure 17 shows a more detailed schematic of the Type A configuration as applied to an HTGR. Due to the very high reactor core temperature delta and the desire to have a highly efficient power generation system, two separate TES systems are combined.

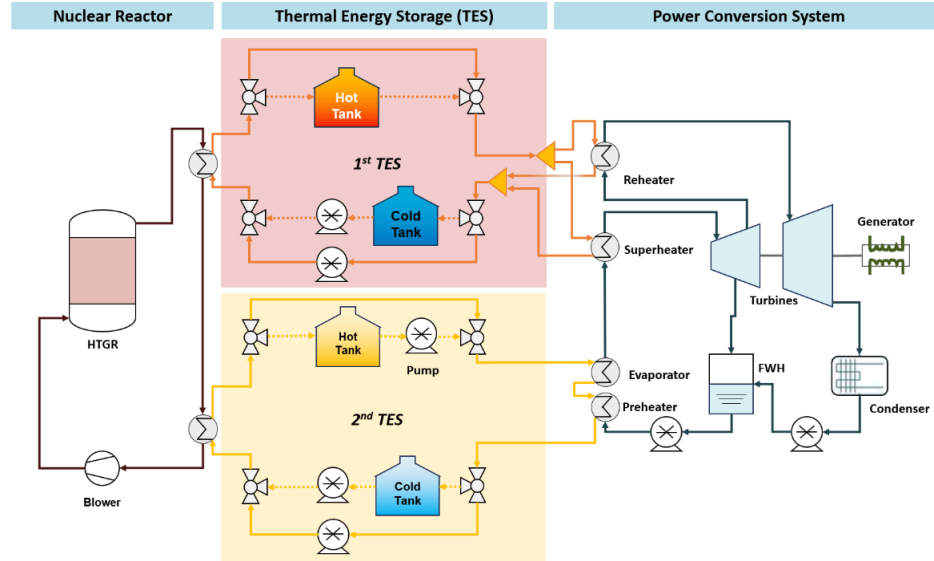


Figure 17. Process flow diagram of the proposed separated high- and low-temperature TES system for HTGR integration [85].

Figure 18 shows the thermodynamic balance of the system when set up with Xe-100 reactor parameters. This system is set up with greater flexibility in the steam cycle design, with features such as reheat cycles and enhanced efficiency. Figure 19 shows the corresponding Q-T diagrams.

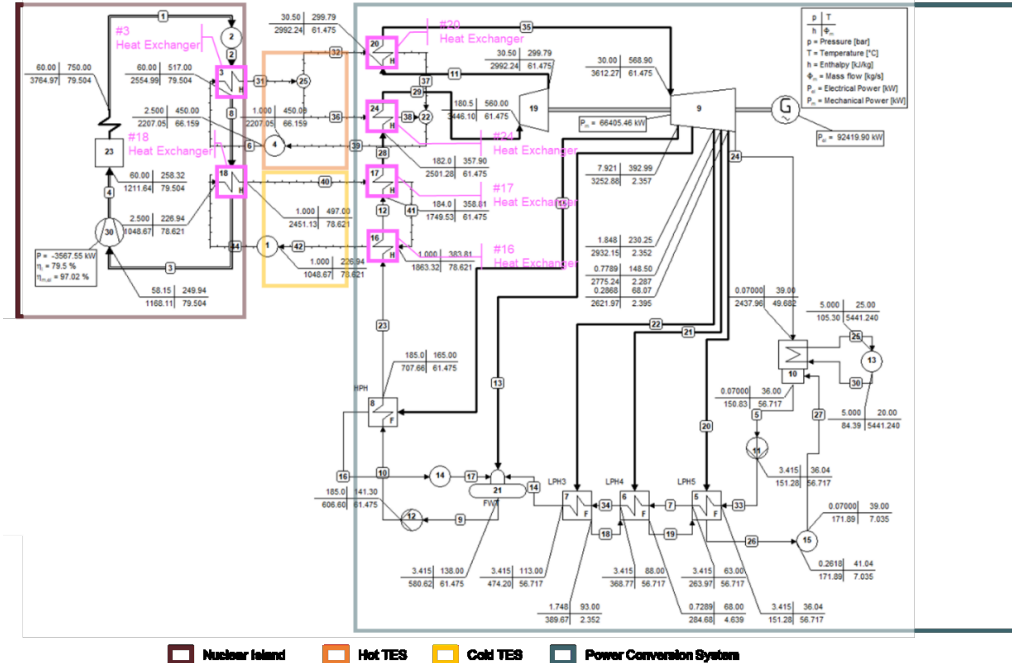


Figure 18. HTGR-CHP-TES coupling approach combining the HTGR-CHP and Type A TES configurations. Thermodynamic balance of the system is achieved using two TES systems to establish

low-and high-temperature TES.

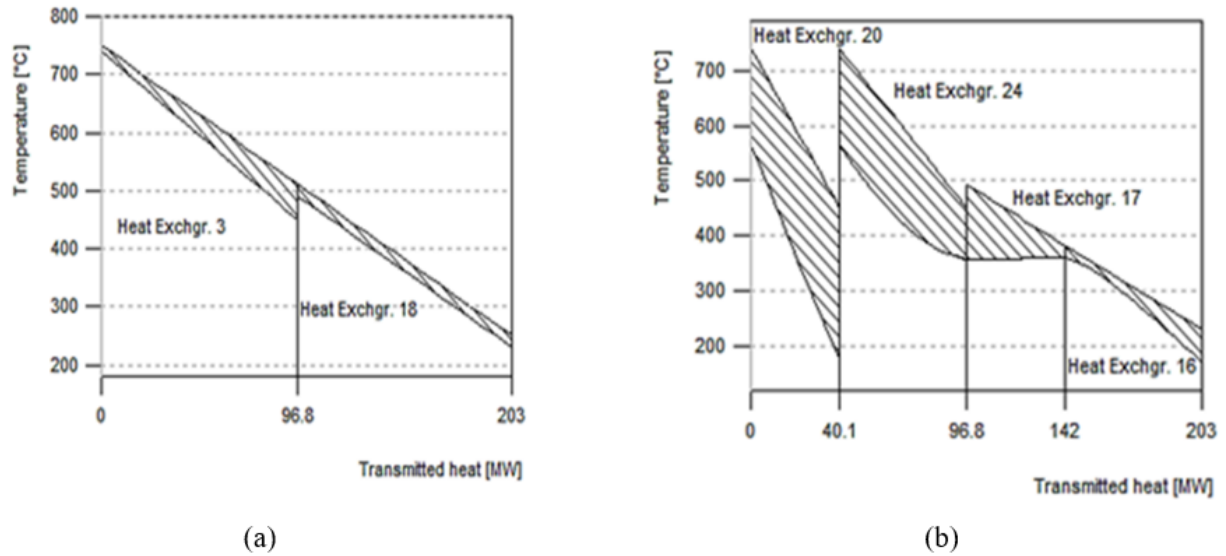


Figure 19. Q-T diagrams of TES (a) charging and (b) discharging.

The Type B approach shown in Figure 20 is similar to a CHP configuration in which the heat application is storage. The original intent of this work was load following for a nuclear system so as to capture benefits from the time dependencies of electricity grid sales prices [86].

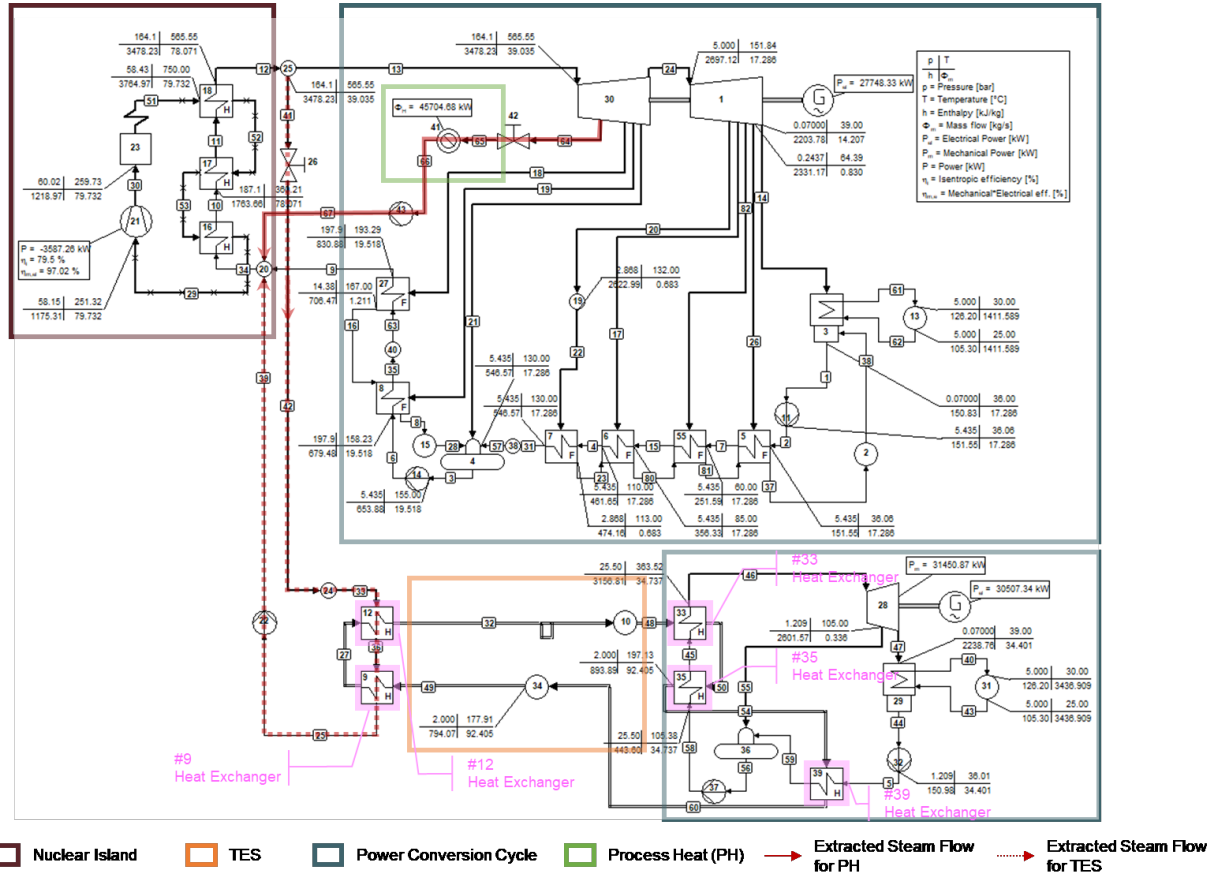


Figure 20. HTGR-CHP-TES coupling approach using HTGR-CHP and the Type B TES.

Figure 21 shows Q-T diagrams of the HTGR-CHP system with the Type B TES. Note that the pinch points in the system arise as steam hits saturation in (a) condensation and (b) boiling.

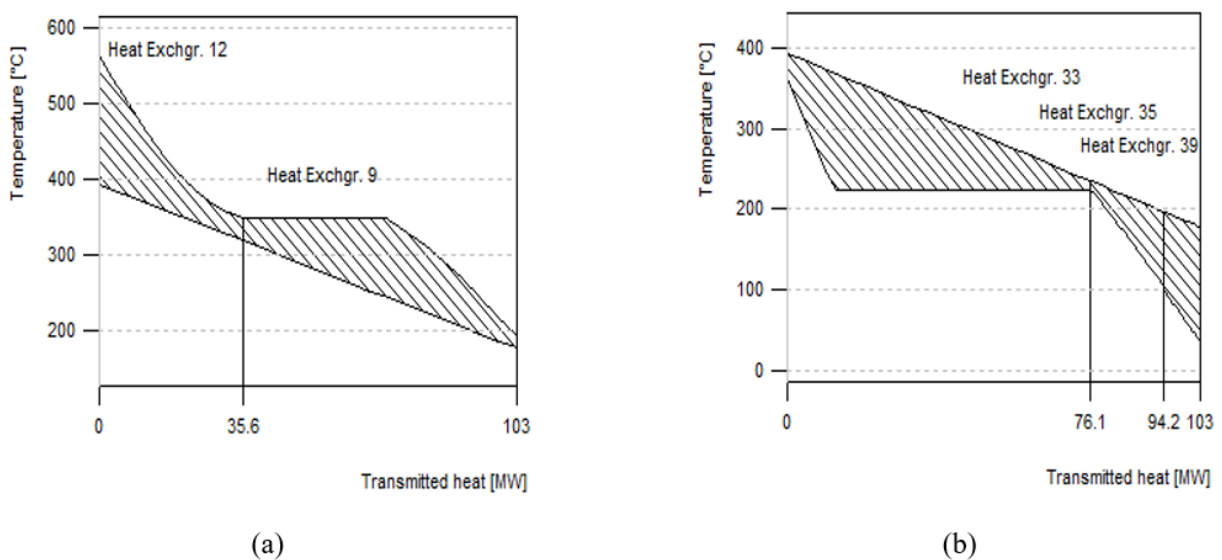


Figure 21. Q-T diagrams of TES (a) charging and (b) discharging.

In an ideal system with high optimistic values of heat exchanger efficiency, a condensate return temperature above the nominal steam generator inlet temperature, very large TES tanks, and active feedwater temperature control, a maximum steam bypass rate can be calculated and the system could reach 39% secondary cycle efficiency (equating to a 97.5% storage system efficiency). With realistic assumptions and maintaining of the condensate temperature, the secondary cycle efficiency drops to 28%, equating to 70% storage efficiency.

Figure 22 shows a thermodynamic balance diagram that integrates the HTGR-CHP configuration with a Type C TES system. The example extraction pressure leveraged is at 110 bar (1595 psia), using a controlled extraction line to allow for modulating the steam demand. The TES then augments the steam extraction occurring at a subsequent extraction point within the turbine system. Due to the small temperature difference between the hot and cold tanks, this system would require large-sized tanks. This system is not deemed advantageous over Type A or Type B storage configurations. It is a configuration in which phase change material TES may offer sufficient performance, but the technology remains at too low a technology readiness level.

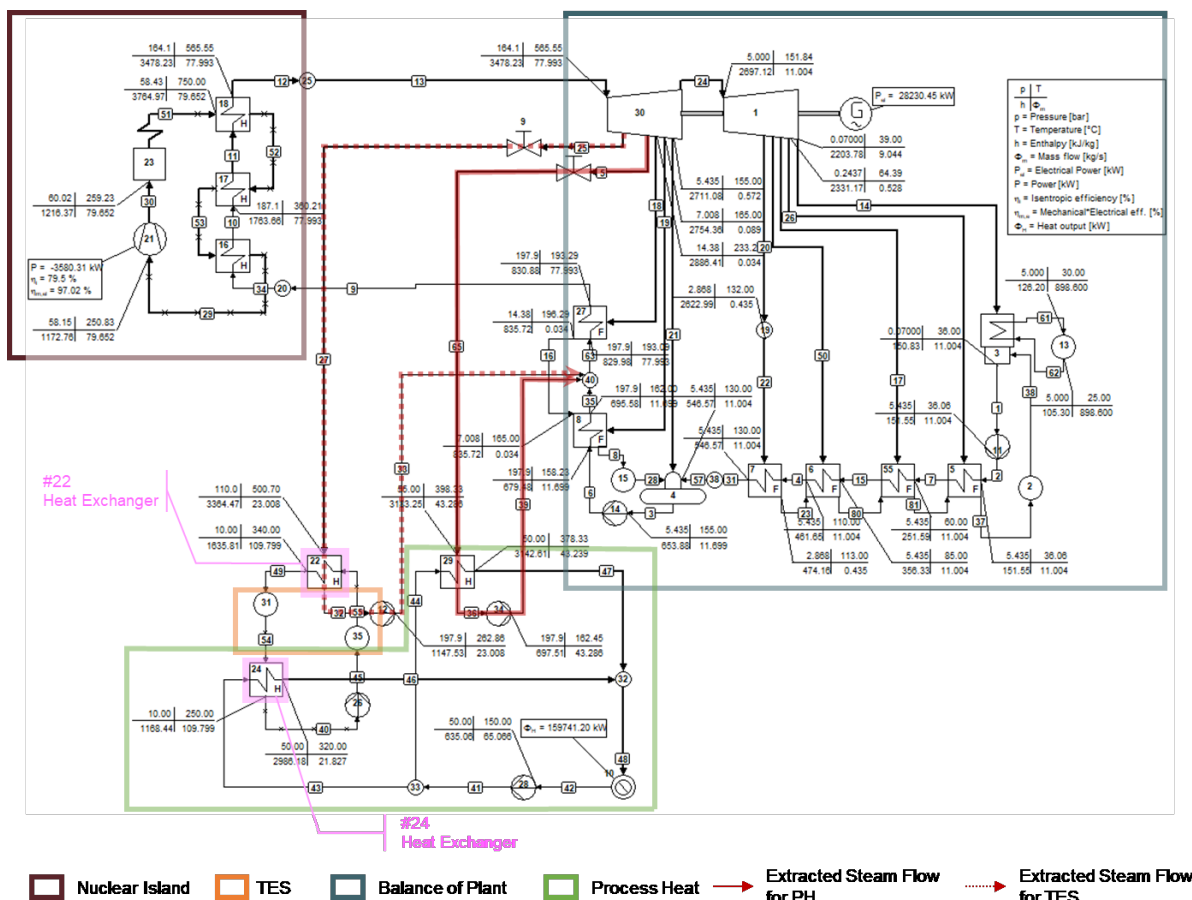


Figure 22. HTGR-CHP coupling approach integrating Type C TES.

Figure 23 shows Q-T diagrams of the HTGR-CHP system coupled with the Type C TES.

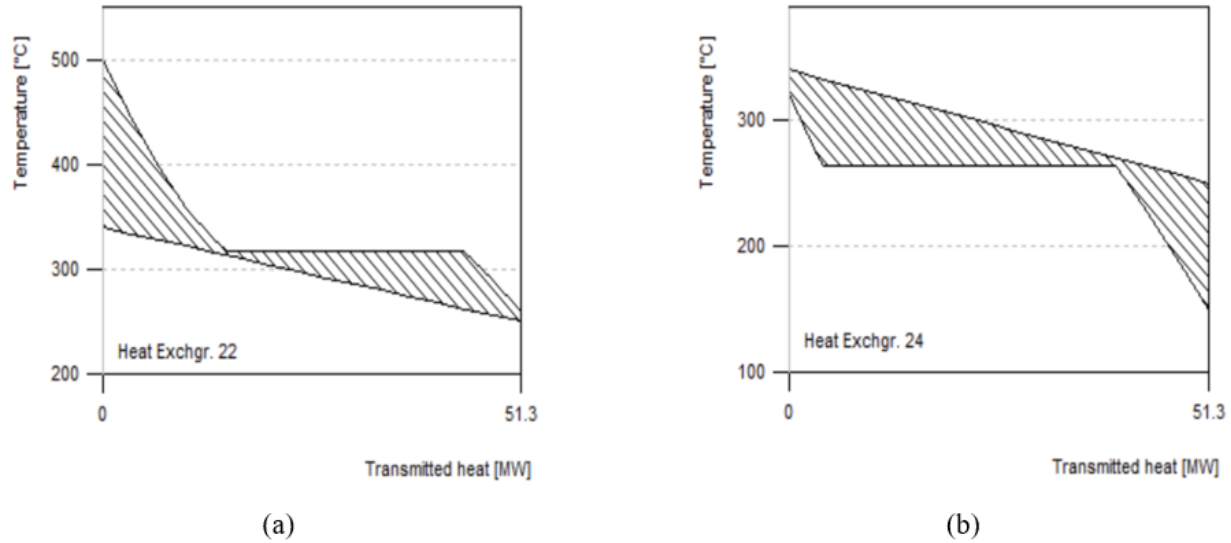


Figure 23. Q-T diagrams of TES (a) charging and (b) discharging.

4.1.5 Thermal Transport Considerations

Figure 24 shows component-level and Q-T diagram of a possible heat transfer station configuration between nuclear and process heat, using the HTGR case. It is recommended that the heat transfer station be collocated with the nuclear plant, bringing cold condensate to the nuclear plant and returning generated steam. This configuration should minimize heat losses and reduce the number of auxiliary systems handling pressurized high-temperature water. In this configuration, condensate from the industrial plant passes through a deaerator before being pumped to the HP steam pressure. This water is preheated by condensate returning to the nuclear steam generator, is evaporated in a drum boiler, and superheated by incoming extracted NPP steam. This steam is then transported across the separation distance for introduction into the HP steam header. If the industrial process condensate is entering the system at a sufficiently cold temperature, an additional heat exchanger leveraging nuclear heat upstream of the deaerator could be introduced.

The LWR case would introduce a compressor just before the integration into the HP header. A small electrical heater may be required to ensure that the compressor only suctions pure steam.

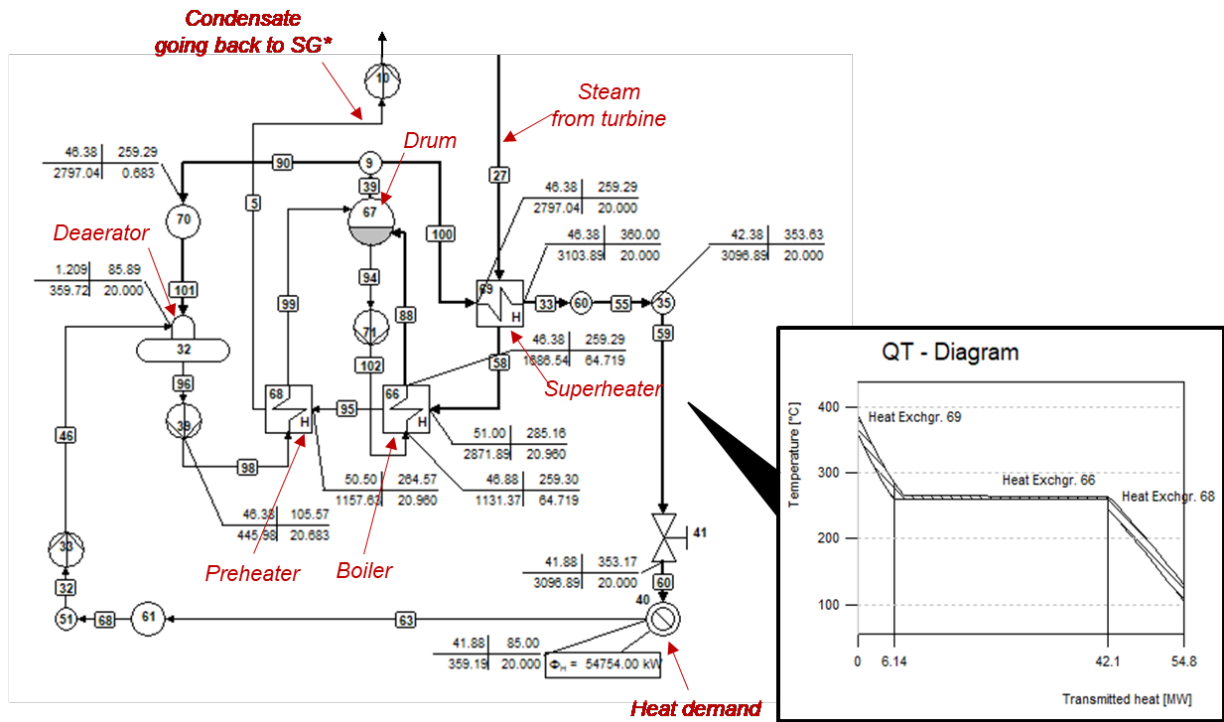


Figure 24. Proposed configuration of the heat transfer station (process steam generation node) interfacing extracted nuclear plant steam and process steam going to the site.

4.2 Synthetic Data Generation

The IES program at INL uses auto-regressive moving average (ARMA) to generate synthetic data for economic optimization studies. Using synthetic data enables more statistically complete system evaluations and avoids the so-called “golden year problem” in which highly impactful but very infrequent events can drive the value proposition of a system. ARMA is a statistical analysis method that generates the characteristics of a dynamic data set and enables the generation of synthetic, and thus different but statistically identical, dynamic data sets [87]. Assuming that the original data set follows a Gaussian distribution about some average, the ARMA method generates statistically equivalent synthetic data sets. If there are non-Gaussian trends in the data, the data must be preprocessed to de-trend them to a Gaussian distribution (e.g., a seasonal reliance on temperature). A key feature in this application is that the original data set cannot be reproduced from the synthetic data set or from the ARMA model itself, thus ensuring the privacy of the original data.

The ARMA algorithm consists of two main generating functions derived from an original data set.

The first is an auto-regressive model of the system:

Here, the value of the synthetic data at time t is a linear function of the previous p values of the synthetic data plus an error term ϵ . The coefficients of the function, the ϕ , are derived from the original data set, as is the distribution from which the error term is drawn.

The second generating function is a moving average model:

The synthetic data values are a linear combination of the previous q error terms, with the θ again being derived from the original data set.

Combining these two terms, synthetic data are generated by the full ARMA model:

Any engineering or economic optimizations completed in this work are deemed equivalent to an analysis performed on the original data. Two ARMA samples are plotted against each other in Figure 25.

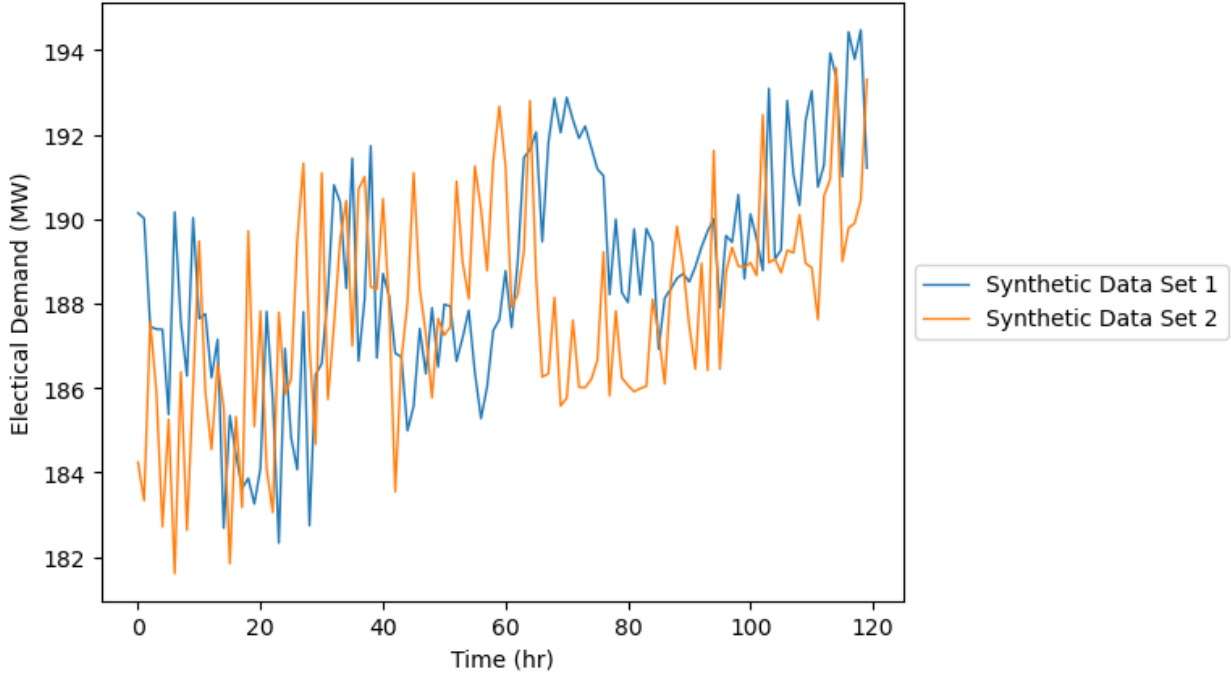


Figure 25. Two ARMA samples compared for a single 5-day cluster. Note that the trends are nearly identical but the specific demand paths are unique.

4.3 Holistic Energy Resource Optimization Network

HERON is a resource capacity optimization tool that was developed at INL to determine the statistically optimal sizing and balance approach for various resources within integrated energy networks. The code was constructed as a plug-in to the Risk Analysis Virtual Environment, using its underlying methods and capabilities to run a bi-level leader-follower optimization that optimizes unit sizing based on a probabilistic dispatch optimization.

The “outer” leader optimization seeks the optimal combination of resource-generating capacities such that an objective function, nominally net present value (NPV), is maximized for a given system. More precisely, the statistical behavior (e.g., expected value) of NPV is maximized. This can reflect minimizing costs or maximizing profits. HERON employs an automated stepping parameter sweep in which the code takes automated steps to navigate across different combinations of installed unit capacities (or “portfolios”), accepting portfolios when the economic objective function is improved and redirecting steps in new directions when the objective function value is worsened. Eventually, as no improvement steps are found, HERON converges to an optimal generation portfolio.

Within the “inner” follower run of HERON, the selected set of unit capacities are pinned and dispatched to meet imposed system requirements in a manner that maximizes the system value. The potential dispatch scenarios (electricity, heat) are repeatedly sampled from ARMA models and run to obtain statistically significant values measured against multiple possible futures. An amalgamation of many independent dispatch scenarios calculates the statistical value of the pinned capacity set, which is

reported back to the “outer” loop of HERON for use as a metric for the expected economic efficacy of that portfolio.

To optimize the dispatch, each unit in the system is represented algebraically in an optimization language. The dispatches of the units at each time step (nominally hourly) are optimization variables, while technical limitations (e.g., minimum/maximum operation and ramping limitations) are implemented as constraints. The economic impacts of variable operation and maintenance costs, fuel costs, production tax incentives, commodity sales, and other hourly costs and revenues are aggregated to provide the objective function to be optimized. For commodity storage such as electric batteries, TES, etc., the constraints also include minimum and maximum commodity levels, charge and discharge rates, round-trip efficiencies, and initial/final commodity levels for the optimization window. The optimization language is written using the Pyomo library in Python, then solved using one of several optimizers (e.g., ipopt or coincbc).

Prior to this analysis, for a given optimization window (e.g., 24 continuous hours), a user-defined initial storage level was defined, and the remainder of the optimization window could use that storage in any optimal manner. This means, for example, that the optimizer could start with the storage full and end with it empty, effectively harvesting “free energy.” To help mitigate this, and as part of this activity, a periodic boundary condition for storage components was implemented. This enables the initial commodity storage level to be optimized by the dispatch optimization algorithm, but requires that the storage end at the same level at which it started. While this requires a sufficiently long optimization window to ensure suitable storage performance, it also enhances the ability to ensure conservation of commodities.

As the SCO system is more complex—with multiple steam headers in addition to the electricity load—the HERON setup for the SCO system will now be presented. Figure 26 shows the initial HERON resource map. It is an automatically generated image produced by HERON during a simulation execution. It is very dense, as the system is set up to be able to flexibly set the sizes of the HTGR, SFR, and LWR systems and respective storage systems, with flexible paths to generate HP, IP, and LP steam to meet thermal demands, as well as the paths to generate electricity (or consume it via a compressor). Figure 27, Figure 28, and Figure 29 give clearer visual representations of the energy map. The only non-dispatchable components are the reactors themselves, which are assumed to always operate at full power. The system demands that must be met are defined at the “HP,” “IP,” “LP,” and “e” nodes for the different heat and electricity loads.

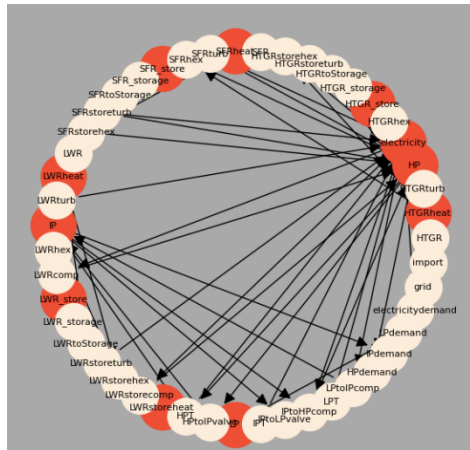


Figure 26. HERON initial resource map at the beginning of the optimization activities.

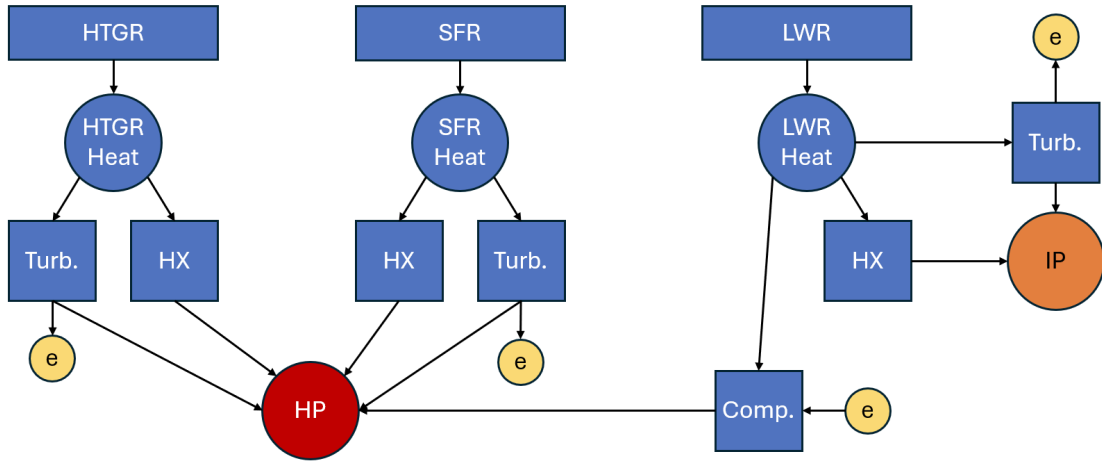


Figure 27. HERON block diagram of heat generation.

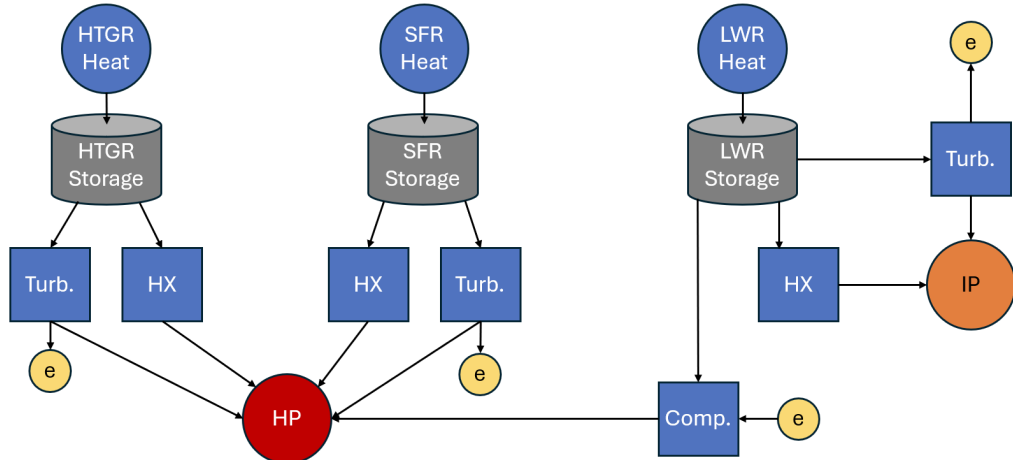


Figure 28. HERON block diagram of heat storage.

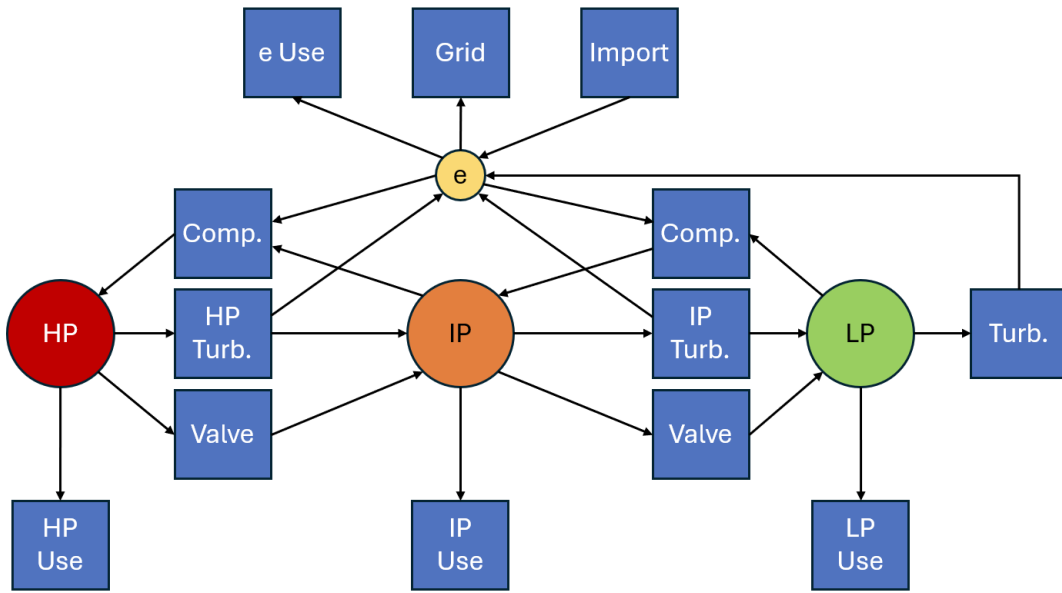


Figure 29. HERON block diagram of heat utilization.

4.3.1 Transfer Functions

HERON defines energy networks in which resources are exchanged between capacity nodes. The rates at which the resources are exchanged are defined by transfer functions. Prior to this study, only linear relationships between commodities consumed and commodities produced were used within HERON to define how, for example, thermal energy is converted to electrical energy. However, in this analysis some of the turbines within CHP units were poorly represented by linear transfer functions; hence, a new quadratic expression for transfer functions was implemented and leveraged to improve the accuracy of the optimization of the heat and power dispatch. The following are example linear transfer functions (the full set of transfer functions are included in the results presented in Section 5.3).

Equation 4 describes how a unit of energy from HTGR heat passed through the backpressure turbine PCC system generates 0.1836 units of electricity and 0.316 units of system steam. (Equation 4 is for Carrollton, which has only one steam resource.) Equation 5 describes the amount of electricity generated when using a backpressure turbine between the HP and LP system lines at SCO. Units are not assigned and must be carefully tracked through the transfer functions.

4.3.2 Cost Information

HERON uses NPV calculations to evaluate the overall system performance of a dispatched energy network. This means that value gained and costs expended must be accounted for. Steam demands must be met in the HERON runs by nuclear energy sources, as there are no other sources of heat in the system. This is true for both the SCO and Carrollton cases. A value of \$500/(kg/s) for all kinds of steam resources is put in as a dummy value to motivate the HERON solver to identify solutions (any positive value would work here, but larger values enable the analysis to be more readily understood by readers). Electricity demand can be met by three sources: nuclear generation at a value of \$1,000/MWh, grid import at a price of -\$1,000/MWh for 10 MWh, and any additional grid import at -\$5,000/MWh, as needed. Selling electricity to the grid is worth a small positive amount: \$5/MWh. These values are chosen to incentivize the optimization model to meet the electricity demand without motivating the solver to just sell electricity. Overall, the combined sales of steam and electricity represent the total net income portion of the NPV. A key realization here is that the absolute values are not drivers of the solution set that HERON generates. This becomes more important as the discussion centers on the cost values, with the relative costs between reactor type costs being more important than the absolute costs.

HERON takes cost values for CAPEX and operational expenditures (OPEX) into account in evaluating the cost portion of an NPV calculation. As no SMRs or μ Rxs have actually been constructed, cost estimates are necessary to make comparisons. Unfortunately, cost estimates from nuclear vendors have proven inaccurate in the early stages of system design and development, with costs rising as more details are added to the designs. Further complicating this venture is the fact that some vendors consider their cost estimates to be a trade secret and are unwilling to make public statements regarding costs. The IES team leveraged a comparative literature assessment to fairly compare the costs of different reactors [88]. This report compiled reactor costs for different categories of reactors and estimated the contributions of various aspects of these systems (e.g. reactor equipment, energy conversion system, electrical equipment, heat rejection system, and indirect costs) to the overall installed-system CAPEX.

A similar analysis was performed for OPEX costs on a reactor-type basis.

Using the input, multiple values are available for use in HERON. Nuclear CAPEX costs are nominally reported in \$/kWe values, which were converted to \$/kWth using 33%, 40%, and 34.5% conversion efficiencies for the LWR, HTGR, and SFR systems, respectively. Using the values for the energy conversion system, a reduced thermal-only reactor CAPEX was determined based on this discount.

The report divided OPEX costs into two categories: staff costs and fuel costs. Due to the more highly enriched and specialized fuel used in HTGR and SFR systems, the fraction of OPEX that is fuel significantly exceeds that for LWR systems. For OPEX, a value of \$25/MWh was used for LWRs. HTGR and SFR OPEX costs were scaled based on the \$25/MWh cost for LWRs, along with the increased portion of costs that are fuel-relative to LWR systems.

Table 5. Nuclear CAPEX and OPEX costs input to the HERON simulations.

	LWR	HTGR	SFR
CAPEX (\$/kWe)	4958	6814	3916
CAPEX (\$/kWth)	1636	2726	1351
CAPEX – Thermal only (\$/kWth)	1493	2477	1299
OPEX (\$/MWh-e)	25	43.1	41.3

TES costs were taken from a second Systems Analysis and Integration report [89].

The HERON simulations in this work only simulated 3-year time windows to reduce computation times. TES systems have 30-year operating lifetimes, and advanced reactor systems are likely to have 60-

year lifetimes or longer. Thus, to obtain an accurate delta NPV between systems, lifetime costs were annualized within the actual HERON input.

Equation 6 was used to modify the capital costs, using an 8% discount rate:

where

- C = capital cost of the system
- = discount rate
- = system lifetime
- = HERON project runtime.

4.4 Siting and Safety Calculations

In the United States, the licensing process for nuclear reactors that are thermally coupled in an IES remains very unclear. Only small demonstrations of relatively minute steam extraction are underway with existing LWRs. No domestic examples of significant heat extraction or fully non-electric applications exist. A significant anticipated hurdle to IES licensing is the process of verifying the independence of tightly integrated nuclear systems. Essentially, can the nuclear system provide heat without being additionally endangered by the integration configuration when, by nature of the integration, the full system is no longer under direct control of the nuclear plant? There are multiple avenues for evaluating the risks and impacts of IES operation, and INL has been leading work to evaluate those risks.

The present research only investigated the introduction of energy from advanced reactors into Dow facilities—which may offer certain advantages. First, advanced reactors are, by definition, safer than traditional nuclear power plants (NPPs), as among other things, they offer walk-away safety during accident conditions. This means advanced reactor designs are more robustly designed to handle a wider range of adverse conditions. Second, there has been a recent push to investigate the creation of a regulatory divide between the nuclear system and the heat application systems [90]. Successful adoption of this regulatory divide would reduce regulatory oversight of the precise BOP configuration, so long as the primary nuclear system remained unchanged and it could be documented that it operated within its design envelope [91]. This would lead to fewer structures requiring advanced protection measures from external hazards, as well as fewer components needing nuclear-quality construction.

Having an industrial facility near a nuclear reactor introduces a range of risks that must be factored into the site selection process. 10 CFR 100.21(e) classifies these criteria under “nearby hazardous land uses.” RG 4.7 expands on these criteria encompassing “industrial, military, and transportation facilities,” stressing the importance of evaluating these facilities and establishing site parameters to mitigate potential hazards and ensure they do not pose excessive risks to the intended facility type [92]. Potential local hazards relevant to a nuclear reactor include vibratory, geotechnical, flooding, and fire hazards, as well as hazards stemming from transportation routes [93]. Each of those kinds of hazards must be evaluated for likely frequency, and their impact on the nuclear plant evaluated.

Nuclear safety analysis, including probabilistic risk assessment, would be necessary for all nuclear and industrial systems in terms of potential hazards such as missiles, security threats, flooding, or any other impacts that could obstruct systems, structures, and components in performing a nuclear safety function. As an initial examination of siting requirements for selected advanced reactors (e.g., Xe-100 by X-energy and VOYGR by NuScale), this report concentrates on vibratory hazards resulting from explosions in the adjacent industrial processes, and will analyze the required separation distance between the boundaries of a nuclear reactor and a target industrial facility—such that the anticipated worst-case scenario does not impact the nuclear system.

Figure 30 shows potential damage stemming from explosion-produced vibratory hazards. Note that refueling water storage tanks, condensate storage tanks, auxiliary feedwater heater tanks, emergency feedwater tanks, service water intakes, and switchyards are all critical external structures in conventional NPPs, and would be impacted by >0.07 bar over-pressurization [94].

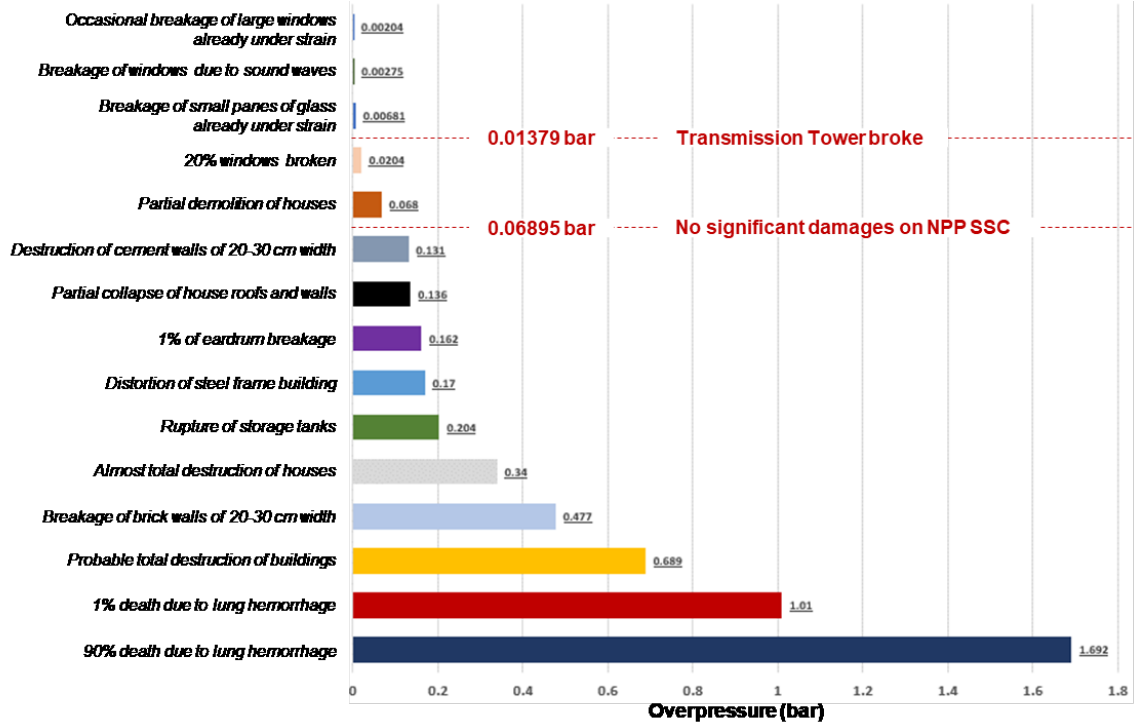


Figure 30. Vibratory hazards resulting from explosions, with different levels of damage caused by different over-pressurization levels [95].

The switchyard is the focus of externally located components, as most of the other safety-critical elements external to a RPV are encased in concrete or steel buildings. Figure 31 shows the total fragility of the switchyard components, with the transmission tower proving the most fragile. The probability of damaging a transmission tower drops to zero at approximately 0.01103 bar [96].

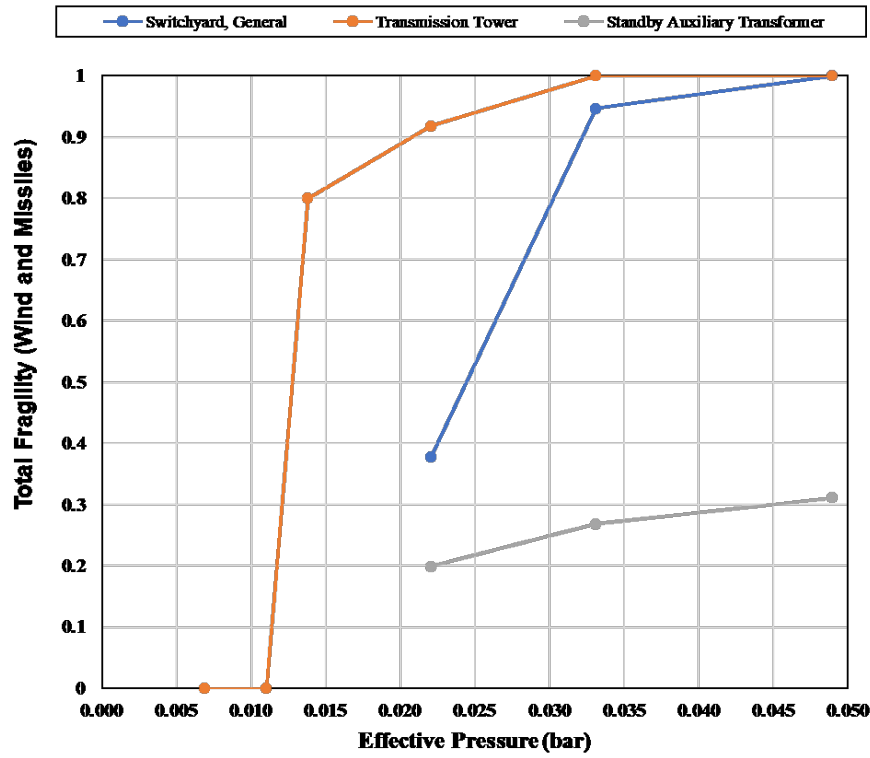


Figure 31. Switchyard component fragility to over-pressurization stemming from vibratory hazards [97].

Additional siting and safety calculations for advanced reactors are executed in this work, largely to inform the thermodynamics of the system. Nominally, a 500 m minimum separation distance was in the initial calculations. We calculated specific relevant values pertaining to the potential interactive risk of the Dow sites, based on the maximum concussive and toxic potential of their chemical loads. Based on these values, the nuclear reactor site is assumed to be placed outside the potential impact zone such that a probabilistic risk is 0, as the maximum impact has no operating impact. Thus, the siting separation must become the greater of the required nuclear regulatory siting separation requirements and the potential external impact radius from incidents initiating at Dow facilities.

The outcomes of the safety and siting calculations map out possible locations where nuclear reactors can be sited near Dow facilities. These mappings, in addition to other considerations in the area (e.g., land ownership, flooding, seismic, transportation patterns, population centers, utility situation, and concussive potential) inform possible locations that Dow can choose to pursue for reactor installation, and they also inform thermodynamic analysis regarding the length of the thermal delivery system.

The work presented in this report assumes that the regulatory definition of the nuclear island is restricted to essentially just those areas that physically interface with the primary reactor coolant, and that PCC systems are open to adjustment without licensing impact. Additionally, we assume that all SMRs and μ Rxs considered have utilized this capability to separate the power conversion system from the licensed primary reactor system. In our thermodynamic calculations, the following assumptions are made: (1) feedwater temperature, (2) steam temperature, and (3) steam pressure are safety-related parameters, based on the notion that the “nuclear islanding” framework exists at the heat rejection side of the steam generator because, combined, they influence the heat balance across the primary heat exchanger. These are crucial for maintaining nominal reactor conditions, as the thermal balance determines the temperature difference (ΔT) across the nuclear core, as well as the system temperatures for various key components such as pumps or compressors. Nuclear power within the core is generally regulated based on primary coolant conditions. Thus, if the conditions on the secondary side can be maintained to ensure that the coolant temperatures remain at nominal levels, it can be assumed that the nuclear reactor will operate nominally—and thus safely as well. It is important to note there is no claim of nuclear safety modeling or analysis having been done in this work. However, it is assumed that maintaining the nominal operating conditions of a given reactor design relies on the safety analysis conducted by reactor vendors, thereby ensuring safe operation.

4.5 Thermal and Electrical Reliability

By 2050, Dow intends to be carbon neutral (Scopes 1, 2, and 3 plus product benefits basis) while continuing to produce high-quality, high-value products that require on-demand thermal and electrical energy. Dow typically employs a “N-2” thermal reliability method and an “N-1” electrical reliability method, with the electrical grid creating “N-2”, at large chemical facilities with onsite electricity generation. By design, two thermal generators and one electrical generator can become unavailable without forcing operational curtailment. Nominally, heat- and electricity-generating assets at Dow sites have been, relative to nuclear systems, low-capital and high-operating-cost systems. Such assets are well positioned as reliable backups, as they incur most of their costs during operation. By contrast, nuclear assets incur most of their costs prior to activation, and economically are best positioned to be operated at maximum power as much as possible to generate revenue and cover the installation CAPEX.

How to approach reliability with nuclear reactors remains uncertain. While unanticipated nuclear outages are uncommon, they do happen. The current operating fleet of LWRs in the United States has a theoretical capacity factor of 93.6% (assuming an average 35-day fueling outage and an 18-month refueling cycle) or 95.0% (assuming a 35-day fueling outage and a 24-month refueling cycle), and it operates with a realized capacity factor of over 90% [98]. This operating capacity factor indicates that well-established nuclear systems can still experience infrequent unanticipated or elongated outages. It is assumed across all engineering projects that the initial operation of complex systems will be more intermittent than typical lifetime operation, introducing additional reliability risks in the early adoption of IES configurations. This will be especially true for relatively untested systems, and this may still be the case by the time that Dow is implementing the solutions proposed in this report.

A few arguments and thoughts must thus be presented to provide a sensible solution, both from a net-zero and an economic standpoint.

First, the solutions proposed in this work allow for CHP solutions from the nuclear system, meaning that thermal and electrical system reliability are interdependent. Do the N-2 and N-1 reliability requirements need to be separately dispatchable? Can the fact that a thermal generation asset can become an electricity generation asset mean that it can serve as both thermal and electrical backup? Either way, this work supplies motivation for nuclear reactor vendors to develop protocols for networking collocated module BOPs such that the system can flexibly assign reactor heat to different BOP configurations, even if the typical core connection is offline due to an unexpected outage or refueling event.

Second, Dow is unlikely to be the actual operator of the nuclear generation assets. Thus, the specifics of how energy is delivered to Dow are uncertain within the context of this analysis, and will need to be

defined via discussions with the local utilities, who are likely either nuclear operators or have peers who are nuclear operators. As such, within the construction, financing, and contracting stages of introducing dedicated nuclear energy, it may suffice for Dow and a local utility to establish a framework by which thermal reliability is well ensured and the electricity consumption at the Dow facility leverages carbon accounting methods within the grid. In this case, N-2 thermal reliability will still need to be installed to account for a refueling outage and an unanticipated outage, but the local utility will entirely guarantee the electricity load requirements.

Third, there are multiple paths to net-zero, including ones in which emitting assets are maintained by being offset via onsite negative emission technologies, carbon credits, and/or negative emissions from different sourcing of materials. While it is more environmentally appealing to never emit than to have to remove emissions, the option should not be taken off the table. Low-capital systems (boilers and other low-carbon steam generators) that can be activated on rare occasions when necessary may be more appealing, even when considering the added infrastructure entailed by needing to remove carbon emissions at a later point.

Overall, this report investigates the systems required to sufficiently cover the demands at SCO and Carrollton. Reliability entrenchment should be analyzed using a diverse set of possible solutions, including the maintaining of emitting assets.

5. RESULTS

This section details the results of the preliminary demand-fitting analysis, system capacities, and siting. Sections 5.1 and 5.2 analyze a single-year dispatch using an assumed reactor configuration. Section 5.3 analyzes the statistical optimal configuration based on the HERON output. Section 5.4 shows carbon emissions reductions at SCO and the Carrollton facility resulting from nuclear power introduction. Section 5.5 shows a hazards analysis at SCO that reduce potential nuclear sites in the immediate vicinity.

5.1 Preliminary Energy Balance Investigation – SCO

A general integration layout is given in Figure 32, with an arrow pointing out the location of nuclear-sourced steam injection into the HP steam header. The active configuration at SCO includes IP steam injection from the HRSG units, which would need to be supplemented through steam letdown from the new nuclear-sourced steam. As previously noted, much of the original equipment may be kept as backup systems regardless, even after nuclear installation.

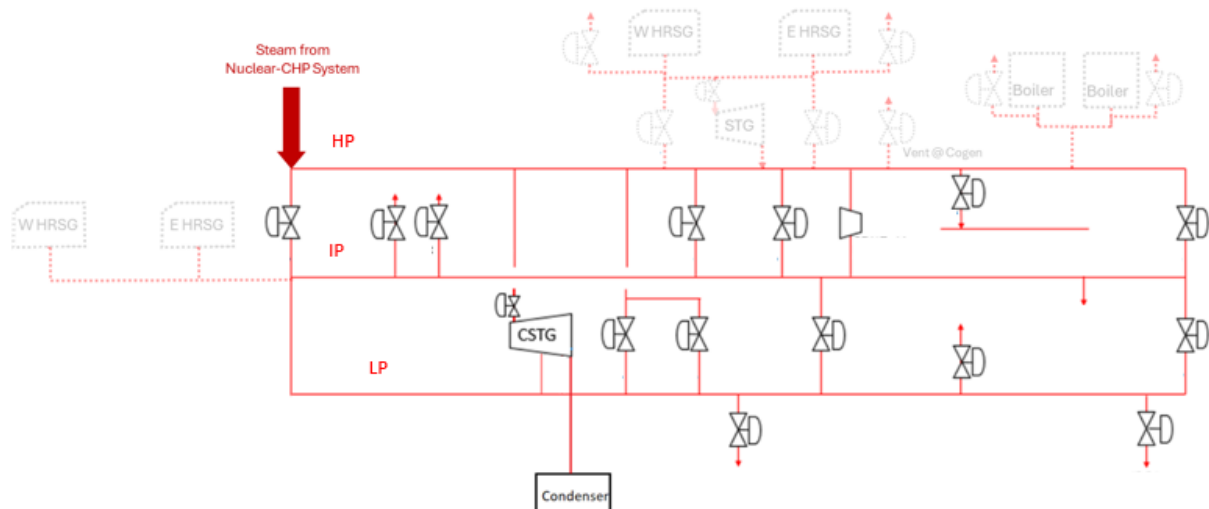


Figure 32. General illustration of nuclear-sourced process steam integration for SCO. The sections with dashed lines could become obsolete after introducing the nuclear-CHP system.

5.1.1 Xe-100 Reactors with PCCs

The SCO site is large enough that four Xe-100 modules would be a good fit for meeting the system demand, as shown in Figure 33. The system combines a single Type 1, two Type 2, and one Type 3 PCC configurations, as established in Section 4.1.1. Based on historic demand, this configuration should be able to meet all thermal demand, with fluctuations in requirements being handled by the two Type 2 CHP modules.

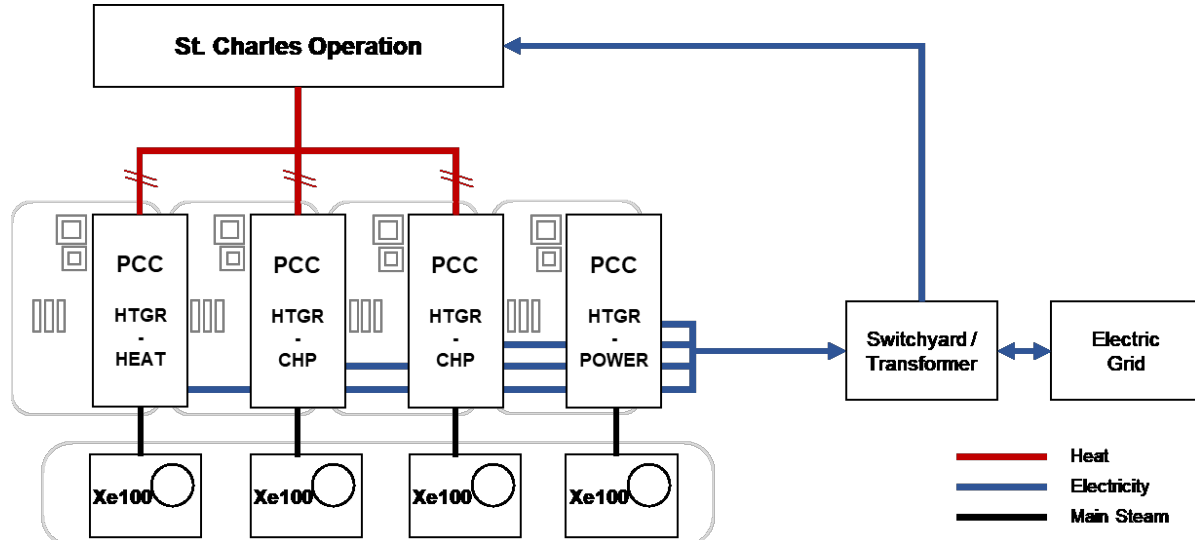


Figure 33. System configuration of the HTGRs with CHPs for SCO, where is the energy conversion (thermal to electric) efficiency.

While the Xe-100 system is designed to feature online refueling and should thus rarely come down for outages during normal operations, for this kind of application it is recommended that interconnections between steam systems be established. The current approach by nuclear vendors isolates each PCC system to a particular core module. This facilitates licensing, as there are no site-specific changes to the types of PCCs the modules may see. However, when one module operates in a unique fashion, it leads to a higher system penalty should that module become unavailable. Two potential approaches could alleviate some of these concerns. The first approach would be to implement common steam buses between the nuclear modules (see Figure 34). As mentioned, this approach may lead to significant licensing challenges. The second approach, which may be simpler to license, would be to establish bypass interconnects so that each reactor core is assigned to a particular PCC at any given time, but the assignments could be changed during times of unavailability. In this configuration, if a uniquely operating core goes down, valves are adjusted and another core directs energy to that PCC until the original core becomes available again. An alternative to interconnecting the reactor PCCs may be to shift the set of PCCs such that more systems than actually required are in the CHP configuration (Type 2), giving the system greater flexibility.

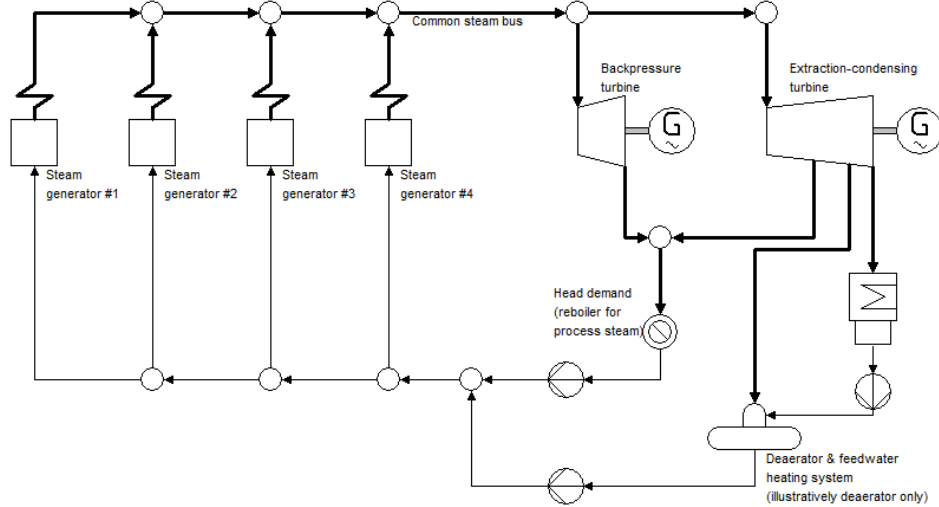


Figure 34. Illustrative representation of the system configuration featuring a common steam bus.

The overall electricity balance of this system, measured against a single synthetic data set (see Figure 35), shows that the system typically exports electricity (seen as values greater than 0). Dow's relationship with Entergy normally limits the amount of electricity that they can export. In a nuclear-integrated future in which Entergy is the operator for the power plants, it is unclear whether this issue will persist. If the answer proves to be yes, options exist for managing excessive over-generation. The first such option is to curtail generation with short-term reactor power load following. The second option is to curtail energy production either via condenser bypass or venting. The final option would be to have a supplemental energy sink in the form of energy storage. TES options were explored in Section 4.1.4 for reactor-side integration, but energy storage could also be implemented within the Dow facilities. Certain conclusions and commentary may be less applicable in this case.

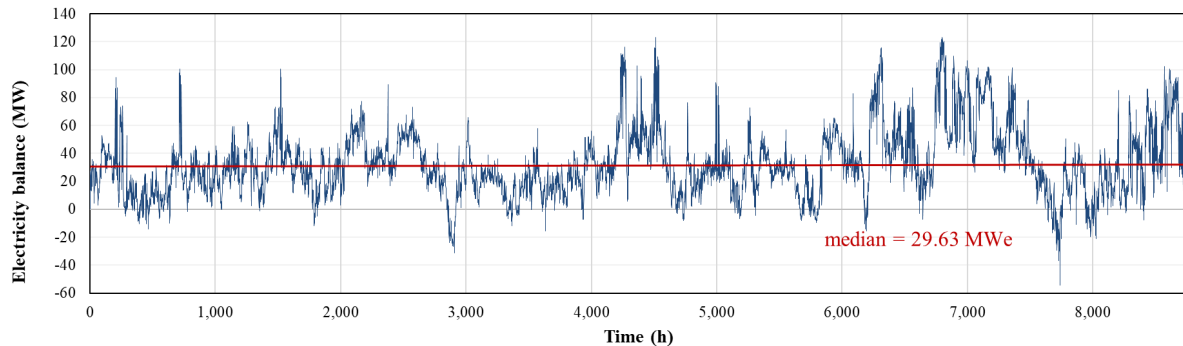


Figure 35. Overall electricity balance, measured against one synthetic data set from SCO, using HTGRs with PCC configurations (detailed in Figure 33).

The specific per-module energy distributions across a 1-year set of synthetic data are shown in Figure 36 for heat and in Figure 37 for electricity. The negative values in Figure 37 indicate an electricity surplus.

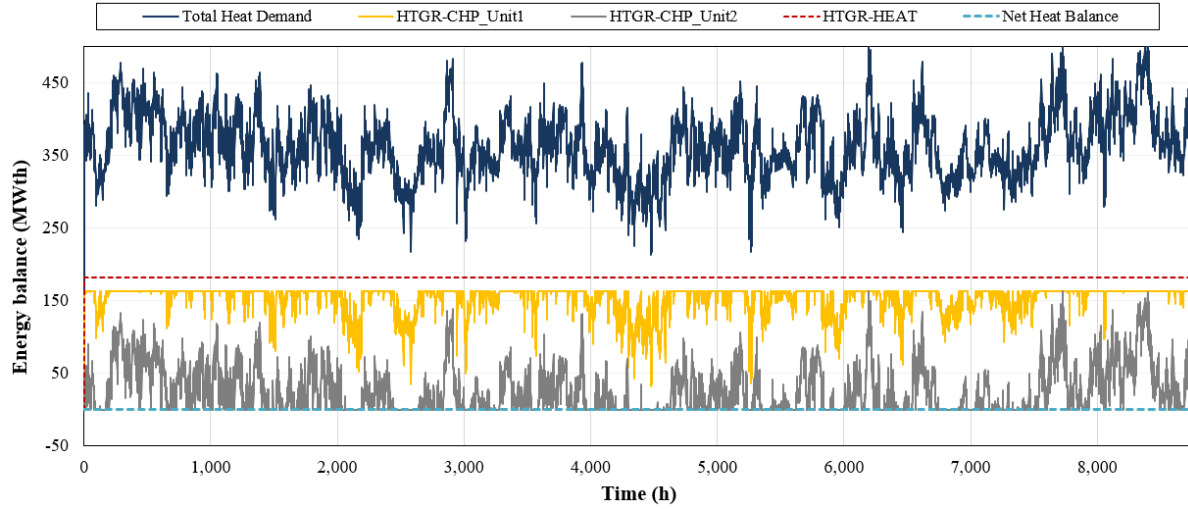


Figure 36. Total heat supply and demand at SCO for 1 year, from a set of four HTGRs.

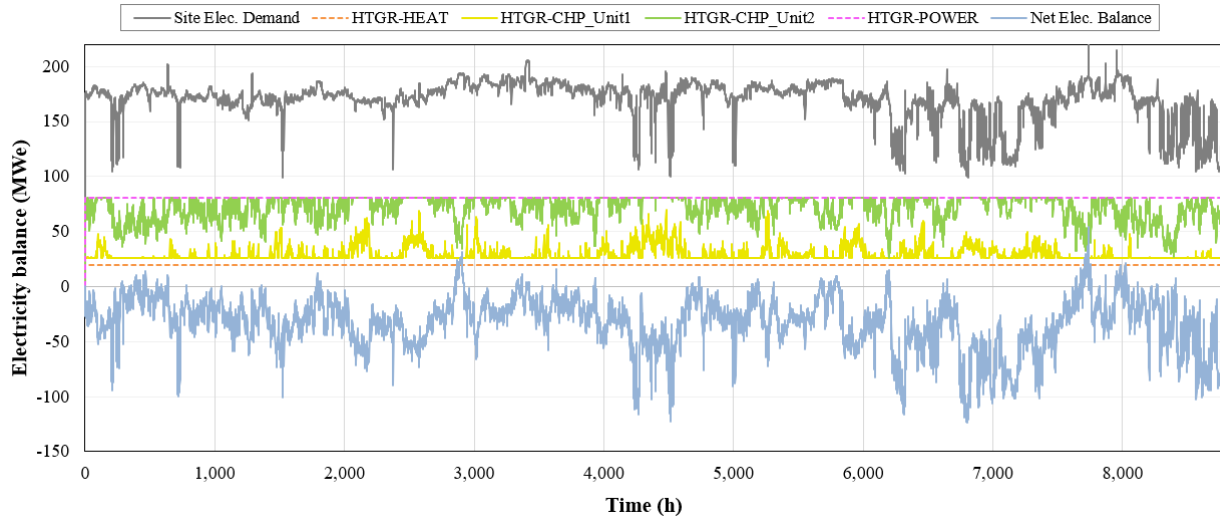


Figure 37. Total electricity supply and demand at SCO for 1 year, from a set of four HTGRs.

5.1.2 Xe-100 Reactors with PCCs and TES

TES has been proposed to address the imbalance between the continuous energy production of nuclear reactors and the fluctuating energy demand at SCO. Figure 38 shows a proposed general system layout of nuclear sources and integrated TES, with TES Type B being added to a PCC Type 1 HTGR system.

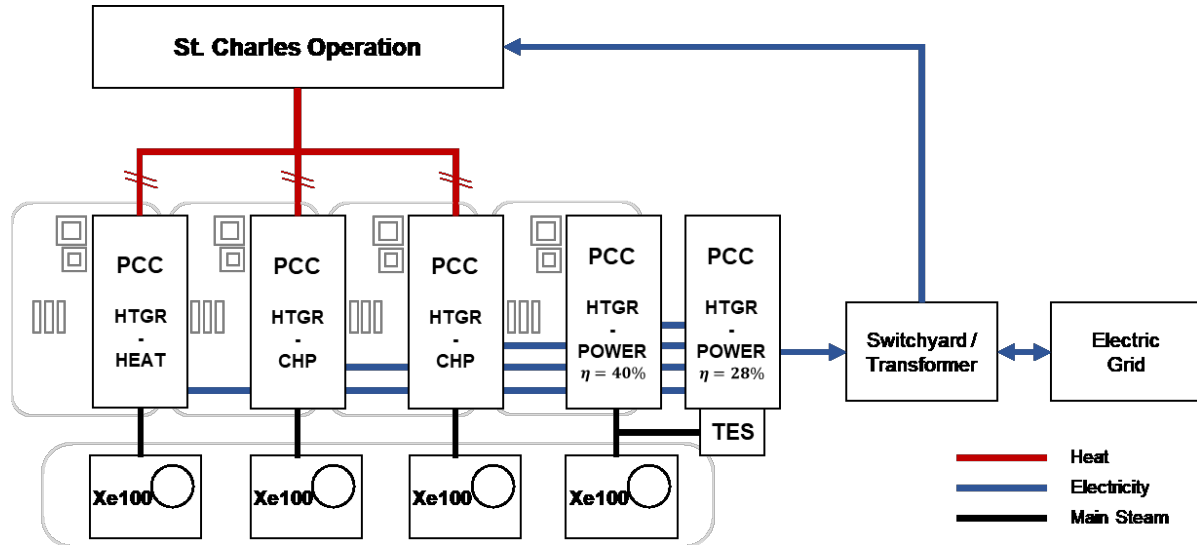


Figure 38. Illustration of the system configuration for the HTGRs with CHPs and TES (Type B) for SCO, where η is the subsystem thermal-to-electric conversion efficiency.

Integrating the TES with the electricity generating unit was a choice based on both control and technical considerations. TES integrated with an electricity-only generating unit simplifies the control system so that it operates very similarly to the nominal module control system: charging the TES when electricity demand is below the nominal system output, and discharging the TES when additional electricity is required. The impact of introducing a TES configured to maximum charge/discharge rates of 80 MWth and a storage capacity of 800 MWh-th is shown in Figure 39. Based on this data sample, the number of grid import occurrences throughout the year drops to three. Figure 40 shows the state of TES charge during the year dispatch profile. Note that storage losses are not accounted for in this dispatch profile. Given the incidental use of storage in this profile, with a cumulative energy dispatch of 2400 MWh-th throughout the year, and accounting for a 1%–2% daily loss in stored heat content, these values should be considered in future detailed investigations.

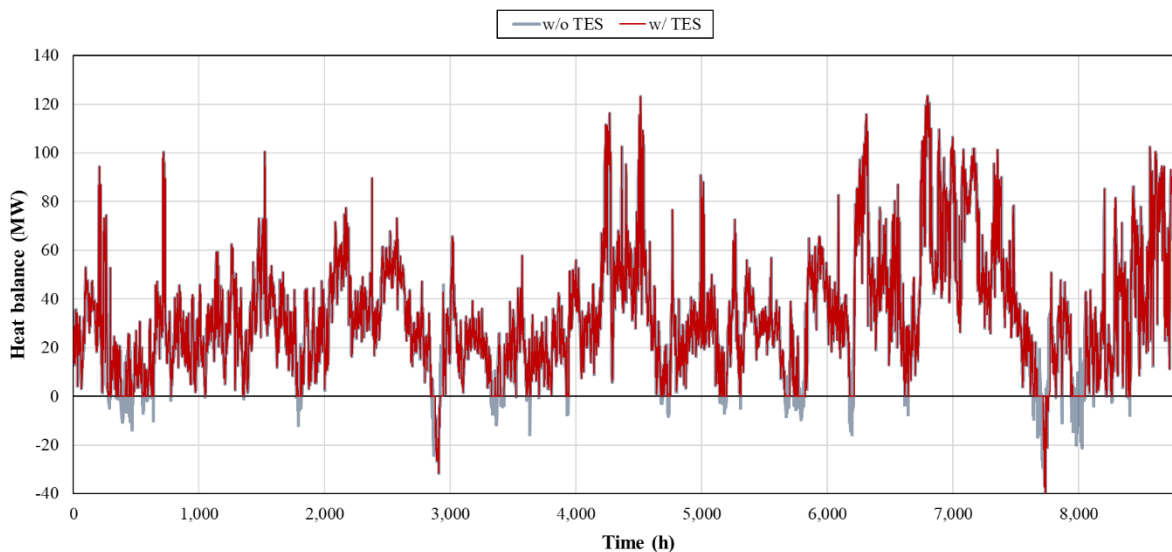


Figure 39. Difference in net electricity balance between cases involving a TES system (red) and cases not involving one (blue).

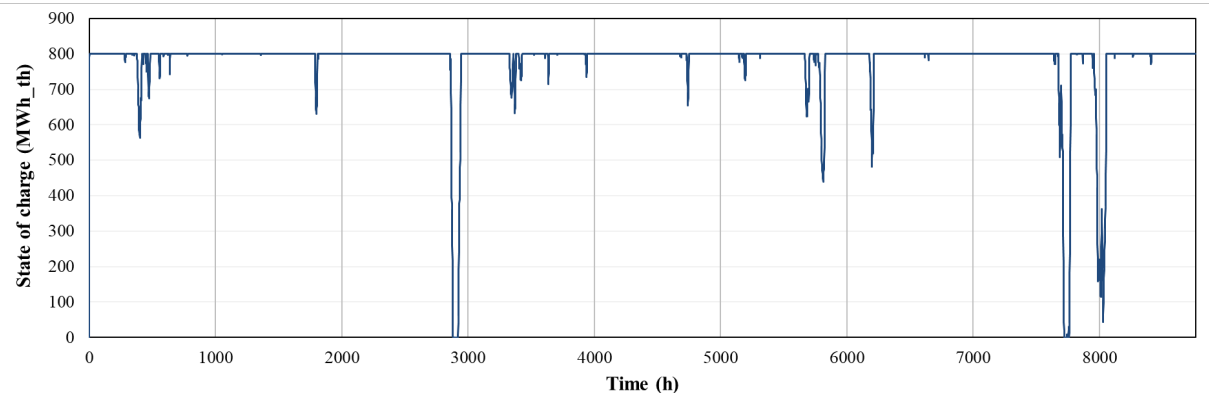


Figure 40. State of TES system charge throughout the year, same data set as Figure 39.

A second TES introduction objective could be to attempt to hold a steady power export to the grid, as opposed to simply avoiding imports. A TES Type A with a maximum power output of 160 MWe and a capacity of 3200 MWh-th, 16 hours, should improve the TES economics, and steadyng the grid output would facilitate grid integration through reducing the need for ancillary grid services. This configuration is shown in Figure 41.

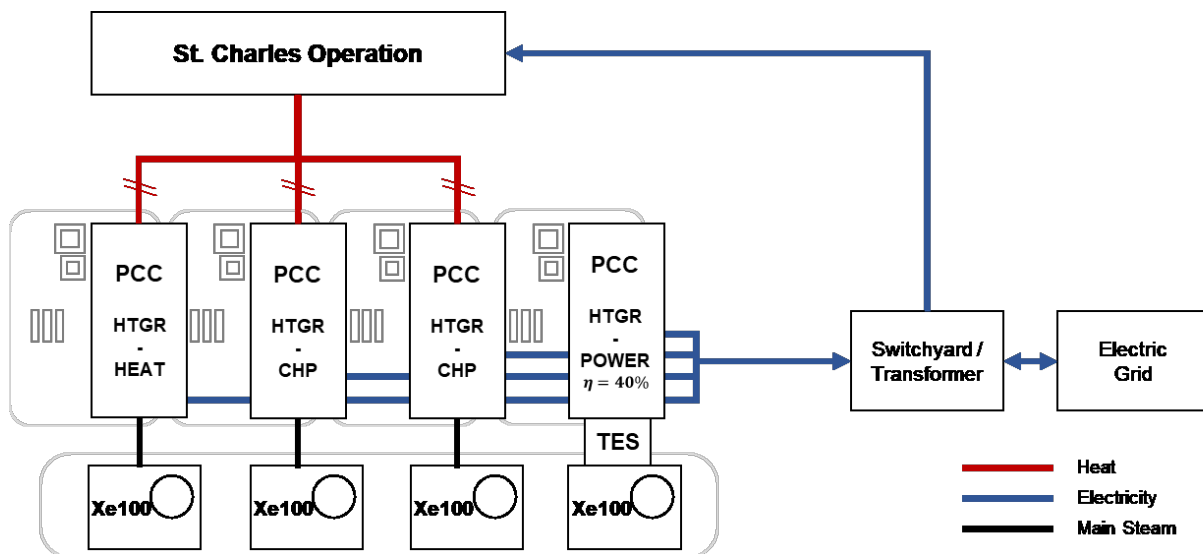


Figure 41. Illustration of the system configuration of the HTGRs with CHPs and TES (Type A) for SCO.

By incorporating a 16-hour storage capacity, the system achieves a continuous power output period 48% of the time, with approximately 11 cycles per year, where a “cycle” is defined as a time in which the storage system passes from greater than 50% charge to less than 50% charge, as shown in Figure 42 and Figure 43.

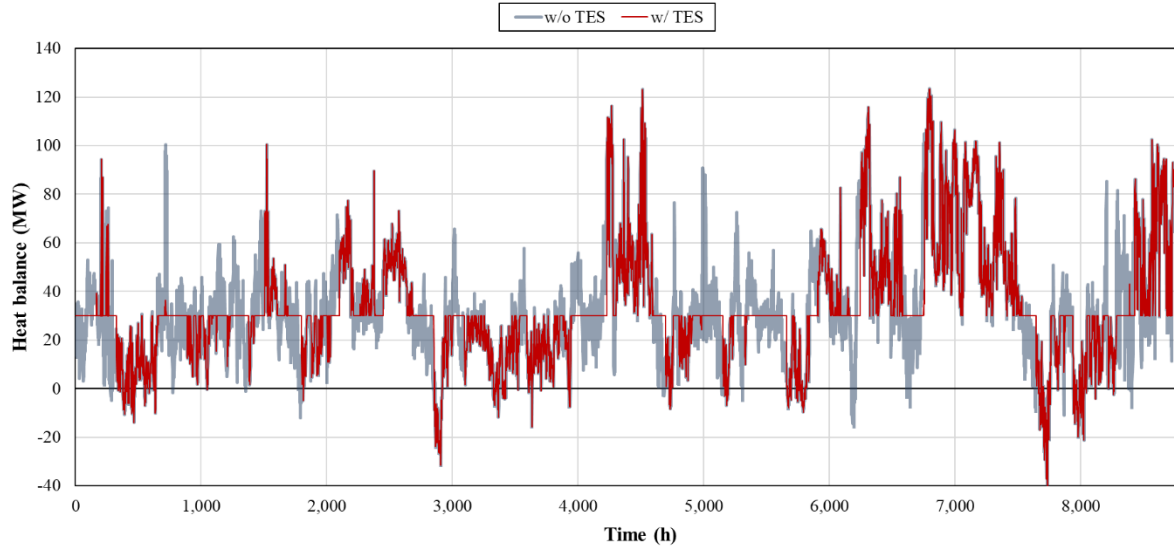


Figure 42. Net electricity generation both with and without TES when the TES is operating in a power-steadying mode, intending to generate 30 MWe.

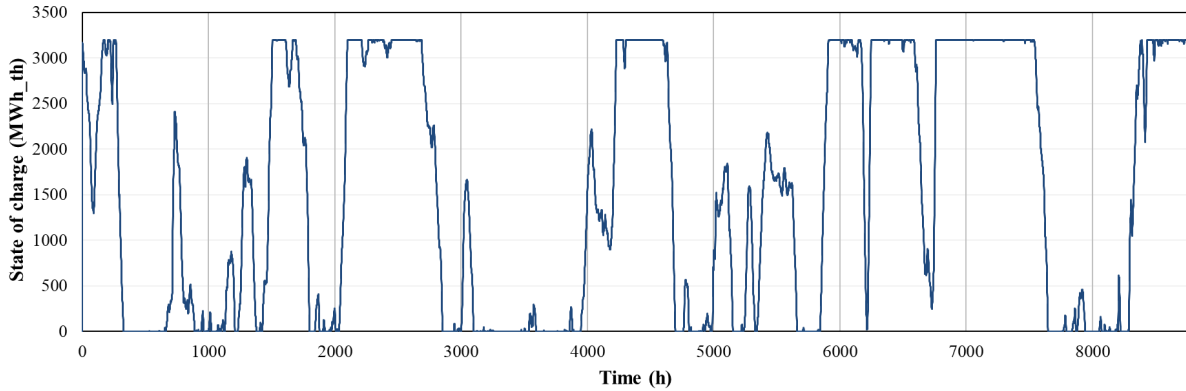


Figure 43. State of TES charge throughout the year when in power-steadying mode at 30 MWe.

Figure 44 shows the relationship between storage capacity and the frequency of meeting the 30 MWe demand, as well as the number of cycles experienced by the TES each year. An inverse relationship exists between storage capacity and the frequency with which storage meets the output throughout the year. The frequency of TES utilization at SCO projects to be significantly less frequent than it would as a grid-centric entity, which would anticipate multiple cycles per week.

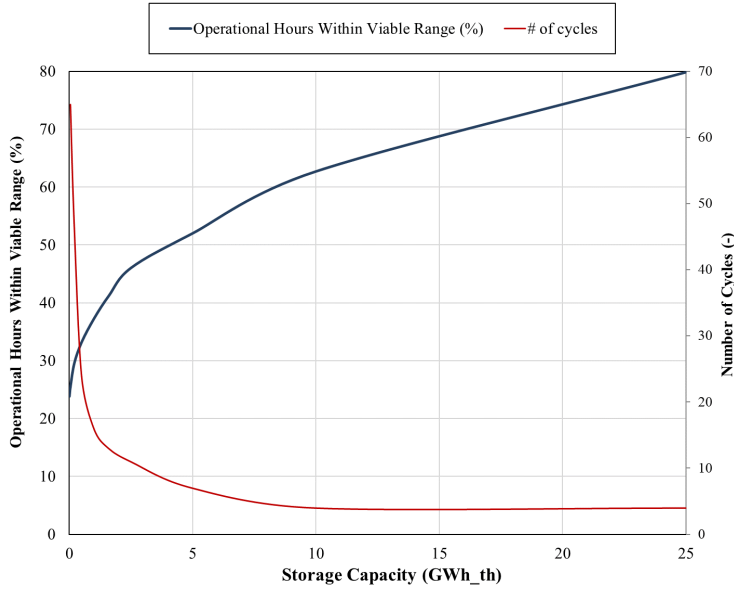


Figure 44. Graph of system parameters as a function of storage capacity.

5.1.3 NuScale Power Modules with PCCs

A bundle of four VOYGR reactors was also identified in this stage of the analysis as being the optimal size for the SCO site. The proposed configuration is shown in Figure 45. Two Type 1 modules are implemented alongside one each of Type 2 and Type 3. The LWR system generates more thermal power per module (hence the reduced number of CHP modules) but produces less electricity, due to reduced efficiencies.

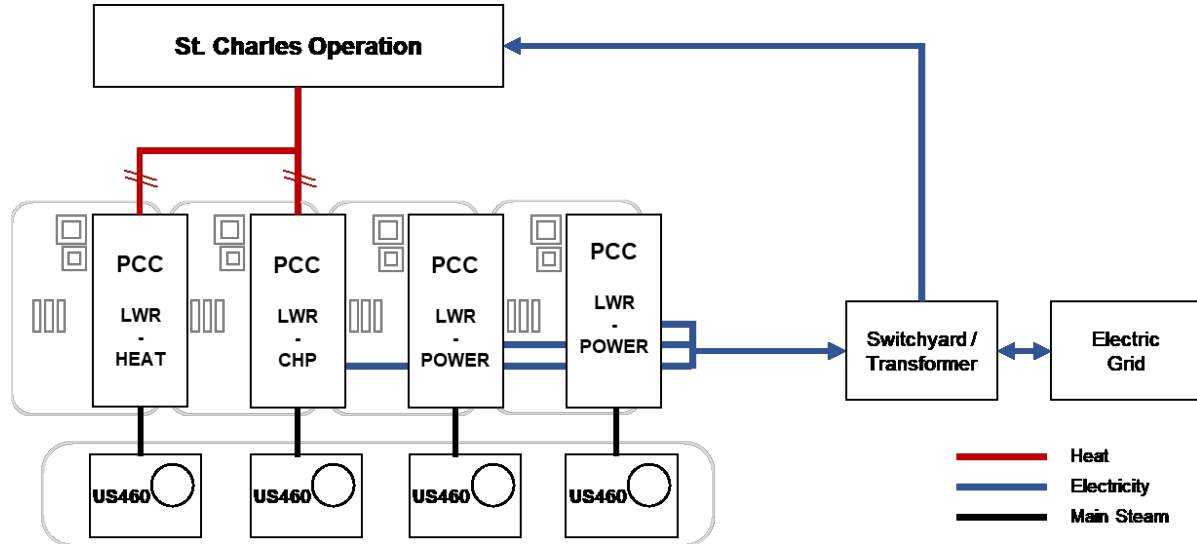


Figure 45. Illustration of the LWR CHP system configuration for SCO.

As seen in Figure 46, this reactor configuration can meet SCO heat demands over a sampled year. The Type 2 system flexes between heat and electricity throughout the year so as to provide heat as needed.

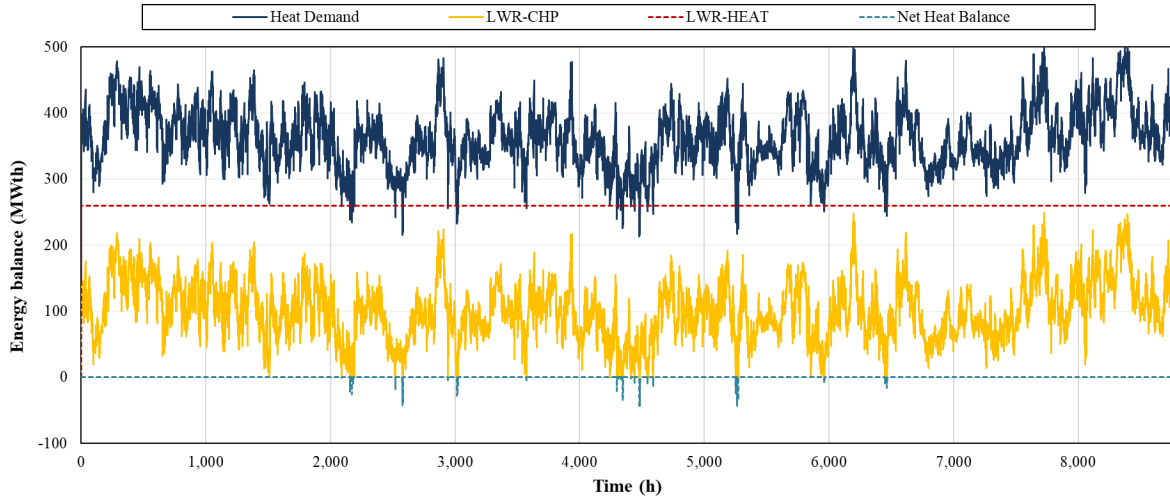


Figure 46. Heat supply and demand from LWRs to SCO.

The hourly year-long electricity balance is shown in Figure 47, with negative net electricity balance values indicating a net surplus of electricity.

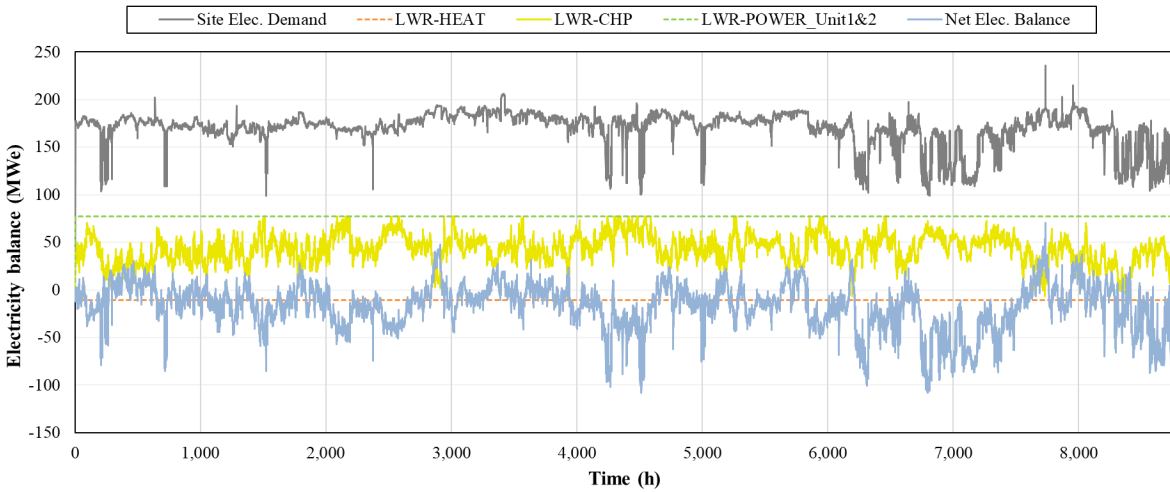


Figure 47. Electricity supply and demand from LWRs to SCO.

The overall electricity balance is presented in Figure 48. The total electricity balance shows a lower overall median export from this system relative to the HTGR configuration, due to differences in design setpoints and larger peaks of the fluctuating values being accentuated due to the reliance on electricity to increase thermal output by increasing the compressor load.

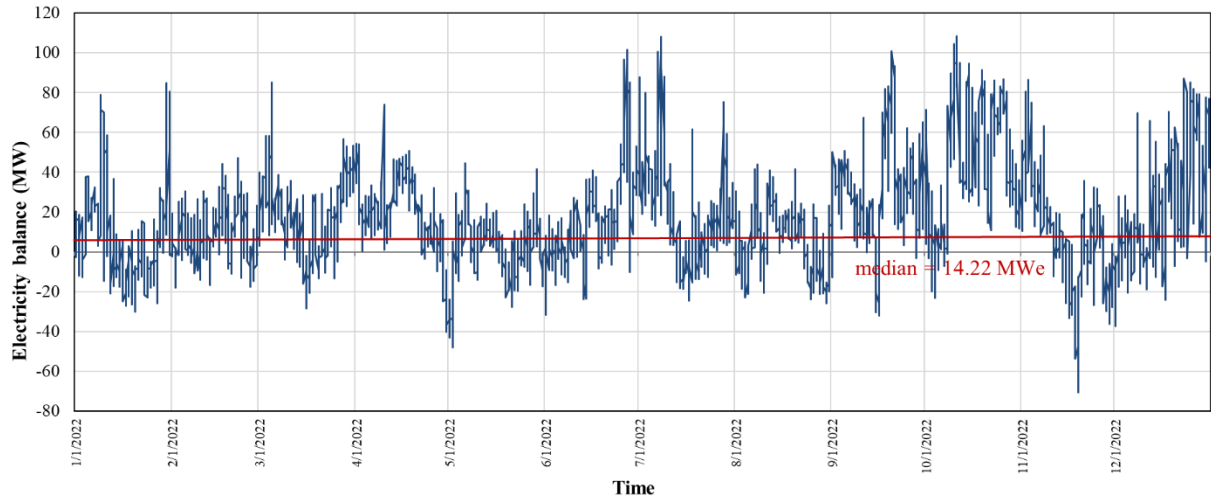


Figure 48. Overall electricity balance of SCO after integrating the proposed NuScale-PCCs system.

As in the HTGR case, power curtailment can be implemented via bypass to the condenser, venting on the reactor or Dow sides, or through TES implementation. TES is not investigated in detail here, but the broad conclusions from Section 5.1.2 should still apply, as they are demand-side driven and not TES-technology driven. The low temperatures within LWR systems drive TES efficiencies even lower, and due to the configurations of most SMR LWRs, only Type B or Type C storage are viable options (since steam generators are embedded within the RPV). Anticipated storage round-trip efficiencies in a Type B configuration for an LWR should be between 60%-83% [86] [99]. At reduced temperatures, solid media (i.e., concrete) storage becomes a competitive option. At these temperatures, liquid sensible heat storage systems either require very large storage systems due to the available temperature delta between the hot and cold tanks for molten salt, or they require a more expensive heat transfer fluid such as a thermal oil.

5.2 Preliminary Energy Balance Investigation – Carrollton

The general integration layout for the DSC site at Carrollton (see Figure 49) is simpler than for SCO, due to the single steam header configuration. It may be advantageous to maintain the current fired boilers at the Carrollton site (or replace them with a cleaner option) to cover both extreme thermal demand peaks or unanticipated outages.

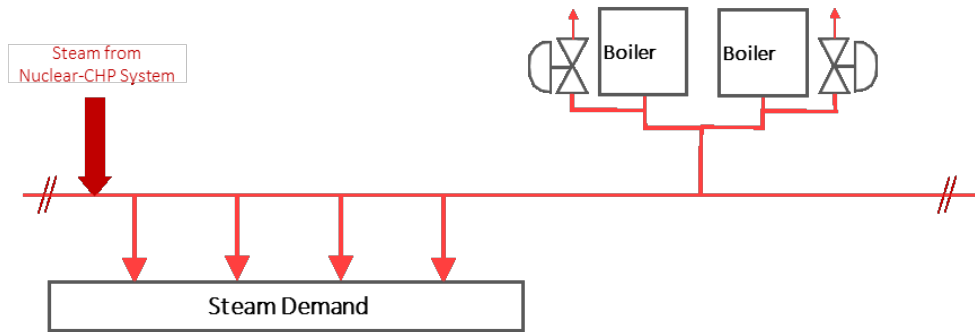


Figure 49. Nuclear integration layout integrating into the Carrollton site process steam system.

5.2.1 Microreactors with PCCs

When considering μ Rxs CHP applications, the systems are typically isolated to either heat or power. Two analyses are covered in this section, one in which this assumption is held and another in which the assumption is relaxed by introducing a backpressure turbine system. The average site requirements are 120 MWth and 20 MWe. It is important to note here that the Carrollton facility does not currently produce electricity onsite.

The first configuration—with μ Rxs dedicated to either heat or power—employs the following assumptions:

- Dedicated power producing units operate at $\eta_{el} = 35\%$
- Dedicated heat production units operate at $\eta_Q = 100\%$

The resulting configuration, shown in Figure 50, has six reactors—two that produce electricity and four that produce heat.

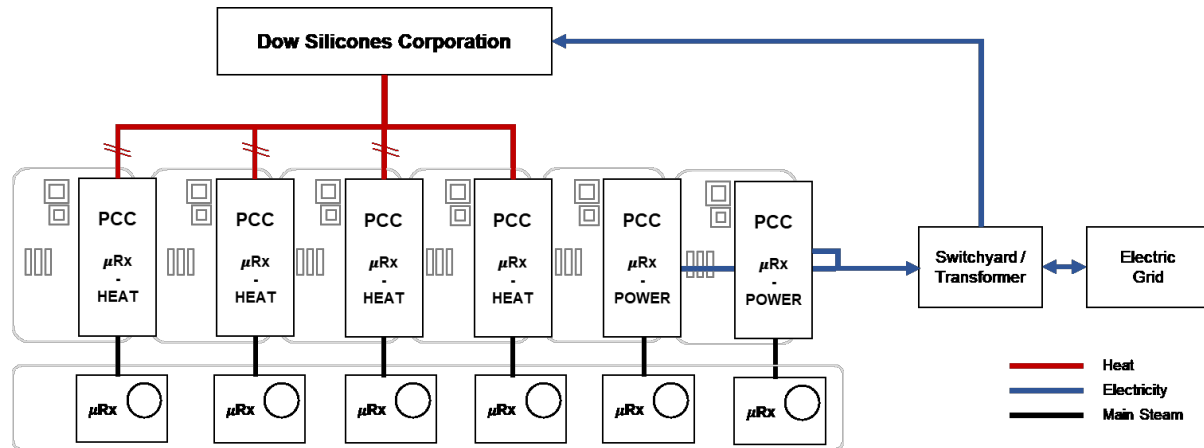


Figure 50. Conceptual nuclear IES configuration for the DSC Carrollton site, considering dedicated power-only and heat-only reactor units.

The second configuration leverages μ Rxs with CHP backpressure systems and no dedicated heat or electricity units. The resulting configuration in Figure 51 has five reactors, highlighting the primary energy savings realized through cogeneration. The efficiency assumption is that the CHP backpressure steam cycles operate with $\eta_{el} = 15\%$ and $\eta_Q = 80\%$.

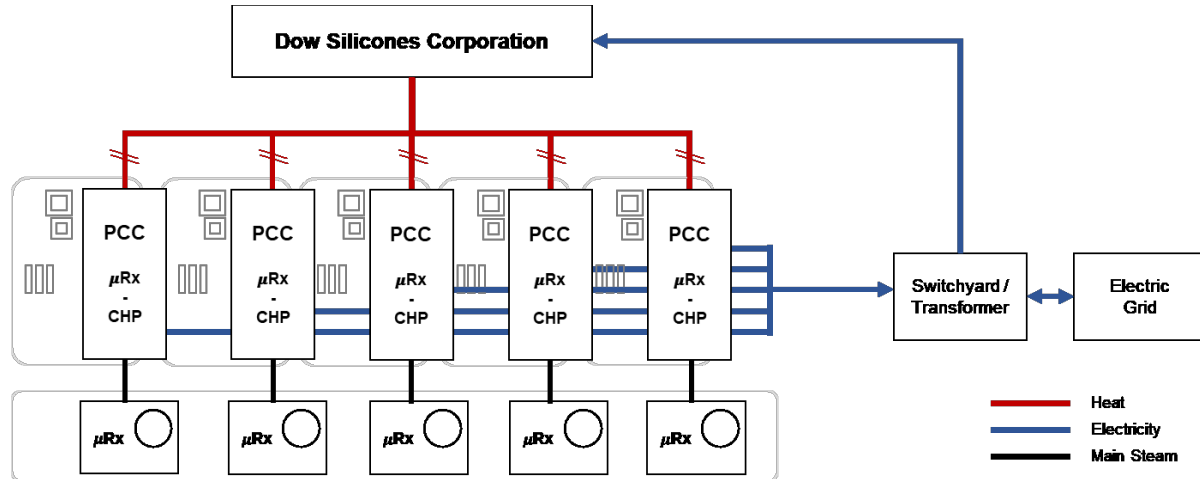


Figure 51. Conceptual nuclear IES configuration for the DSC Carrollton site, considering backpressure PCC systems for each reactor unit.

If all reactors are operated in baseload mode, Figure 52 shows that the DSC Carrollton facility would frequently operate at a thermal deficit if relying only on the μ Rxs. The electricity demand is generally completely covered throughout the analysis period.

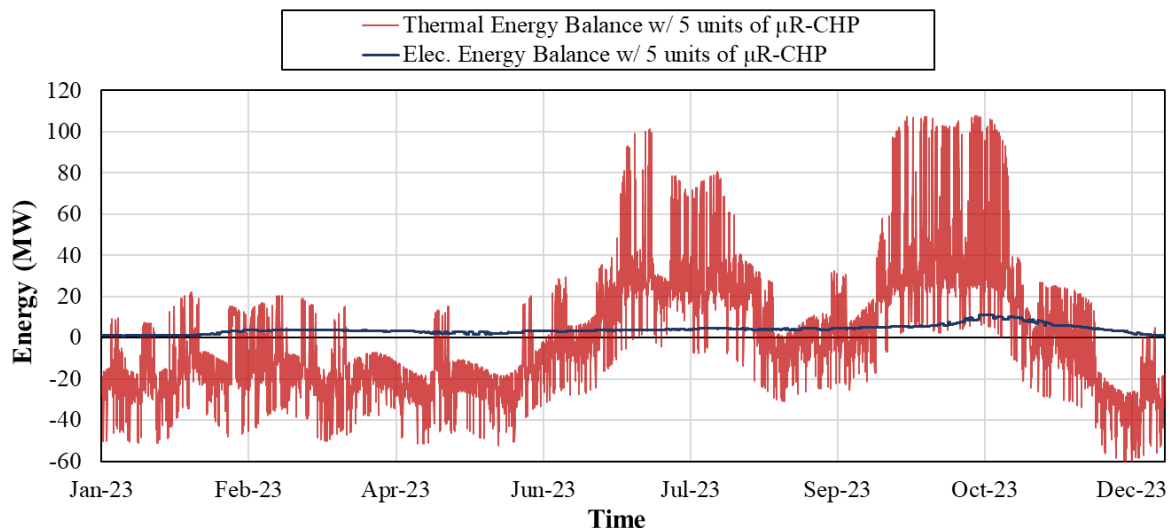


Figure 52. Thermal and electrical net balances for the DSC Carrollton site, leveraging five μ Rxs in a baseload backpressure configuration.

Figure 53 shows that adding a sixth μ Rx would eliminate most—but not all—the heat deficits, while simultaneously raising the net electricity export to an average of about 10 MWe (i.e., around 50% of the nominal electricity draw at Carrollton). Due to this significant over-generation, subsequent analysis in this section assumes that five μ Rxs are installed.

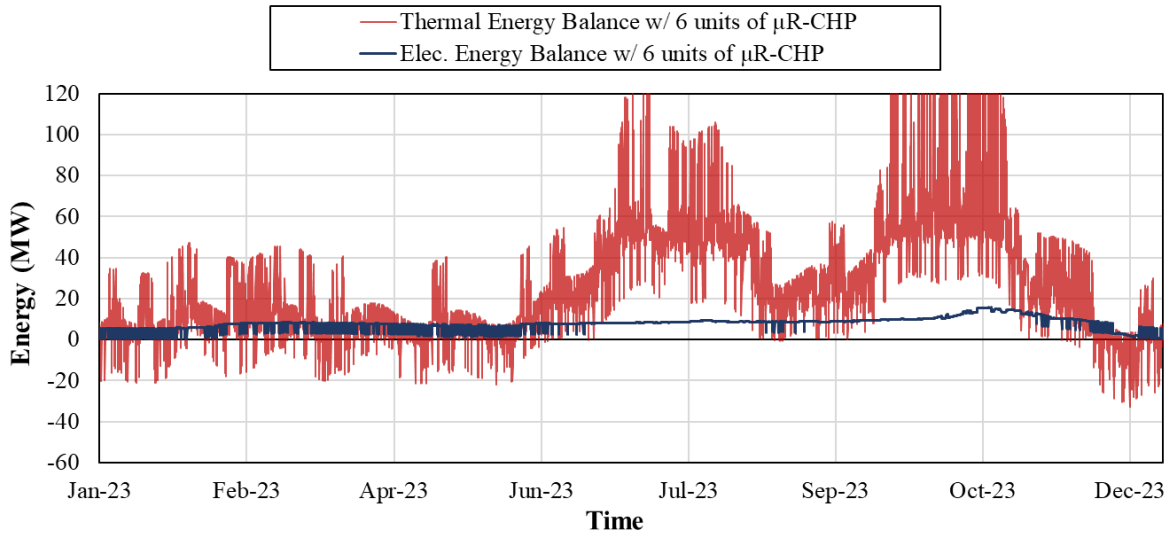


Figure 53. Thermal and electrical net balances for the DSC Carrollton site, leveraging six μ Rxs in a baseload backpressure configuration.

The thermal energy supply deficit should be able to be made up for by the existing boilers or replacement generating assets. Electricity is assumed to be balanced by the grid. Note that due to a lack of hourly data, the electricity fluctuations are unknown, meaning it is also unknown how well KUC would accept distributed generation at Carrollton. The site may need to exercise load following to reduce electrical intermittency.

The thermal energy supply deficit is assumed to come from the natural gas boilers, and electricity is balanced via connection to the electrical grid. To reduce natural gas consumption, the dispatch algorithm for one μ Rx is modified from continuous baseload backpressure generation to allow for turbine bypass, slightly increasing heat production in periods of deficit, and thus producing less power. The resulting auxiliary boiler profile is shown in Figure 54, as compared to the average μ Rx.

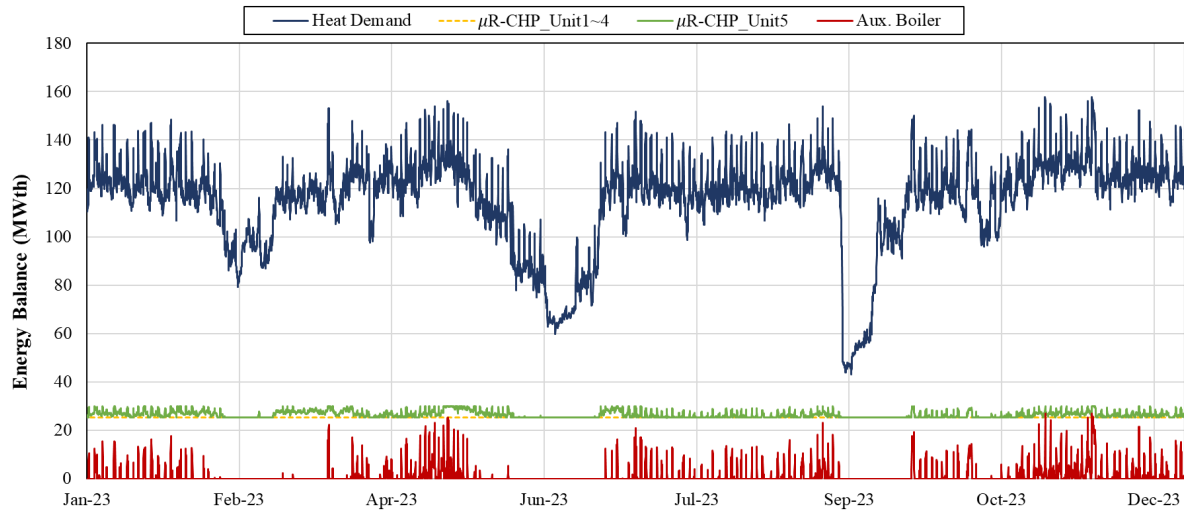


Figure 54. Thermal energy dispatch from the auxiliary boilers required to meet the thermal demands at the DSC Carrollton site via a five- μ Rx configuration.

Increasing the thermal dispatch from the final μ Rx results in corresponding decreases in electricity output. Negative values in Figure 55 indicate net electrical export from the site to the grid. The nominal electricity generation from one backpressure turbine μ Rx is added as a reference value.

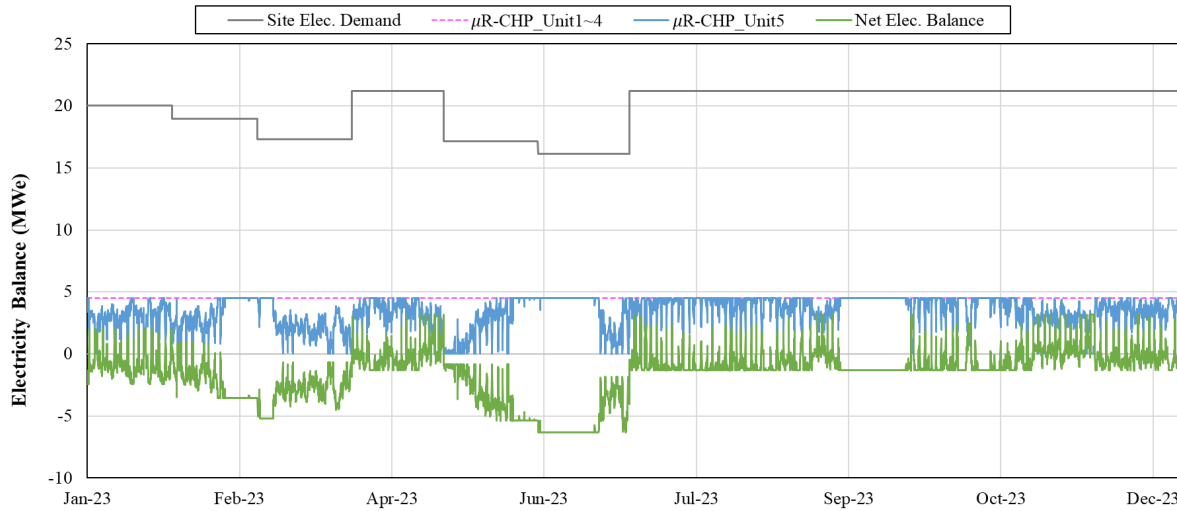


Figure 55. Resulting net demand electricity fluctuations from the backpressure turbine bypass in one μ Rx.

5.2.2 Microreactors with PCCs and TES

Frequent oscillations in demand indicate that a storage system may be able to be readily applied to reduce the need for auxiliary boilers and heat curtailment during low demand. TES was introduced to a single production module, with charging and discharging rates limited to 25 MWth and a total capacity size of 100 MWh-th. No changes for the backpressure turbine system were introduced, and the turbine was constrained to its nominal load, causing the maximum electricity generation to remain at 4.5 MWe. This configuration is shown in Figure 56.

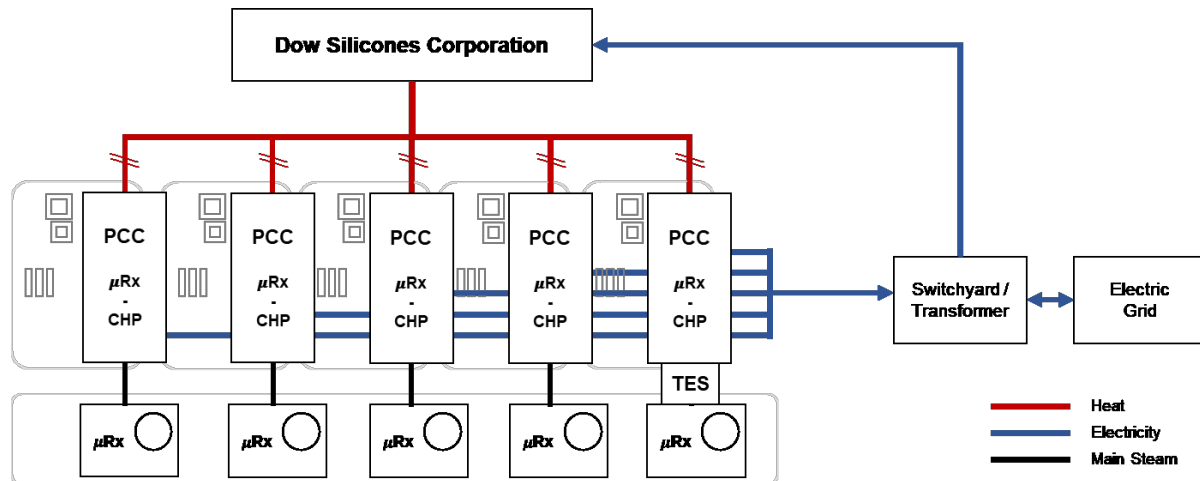


Figure 56. Conceptual nuclear IES configuration for the Carrollton site, considering backpressure CHP systems for each reactor unit and a TES system coupled to one of the units.

The TES has high utilization across non-outage periods, as seen in Figure 57. The TES unit is rarely used in 100% charge or discharge mode. Introducing TES greatly reduces the reliance on natural gas boiler systems, as can be seen by comparing the values in Figure 57 and Figure 54.

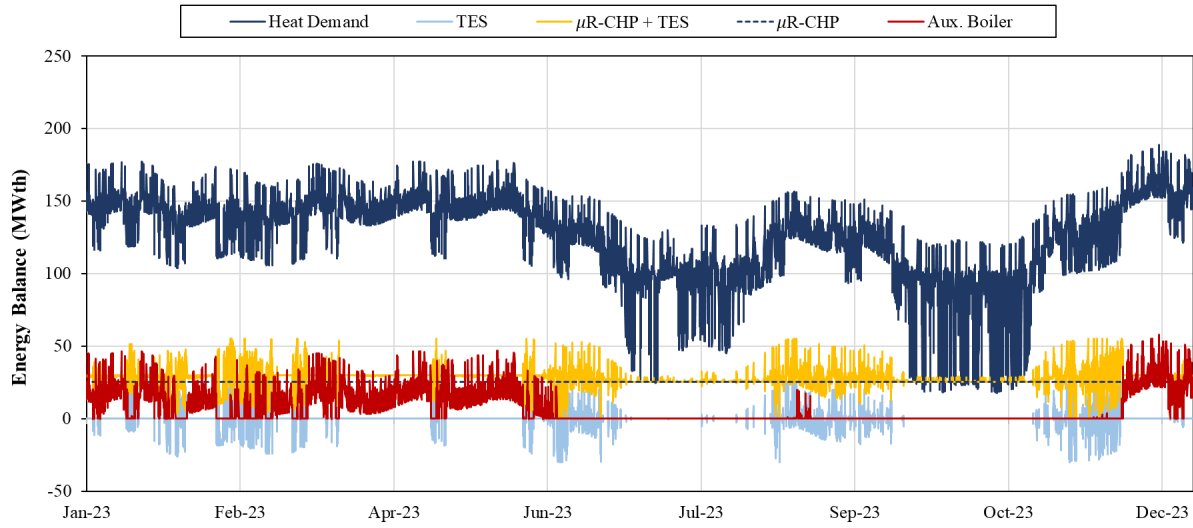


Figure 57. One year of thermal dispatch from the proposed DSC's IES, with TES integrated into one module.

The net electricity balance, with negative values in Figure 58 representing exports, has a shape similar to that of the system without TES, but operates with generally smaller-magnitude swings in electricity generation.

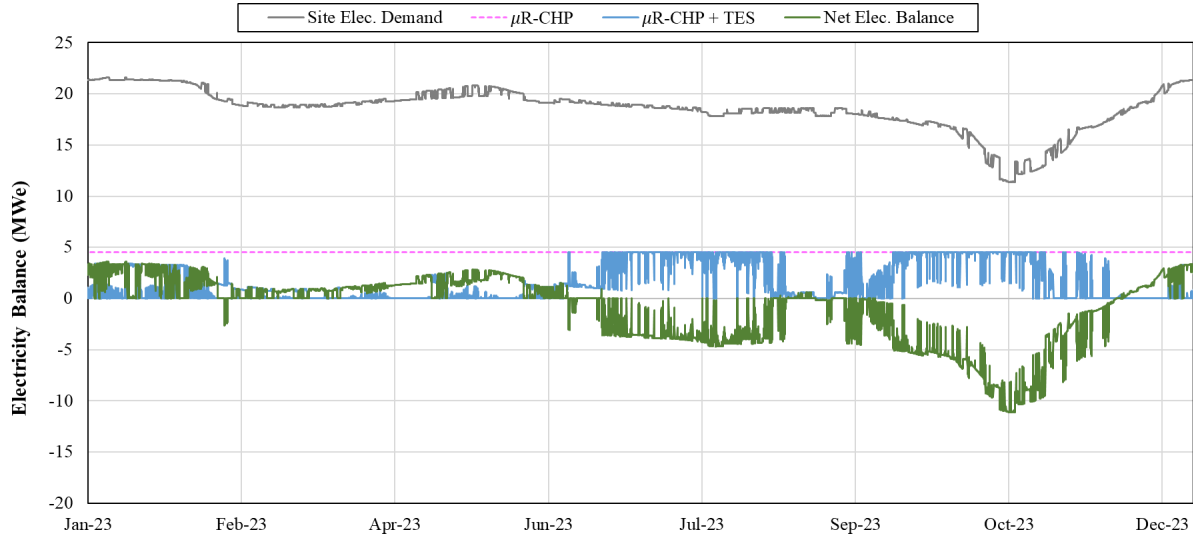


Figure 58. One year of electricity generation from the proposed Carrollton IES, with TES integrated into one module.

A two-step sensitivity study on TES size was exercised, and the results are shown in Figure 59–Figure 62. Figure 59 shows the net nuclear heat and electricity balances across 1 year of operation at Carrollton. Figure 60 shows the TES content across the same year of operation.

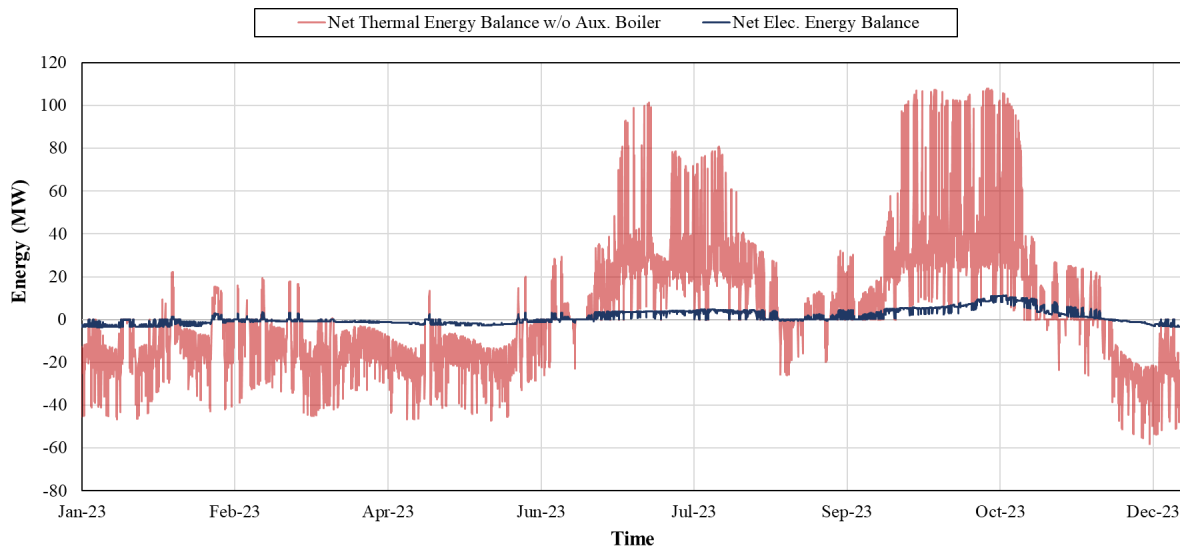


Figure 59. Thermal and electrical energy balance of the site with 100MWh-th storage is installed.

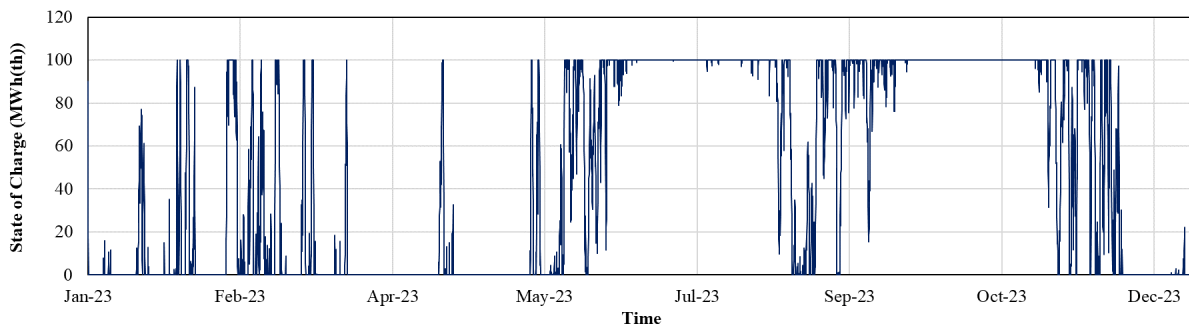


Figure 60. State of charge across operation for a 4-hour (100 MWh_{th}) TES system.

Figure 61 and Figure 62 show the net Carrollton energy production and TES storage content, respectively, when the storage capacity is expanded to 600 MWh-th, with 24 hours of storage. As anticipated, there are fewer periods of required auxiliary heating in this system, and the storage system takes longer to fully charge and discharge, leading to fewer cycles throughout the 1-year dispatch profile.

The impact of varying storage capacity is shown in the net heat and power profiles and TES state of charge across a 1-year period, first for the case of a 4-hour storage capacity (100 MWh_{th}), as reflected in Figure 59, and then for a 24-hour storage capacity (600 MWh_{th}), as reflected in Figure 61. TES can partly balance out the net balance profile, but there are long periods of excess energy or demand that again go beyond the capabilities of even large storage systems. Thus, the overall impact of TES is only moderate, as displayed in a sensitivity study conducted on the main parameters pertaining to TES capacity (see Figure 63).

Most of the energy imbalance following nuclear integration cannot be balanced with TES in this operation mode. Demand-side management may significantly improve the situation, both prior to TES and with it. TES may still be useful for balancing peaks, especially if curtailed thermal energy was to be converted to power and exported to the grid. When also connecting TES to electric heaters, additional benefits may arise from providing grid auxiliary services; eventually, TES could also be charged during periods of negative electricity prices. Such an integrated system might even require fewer reactor systems to achieve a similar reduction in the reliance on fossil fuels.

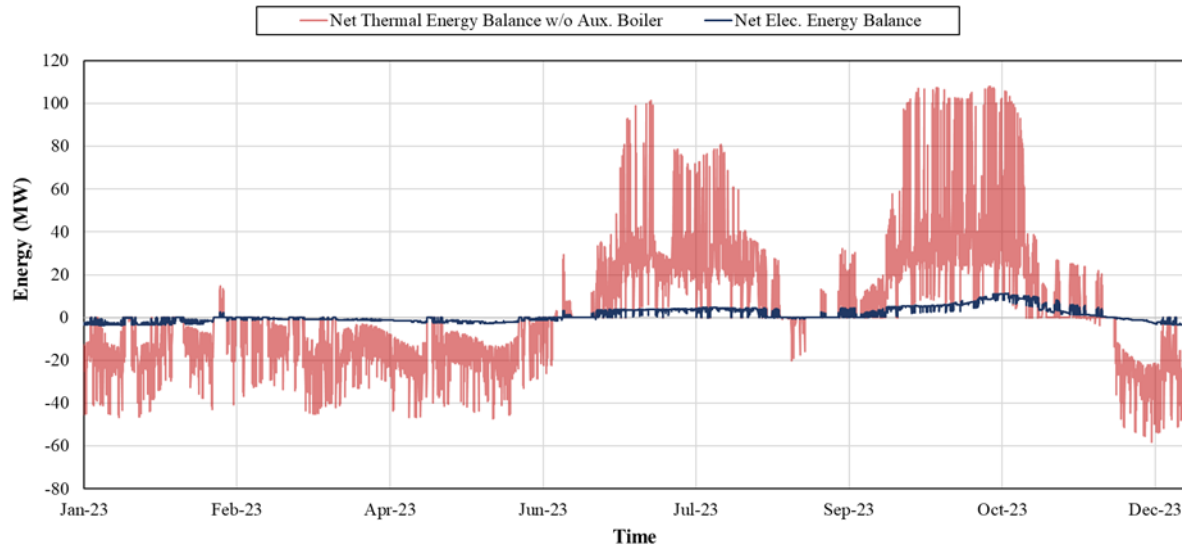


Figure 61. Energy balance of the site and state of charge of the storage system in time for a 24-hour (600 MWh_{th}) TES system.

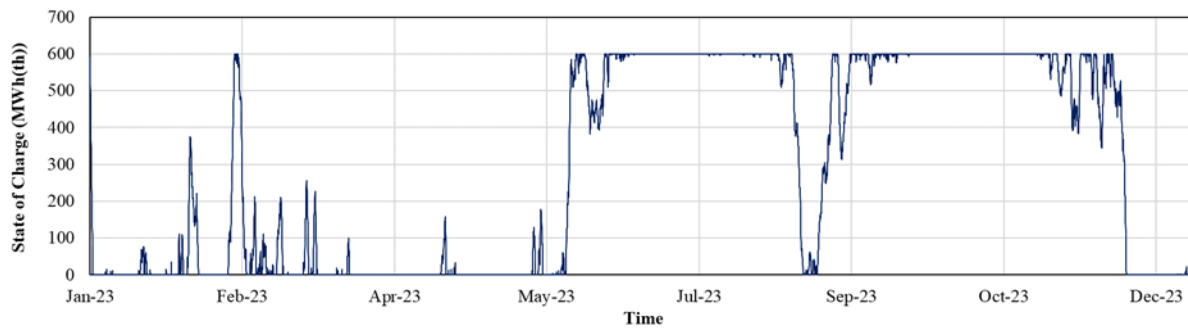


Figure 62. State of charge for a 24-hour (600 MWh_{th}) TES system.

Figure 63 maps the impact of increasing the TES size for one module at the DSC Carrollton site. As with the effect of increasing storage size at SCO, the number of cycles decreases with increasing storage size. The impacts on net electricity import/export are not pronounced with significantly increasing storage size. The slopes of thermal energy curtailment, thermal energy from auxiliary boilers, electricity imported, and electricity exported all have small negative slopes with respect to TES capacity.

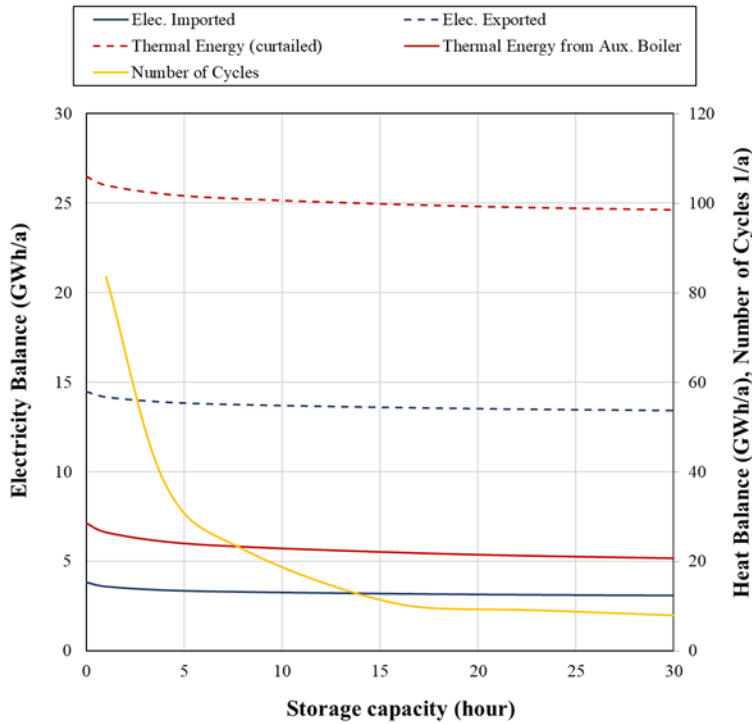


Figure 63. Reduction of annual external energy demand, electricity export, and heat curtailment—based on TES capacity—along with the annual number of TES cycles.

5.3 System Capacities Analysis with HERON

HERON was unable to establish a preferred reactor type at the SCO site, as 1250 MWth of LWR capacity, 800 MWth of HTGR capacity, 1000 MWth of LWR and 200 MWth of HTGR, and 750 MWth of LWR and 400 MWth of HTGR were effectively statistically indistinguishable, within 5%, on a net present value basis. At the Carrollton site, the optimal nuclear installation capacity was found to be 172.8 MWth, with a TES installation of 310.3 MWh-t.

5.3.1 St. Charles Operations

The SCO optimization was accomplished using a few different sweeps in HERON, partly thanks to simplifying the analysts' output interpretation burden by reducing the number of optimization variables. Once an initial optimization sweep had identified that a combination of different technologies may be preferable, optimization sweeps using discrete reactor sizes were exercised to identify economic valuations of specific reactor size and technology combinations. With identified reactor sets, two more optimization runs were performed to validate the selection of specific PCC types and to identify the value of TES at SCO.

The goal of the first HERON optimization study for the SCO site was to identify the potential reactor technologies. The initial problem set was quite large, so some preliminary runs were executed to rule out certain components, based on the inner dispatch optimization. Components that went unused were eliminated, such as the option to use a heat exchanger rather than a backpressure turbine to convert SFR or HTGR heat into HP steam. The unused options were then removed from subsequent runs. The SFR option was also removed, as the reactor vendor study showed the smallest SFR option to be 1000 MWth, whereas the initial selection showed SFR sizes of around 200 MWth, meaning that a realistic SFR option did not exist.

The initial full optimization search method, using fixed TES sizes, was inconclusive for determining a true optimal reactor configuration, due to an apparently non-smooth solution space in which the variation in the ARMA samples was at least as—or perhaps more—impactful than the variation in selecting more HTGR or more LWR capacity to install. Thus, to obtain a more practical, straightforward result, discrete reactor sizes were evaluated via a parameter sweep using the set of parameters listed in Table 5.

Table 6. All components, capacities, transfer functions, CAPEX and OPEX values, and generation or consumption prices used in the discrete reactor sweep in HERON.

Component	Produces	Capacity	Consumes	Transfer Function	CAPEX (\$/KWth)	Variable O&M (\$/MWh-th)	Unit Price
LWR	LWR_heat	[0:250:1250]	N/A	Source	1492.88	8.25	N/A
LWR_turb	IP, electricity	inf	LWR_heat	$2.319*LWR_heat$ $=.0015*electricity+1*IP$	N/A	N/A	N/A
LWR_comp	HP	inf	LWR_heat electricity	$2.319*LWR_heat+.2138*$ $electricity=1*HP$	N/A	N/A	N/A
LWRtoStorage	LWR_store	inf	LWR_heat	$1*LWR_heat=1*LWR_store$	N/A	N/A	N/A
LWR_storage	LWR_store	1000	N/A	Storage	N/A	3.5	N/A
LWR_turb	IP, electricity	inf	LWR_store	$2.359*LWR_store$ $=.0663*electricity+1*IP$	N/A	N/A	N/A
LWR_comp	HP	inf	LWR_store electricity	$2.249*LWR_store+.2093*$ $electricity=1*HP$	N/A	N/A	N/A
HTGR	HTGR_heat	[0:200:1000]	N/A	Source	2476.73	17.25	N/A
HTGR_turb	HP, electricity	inf	HTGR_heat	$2.886*HTGR_heat$ $=.3334*electricity+1*HP$	N/A	N/A	N/A
HTGRtoStorage	HTGR_store	inf	HTGR_heat	$1*HTGR_heat=1*HTGR_store$	N/A	N/A	N/A
HTGR_storage	HTGR_store	1000	N/A	Storage	N/A	N/A	N/A
HTGR_turb	HP, electricity	inf	HTGR_store	$2.829*HTGR_store$ $=.2962*electricity+1*HP$	N/A	3.5	N/A
HPT	IP, electricity	inf	HP	$1*HP=.227*electricity+.97*IP$	N/A	N/A	N/A
IPT	LP, electricity	inf	IP	$1*IP=.146*electricity+.95*LP$	N/A	N/A	N/A
LPT	electricity	inf	LP	$1*LP=.293*electricity$	N/A	N/A	N/A
HPdemand	N/A	ARMA(HP)	HP	Sink	N/A	N/A	500
IPdemand	N/A	ARMA(IP)	IP	Sink	N/A	N/A	500
LPdemand	N/A	ARMA(LP)	LP	Sink	N/A	N/A	500
Edemand	N/A	ARMA (electricity)	electricity	Sink	N/A	N/A	1000
grid_sell	N/A	10	electricity	Sink	N/A	N/A	5
import1	electricity	10	N/A	Source	N/A	N/A	-1000
import2	electricity	inf	N/A	Source	N/A	N/A	-5000

The LWRs were analyzed in 250 MWth increments based on the VOYGR size, and the HTGR capacity was analyzed in 200 MWth increments based on the Xe-100 design. This analysis could be readily repeated for different nuclear design capacities, but as seen in Figure 64, unless a change in the relative costs of HTGRs and LWRs is realized, nuclear capacity meeting demand is presently effectively an identical result between the technologies. Figure 64 is a heat map showing the resulting NPV of these systems. Note that a low NPV could result either from a higher CAPEX-OPEX combination stemming from installation, or due to a reduced income as a result of not meeting system demands. Unfortunately, the heat maps mostly show that nearly all the systems capable of meeting demand are, statistically, equally valuable to the overall system, with some of the definition being lost due to the extremely low value of having zero installed nuclear power.

The NPV values calculated by HERON were adjusted such that the highest NPV is always \$0. As stated before, absolute NPV is not well defined here, as the positive value of meeting demand is arbitrary on an absolute scale and is only added to motivate the solution algorithm to find an optimal location.

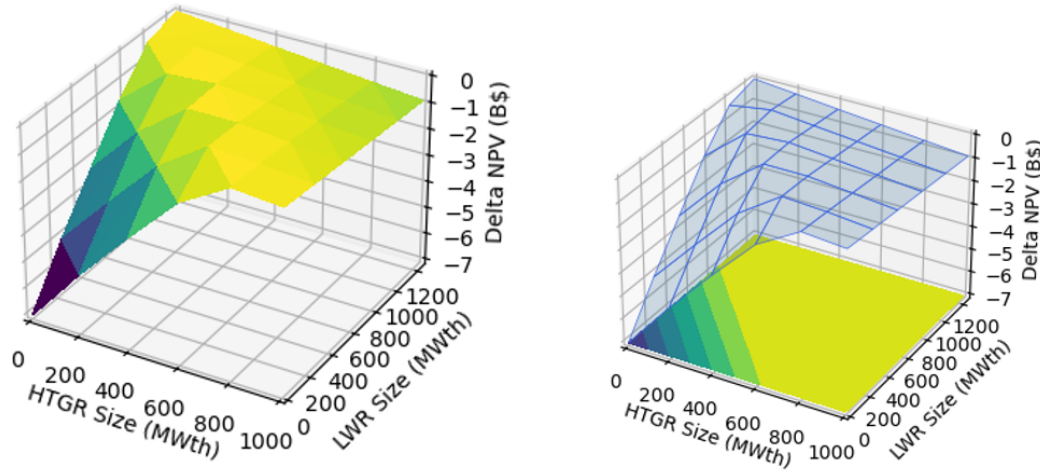


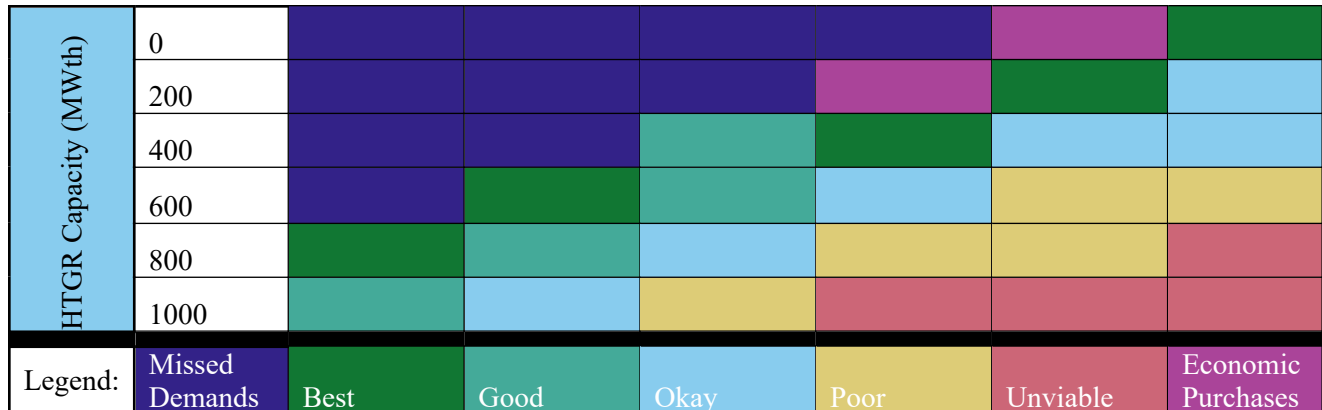
Figure 64. Heat map and projection of the project NPV in regard to different reactor sizes.

Table 7 shows the full set of results when sweeping across potential LWR and HTGR capacities. Precise values are not included as the inputs have significant uncertainty, and no sensitivity analysis was done as the focus of the work was dynamic load balancing and not economic valuation. Rather, solutions were graded based on the NPV and categorized into “best,” “good,” “okay,” “poor,” and “unviable” based on the economic evaluation of the system. “Best” solutions were within 5% of the optimal economic calculation. “Good” solutions were within 10%. “Okay” solutions were within 20%. “Poor” solutions were within 30%. “Unviable” solutions exceeded 30% of the optimal net present value calculations. Solutions graded in dark blue, “Missed Demands,” were unable to sufficiently meet demand and are therefore considered unviable solutions. Solutions graded in dark red, “Economic Purchases,” also missed significant demand, but purchases kept the net present value equivalent to the “okay” category or better.

The trend of the table follows clear logic: the solutions that minimize capacity while still meeting demand are the optimal economic scenarios. It is an important result that, at the moment, economic costs used (shown in Table 5) indicate that both the LWR and HTGR nuclear systems are viable integration candidates using the proposed configurations.

Table 7. Economic evaluations of various nuclear integration scenarios, showing systems that were able to meet dynamic load demands and those unable.

Scenario Evaluation					
	LWR Capacity (MWth)				
	0	250	500	750	1000



While some mixed-reactor solutions are in the “Best” category, further discussion will focus on single reactor-type solutions, as these will take advantage of so-far unaccounted for learning rates and should, in the end, improve economics to sway the “Best” solutions towards single reactor-type solutions.

LWR-only System

To evaluate the dispatch of the identified LWR-only optimal configuration, a limited HERON case with only the LWR system was set up. Table 8 shows the components, transfer functions, costs, and revenues for the established system. Preliminary analysis showed that storage did not have a utility within this five-LWR configuration and was removed for this HERON run.

Table 8. New HERON input parameters for the LWR-only case used to obtain dispatch.

Component	Produces	Capacity	Consumes	Transfer Function	CAPEX (\$/KWth)	Variable O&M (\$/MWh-th)	Unit Price
LWR	LWR_Heat	1250	N/A	Source	1492.88	8.25	N/A
PCC	electricity	308	LWR_heat	$1*LWR_heat$ $=0.308*electricity$	N/A	N/A	N/A
Compressor	HP	inf	LWR_heat electricity	$2.319*LWR_heat+$ $0.1022*electricity=1*HP$	N/A	N/A	N/A
RX_stepdown turb	IP electricity	inf	LWR_heat	$2.319*LWR_heat=$ $0.0015*electricity+1*IP$	N/A	N/A	N/A
HP2IPTurb	IP electricity	8.6	HP	$1*HP$ $=0.2386*electricity+1*IP$	N/A	N/A	N/A
HP2LPturb	LP electricity	88.19	HP	$1*HP$ $=0.39727*electricity+1*LP$	N/A	N/A	N/A
HP2IPvalve	IP	inf	HP	$1*HP=1*IP$	N/A	N/A	N/A
IP2LPvalve	LP	inf	IP	$1*IP=1*LP$	N/A	N/A	N/A
HPdemand	N/A	ARMA(HP)	HP	Sink	N/A	N/A	500
IPdemand	N/A	ARMA(IP)	IP	Sink	N/A	N/A	500
LPdemand	N/A	ARMA(LP)	LP	Sink	N/A	N/A	500
Edemand	N/A	ARMA (electricity)	electricity	Sink	N/A	N/A	1000
grid_sell	N/A	10	electricity	Sink	N/A	N/A	5
import1	electricity	10	N/A	Source	N/A	N/A	-1000
import2	electricity	inf	N/A	Source	N/A	N/A	-5000

Figure 65-Figure 68 show the dispatch for reactor heat and the system balances for meeting steam demands. With the nuclear reactors set to constantly generate full power, there is frequent over-generation, as seen in Figure 65, that is wasted as the plant operates between 1000 MWth and 1250 MWth. Three, and occasionally a portion of a fourth, modules are generally used for electricity generation. Figure 66 shows an interesting development, that the HP steam line within the SCO plant is now entirely servicing loads and not being used as a buffer to generate IP and LP steam. This would be a marked change from the current system. This result arises as electricity is required via the compressor to generate HP steam from the system.

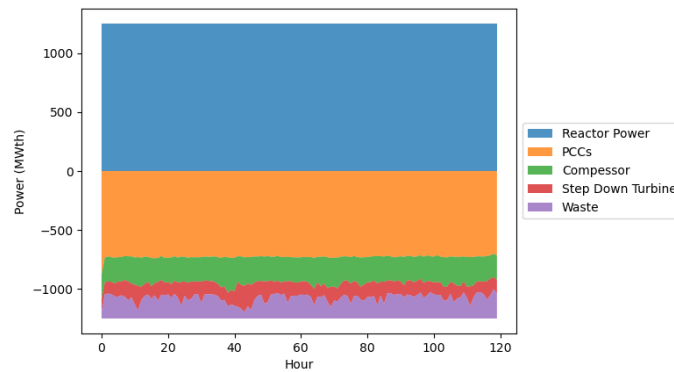


Figure 65. Reactor heat dispatch across five-day cluster for LWR-only case.

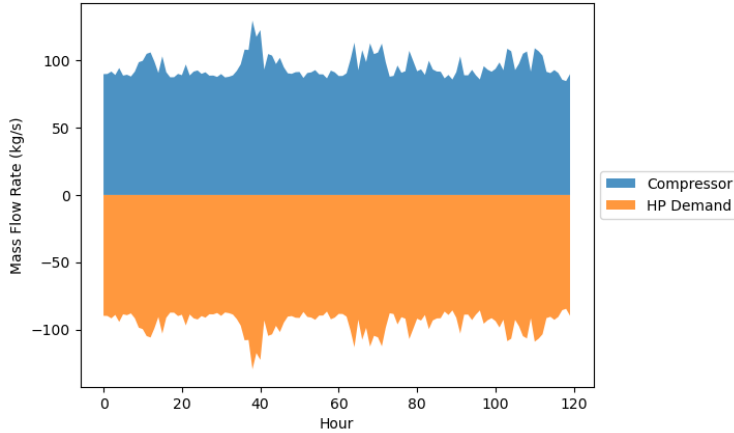


Figure 66. HP steam demand and production across five-day cluster for LWR-only case.

The IP steam load is met entirely via the small backpressure (“Step Down”) turbine included as an option within the LWR system, shown in Figure 72. This system produces a small amount of electricity while meeting the steam demand, and thus is a very valuable path by which to interface with the Dow chemical facility. Practically, this system would likely be configured at the SCO facility at a junction splitting steam generated at the nuclear facility site into steam passing through the compression system into the HP steam header, and another stream passing through a small turbine and into the IP steam header. Figure 73 shows that the LP steam is entirely generated through a letdown valve from the IP steam, again avoiding consuming the HP steam that is more energetically expensive to generate.

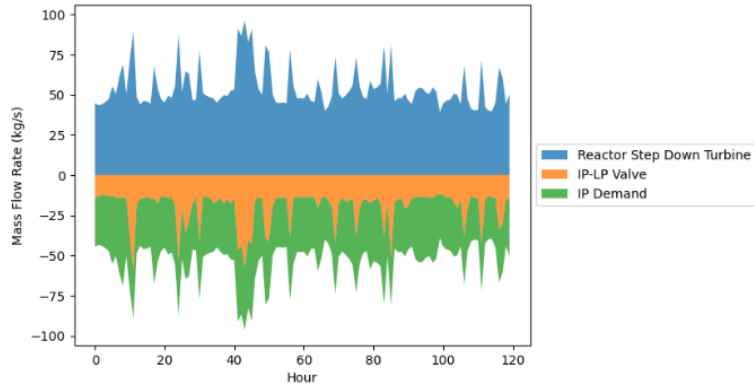


Figure 67. Total IP steam demand and production across five-day cluster for LWR-only case.

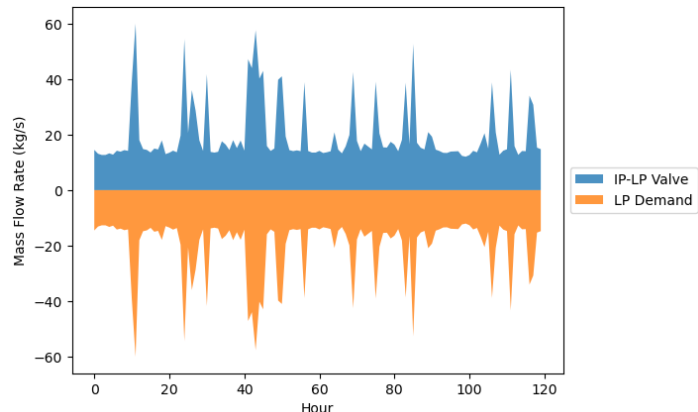


Figure 68. LP steam demand and production across five-day cluster for LWR-only case.

HTGR-only System

Based on the results from the first HERON run for the SCO site, a second HERON input file was created to compare BOP configurations for the HTGR configuration. The system was set up with a fixed capacity of 800 MWth of installed HTGR. It was assumed that a fixed-capacity 1000 MWh-th TES was installed that could dispatch heat to an additional system. Type 1, 2, and 3 PCC configurations were implemented in the HERON run, with the transfer functions listed in Table 9, along with a fourth heat-rejection system that was simply a heat exchanger that provided all heat directly to the Dow facility. This HERON configuration considered all steam to be delivered directly into the HP header line, more akin to the current Dow steam configuration. The components in the HERON run are listed in Table 9.

Table 9. System components included in second HERON optimization run for SCO.

Component	Produces	Capacity	Consumes	Transfer Function	CAPEX (\$/KWth)	Variable O&M (\$/MWh-th)	Unit Price
HTGR	HTGR_Heat	800	N/A	Source	2476.73	17.25	N/A
HTGR_storage	HTGR_store	1000	N/A	Storage	N/A	N/A	N/A
HTGRtoStorage	HTGR_store	inf	HTGR_heat	1*HTGR_heat=1*HTGR_store	N/A	N/A	N/A
Type3BOP	HP electricity	[0:22:44]	HTGR_heat	1*HTGR_heat =0.1045*electricity+0.712*HP	284.15	N/A	N/A
Type2BOPe	electricity	[0:81:324]	HTGRheatT2	poly1	161.71	N/A	N/A
Type2BOPh	HP	[0:133:532]	HTGRheatT2	poly2	0	N/A	N/A
Type1BOP	electricity	[0:84:252]	HTGR_heat	1*HTGR_heat =0.404*electricity	158.98	N/A	N/A
Type4BOP	HP	[0:168:168]	HTGR_heat	1*HTGR_heat=1*HTGR_store	0	N/A	N/A
Type2sBOPe	electricity	81	HTGR_store	poly1	161.71	N/A	N/A
Type2sBOPh	HP	133	HTGR_store	poly2	0	N/A	N/A
HTGR2Type2	HTGRheatT2	[0:200:800]	HTGR_heat	1*HTGR_heat=1*HTGRheatT2	N/A	N/A	N/A
HP2IPturb	IP electricity	8.6	HP	1*HP =0.2386*electricity+1*IP	N/A	N/A	N/A
HP2LPturb	LP electricity	88.19	HP	1*HP =0.39727*electricity+1*LP	N/A	N/A	N/A
HP2IPvalve	IP	inf	HP	1*HP=1*IP	N/A	N/A	N/A
IP2LPvalve	LP	inf	IP	1*IP=1*LP	N/A	N/A	N/A
HPdemand	N/A	ARMA(HP)	HP	Sink	N/A	N/A	500
IPdemand	N/A	ARMA(IP)	IP	Sink	N/A	N/A	500
LPdemand	N/A	ARMA(LP)	LP	Sink	N/A	N/A	500
Edemand	N/A	ARMA (electricity)	electricity	Sink	N/A	N/A	1000
grid_sell	N/A	10	electricity	Sink	N/A	N/A	5
import1	electricity	10	N/A	Source	N/A	N/A	-1000
import2	electricity	inf	N/A	Source	N/A	N/A	-5000

The steam extraction CHP plants use the following polynomial transfer functions in Equations 7 and 8 to accurately model the change in system efficiency as the plant is flexed:

Successful PCC combinations are shown in Table 10. The optimal combination showed one electricity module, two CHP modules, and one module that provided only heat to the SCO site. The TES can produce electricity, so HERON used this option to meet some of the electricity demand in the system. Unsurprisingly, the difference in NPV was not very large across different PCC selections, as the total reward for each system was approximately equal, given that they met demand, and the relative cost differences between the various PCC equipment were simply not that large relative to the rest of the system. The second most valuable system matches the configuration set proposed in Section 5.1.1.

Table 10. Delta NPVs for different configurations of PCCs.

Type 1	Type 2	Type 3	Type 4	Delta NPV (M\$)
3	0	0	1	-19.7
2	1	0	1	-16.7
3	1	0	0	-17.5
1	2	0	1	0.0
2	2	0	0	-27.4
0	3	0	1	-17.0
1	3	0	0	-17.1
0	4	0	0	-37.8
3	0	1	0	-19.7
2	1	1	0	-12.0
1	2	1	0	-4.7
0	3	1	0	-25.5
2	0	2	0	-17.0
1	1	2	0	-19.8
0	2	2	0	-40.6

Further investigation into using the TES system at SCO indicated that it was not fully being used as a storage system, but more so as an alternative electricity generation method. Further, storage's impact on the NPV was less than the statistical standard deviation found in each scenario's dispatch results. Combined, these two facts indicate that storage does not have a clear value case at SCO. Thus, the HERON optimization was rerun without TES included in the system. The resulting NPVs and PCC selection are shown in Table 11.

Table 11. Delta NPVs for different configurations of PCCs without TES.

Type1	Type2	Type3	Type4	Delta NPV (M\$)
2	1	1	0	-3.1
2	1	0	1	-3.2
2	2	0	0	0.0
1	2	1	0	-5.2
1	2	0	1	-13.3
1	3	0	0	-0.9
0	4	0	0	-8.7

The optimal PCC type shifts to include two Type 2 and two Type 1 configurations, although this system is found to convey nearly the same value as having three Type 2 configurations and one Type 1 configuration.

Figure 69 shows how the HTGR heat is dispatched between the Type 1 and Type 2 configurations, curtailing some of the heat production via waste that was directed to Type 2 CHP configurations. The system, across this entire cluster, is always operating under a net excess of energy. Note that the system is limited in terms of the amount of energy that can be sold to the grid, which is why some of the thermal energy is being wasted. In actuality, it would be curtailed via load follow or energy dumping, or sold as electricity to the grid.

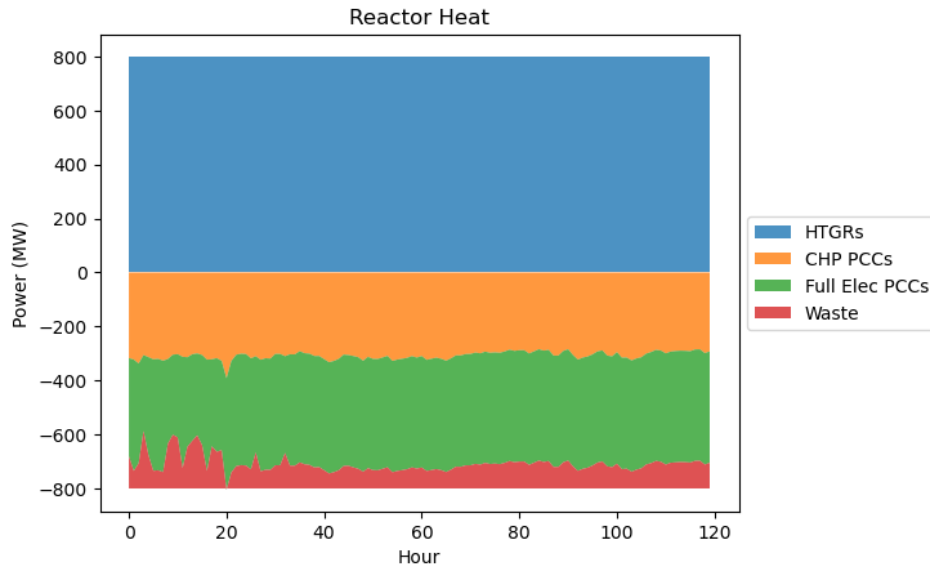


Figure 69. HERON dispatch of reactor heat across a 5-day dispatch cluster for SCO, with two Type 2 and two Type 3 PCCs.

The HP steam demand was sampled from the generated ARMA. As nuclear is the only method of generating heat in the system, HERON is highly motivated to meet the demand at all times. Figure 70 shows that the two CHP unit sources of HP steam appear to operate at the same values throughout the 5-day dispatch cluster. The HP steam is used almost constantly as an IP steam source via the IP turbine. The LP demand through the turbine and valve modulates a between these sources. None of the hourly jumps appear sufficiently severe to cause any challenges to the system ramping capabilities.

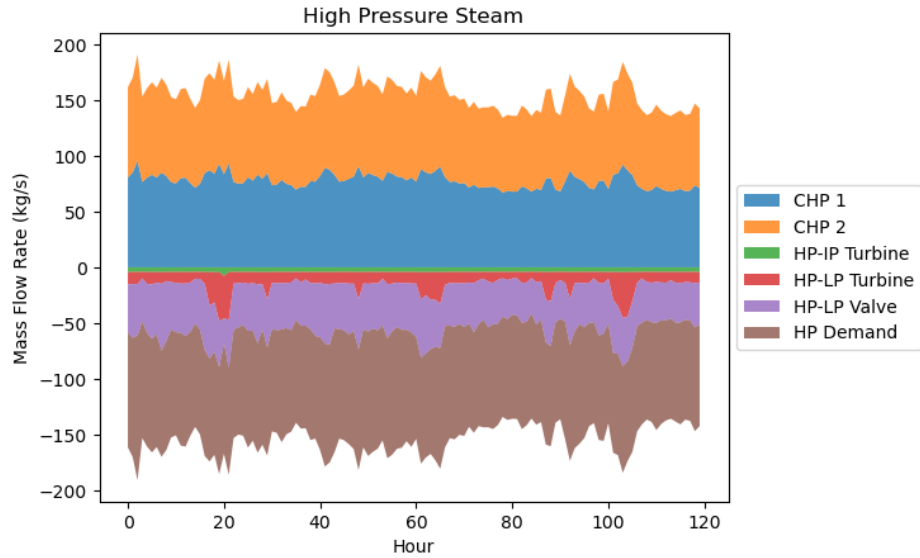


Figure 70. Sources and applications of HP steam in the SCO case, per HERON dispatch. Positive values indicate HP steam sources, negative values indicate HP steam applications. IP steam can be used in two ways: demand in the plant and letdown to the LP system. Figure 71 shows that a majority of the IP steam is sourced directly from the HP network via the letdown valve, indicating that the system is shedding energy to generate IP steam, as opposed to leveraging the HP-IP backpressure turbine. Most of the IP steam is consumed, but some is let down further into the LP system.

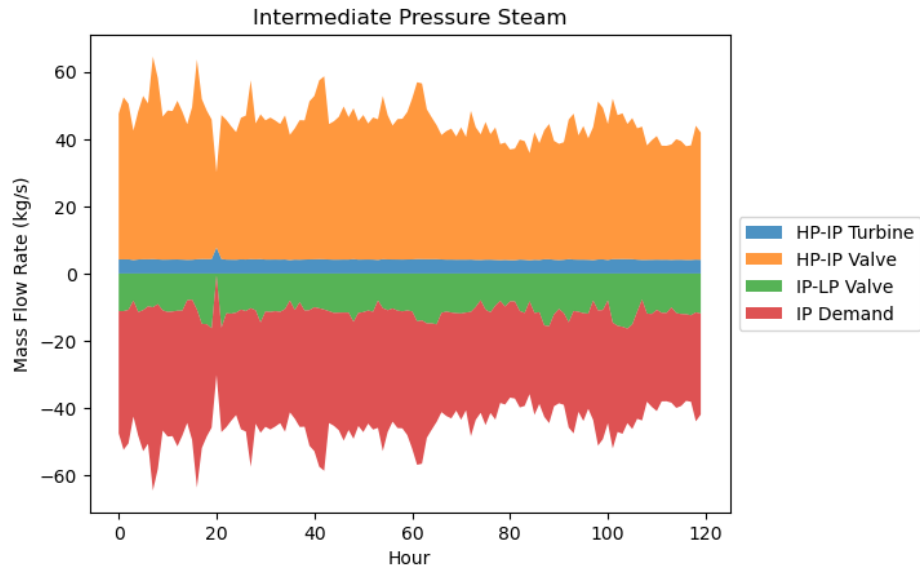


Figure 71. Sources and applications of LP steam in the SCO case, per HERON dispatch. Positive values indicate IP steam sources, negative values indicate IP steam applications.

LP demand is highly variant across the 5-day dispatch cluster shown in Figure 72. Both the HP-LP backpressure turbine and the IP-LP valve are used consistently throughout the dispatch to meet demand. The ratio between them appears to shift depending on the specific time, with the HP-LP backpressure turbine taking on additional load with higher levels of LP demand.

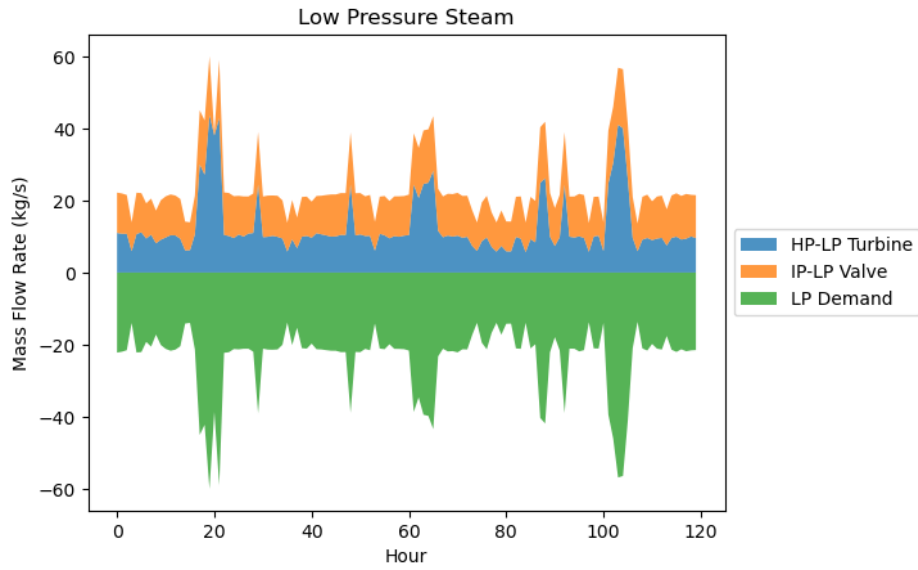


Figure 72. Sources and applications of LP steam in the SCO case, per HERON dispatch. Positive values indicate LP steam sources, negative values indicate LP steam applications. Within this 5-day cluster, the electricity demand is very consistent, as reflected by the brown color in Figure 73. There is a small change at around hour 20, but the system is largely running in near-constant fashion. Based on Figure 3, it is a reasonably consistent trend at SCO that, over short periods of time, the electricity load remains consistent outside of any extreme changes. The small variations in electricity load are handled in the HERON dispatch by the CHP Type 2 plants, and the electricity-only generating systems operate at what appears to be a constant rate. The system is always operating at an electricity surplus (indicated by the pink line at the bottom), with electricity being dispatched to the electrical grid.

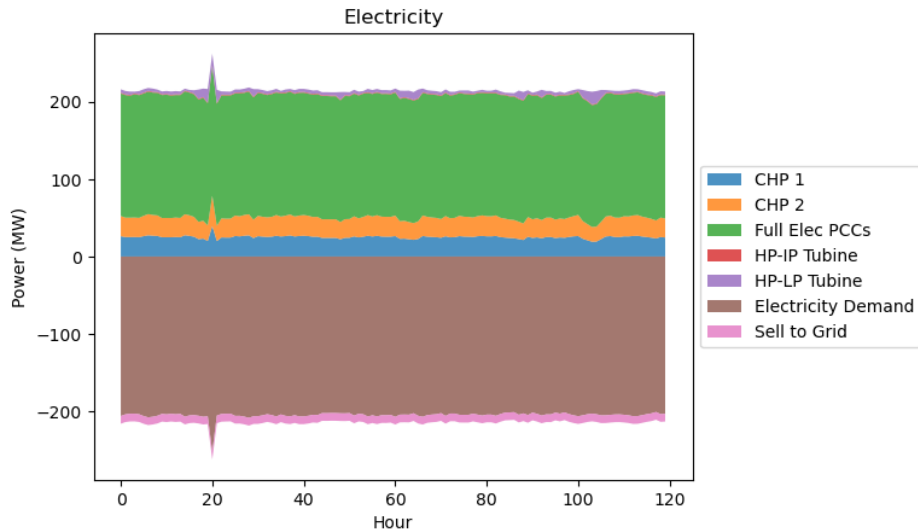


Figure 73. Sources and applications of electricity in the SCO case, per HERON dispatch. Positive values indicate electricity generation sources, negative values indicate electricity consumption.

Within the presented dispatch cluster, the results show that the system is readily meeting all system demands for heat and electricity. Excess capacity is noted in the system from an electrical standpoint via the dispatch of heat through valves instead of through turbines between the various steam headers. Were there a larger market for selling electricity to the grid, the turbines would be expected to be preferred over valves, as they generate value. However, grid sales are limited and thus the valves are leveraged to meet the steam demand. Between this observation and the heat being wasted (see Figure 69), we see that the set of four HTGRs would frequently be slightly oversized for SCO. However, at hour 20, the electricity production sees a minor spike in demand, and the corresponding increases in demand across the system use up the excess energy almost entirely. As meeting demand is paramount to the value of the system, some overgeneration is not only expected, but likely desirable.

5.3.2 Carrollton Site

The HERON input for the Carrollton site was set up differently (see Table 12). A generic μ Rx design was sized, since all μ Rxs surveyed would be readily capable of delivering steam to the Carrollton steam header. HERON optimized the size of the installed μ Rx system and an associated TES. The optimized solutions were a μ Rx installation of 167.3 MWth and a storage size of 183.2 MWh-th.

Table 12. HERON components, links, transfer functions, and values input for the Carrollton facility case.

Component	Produces	Capacity	Consumes	Transfer Function	CAPEX (\$/KWth)	Variable O&M (\$/MWh-th)	Unit Price
mRX	RX_Heat	Optimized	N/A	Source	4940	38	N/A
mRX_storage	RX_Heat	Optimized	N/A	Storage	18.3	3.5	N/A
Rxcondturb	electricity	inf	RX_heat	$1*RX_heat = 3773*electricity$	N/A	N/A	N/A
RXBPturb	electricity steam	inf	RX_heat	$1*RX_heat = 1*.1836*electricity + .3016* steam$	N/A	N/A	N/A
RXHX	steam	inf	RX_heat	$1*RX_heat = .466*steam$	N/A	N/A	N/A
steamdemand	N/A	ARMA(steam)	steam	Sink	N/A	N/A	500
Edemand	N/A	ARMA(electricity)	electricity	Sink	N/A	N/A	1000
grid_sell	N/A	10	electricity	Sink	N/A	N/A	5
import1	electricity	10	N/A	Source	N/A	N/A	-1000
import2	electricity	inf	N/A	Source	N/A	N/A	-5000

As was done for the SCO analysis, a parameter sweep across a subset of μ Rx installation sizes and TES capacity sizes was executed to develop a heat map showing NPV's sensitivity to the installed capacity. The resulting heat map and its projection are shown in Figure 74. The Carrollton facility shows strong sensitivity, in terms of NPV, to reactor size, and weaker sensitivity to TES installation.

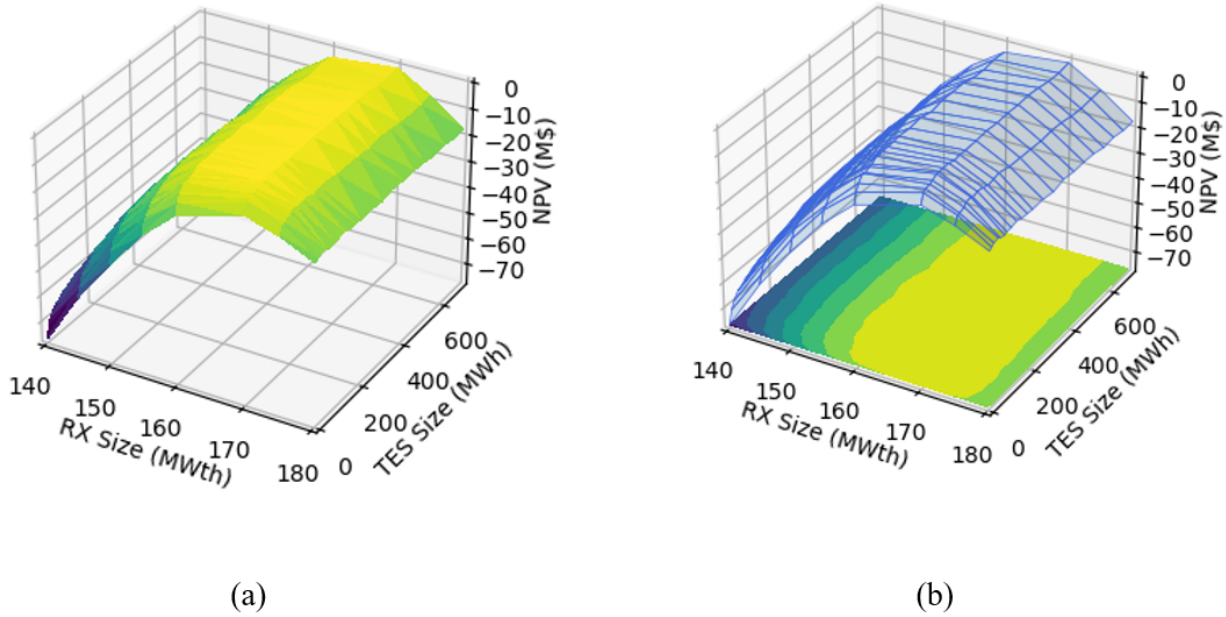


Figure 74. NPV (a) heat map and (b) projection measured against reactor TES sizes.

Figure 75 shows the impact of changing the TES capacity at the Carrollton site. The output values are defined to a reference \$0 without TES capacity installation as the reference case. The change in NPV increases rapidly with some TES introduction, as the system becomes more flexible and can meet demand more effectively. However, a peak is found at a low amount of storage as utilization decreases.

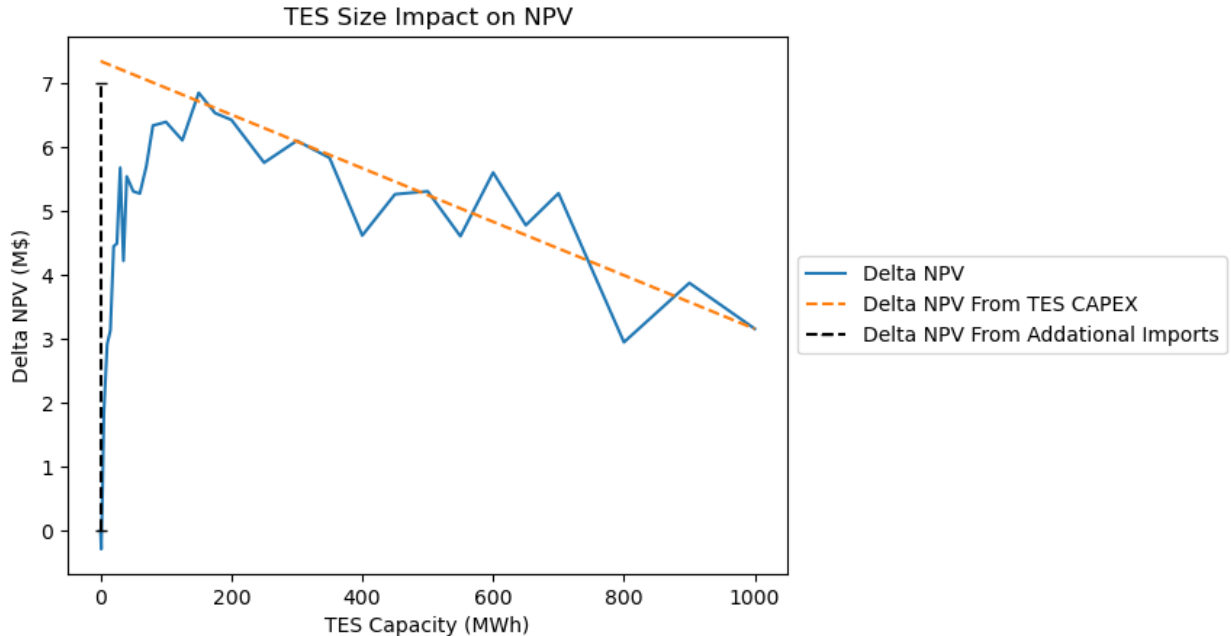


Figure 75. Measured impact of installed storage capacity at Carrollton.

Figure 76 and Figure 77 show the reactor heat and TES level for a five-day cluster of HERON dispatch for the identified Carrollton configuration. Figure 76 shows that the heat generated from the microreactors is mostly distributed between the BP turbine and the direct heat exchange system delivering

heat. The TES is consistently either charging or discharging throughout this period, as seen in Figure 78, but does not consume or produce a majority of the power at any time. As the system charges the TES, reducing some of the available steam load to the plant, steam is directed through the direct heat exchangers to meet steam demand, as seen in Figure 78. When this occurs, electricity production is reduced and grid import is required to meet electricity demand, seen in Figure 79. This optimal solution has a net negative electricity profile, with some electricity imports seen but no comparable grid sales included. The combined system leverages intermittent decreases in steam demand to store heat for the intermittent over-average steam dispatches required.

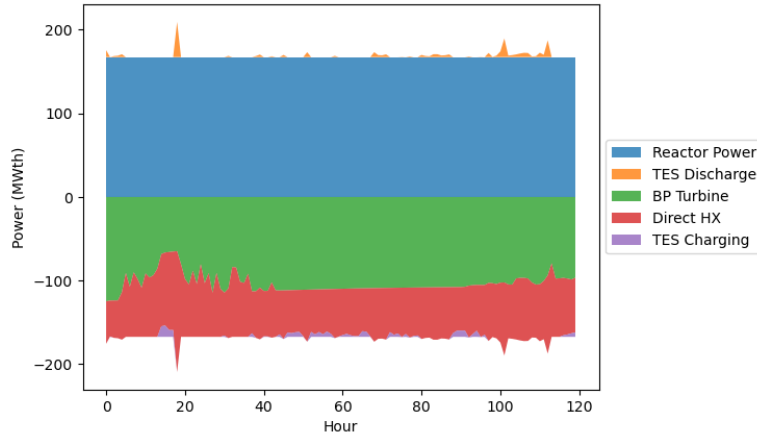


Figure 76. HERON dispatch of reactor heat across a five-day dispatch cluster for Carrollton.

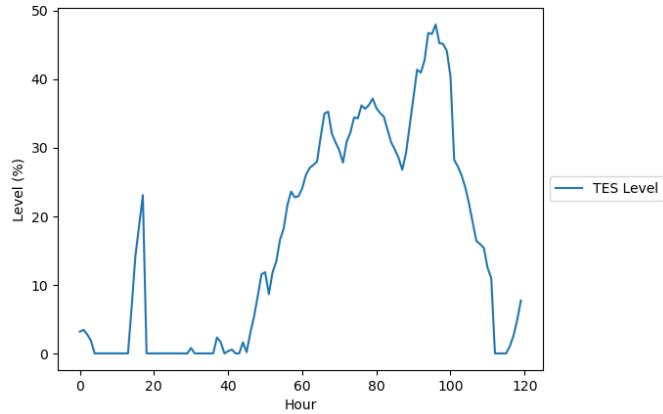


Figure 77. TES storage level across a five-day dispatch cluster for Carrollton.

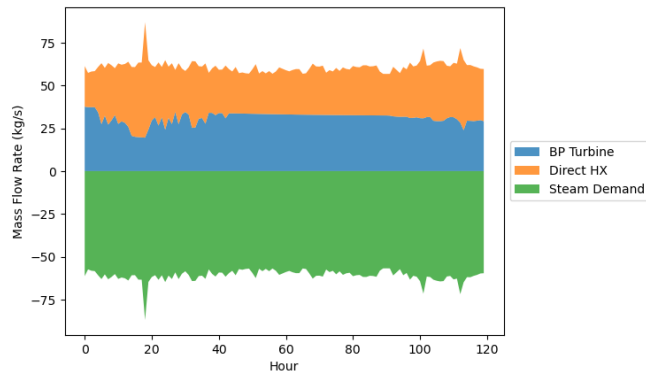


Figure 78. Sources and applications of steam in Carrollton case per HERON dispatch. Positive values indicate steam sources, negative values indicate steam applications.

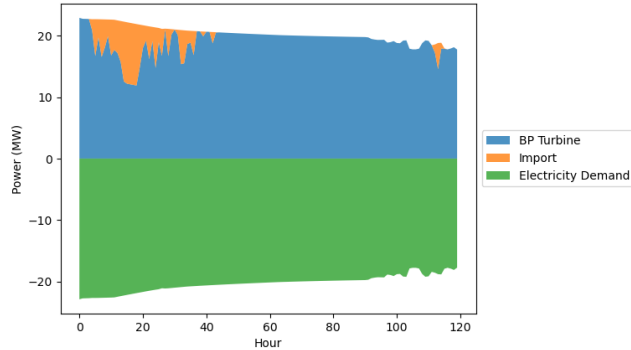


Figure 79. Sources and applications of electricity in DSC case per HERON dispatch. Positive values indicate electricity generation sources, negative values electricity consumption.

5.4 Carbon Emission Reduction

5.4.1 St. Charles Operations

Integration of SMRs at the SCO site is intended to replace fossil-fuel-based boilers and CHP units with zero-carbon steam and power for the site. The Scope-1 CO₂ emissions at SCO totaled ~2.7 million tons per year, with ~2.1 million tons coming from stationary combustion sources [100] [62]. These emissions largely stem from fossil fuel combustion to generate steam, power, and heat for the ethylene cracking furnaces, in addition to the fossil fuel loads required to generate facility-wide steam and electricity. Installation of integrated SMRs to supply clean steam and power should reduce the total CO₂ emissions at the site by ~615,000 tons per year (~30% of combustion emissions), as shown in Figure 80.

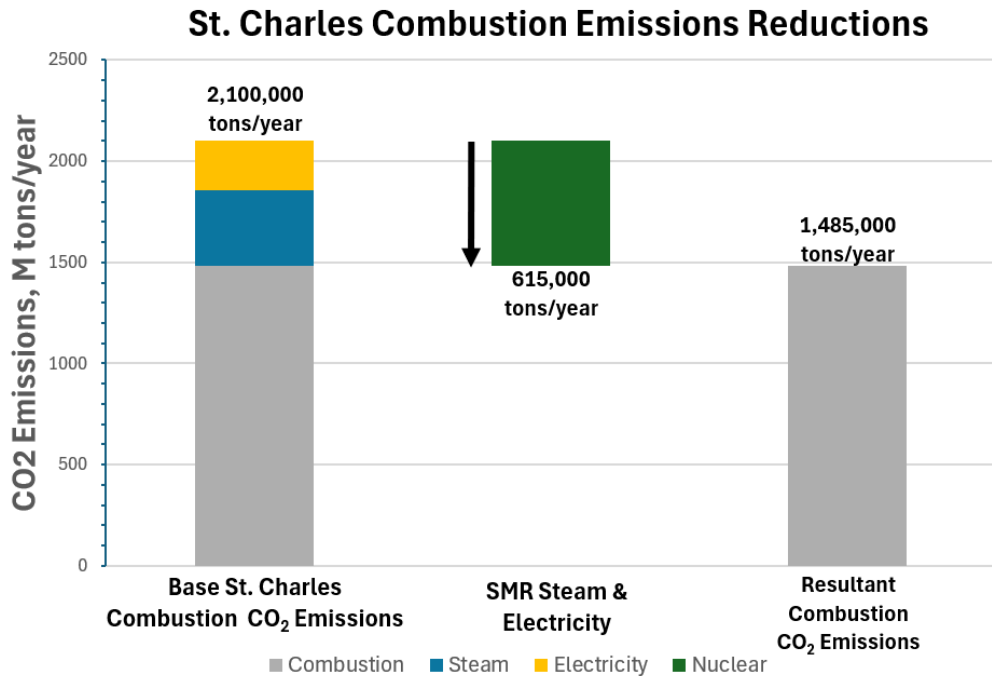


Figure 80. SCO combustion CO₂ emissions and the reduction achieved through SMRs.

The remaining emissions from SCO are attributed to the heat supplied to the cracking furnaces via combustion of fossil fuel and would not be accounted for by replacing the fired boilers onsite.

5.4.2 Carrollton Site

Integration of μ Rxs with the DSC Carrollton site is intended to replace the fossil-fuel-based boilers with zero-carbon steam and power for the site. In 2021, the Scope-1 combustion CO₂ emissions from the Carrollton site totaled ~174,000 tons per year [68]. These emissions primarily stem from fossil fuel combustion to generate steam used in the plant. Successful installation and integration of μ Rxs will introduce a clean source of steam (and electricity) that will reduce the Scope-1 (and Scope-2) emissions at the facility. The reduction in combustion CO₂ emission from the site by supplying clean steam is estimated to total ~174,000 tons per year (~100%), as shown in Figure 81.

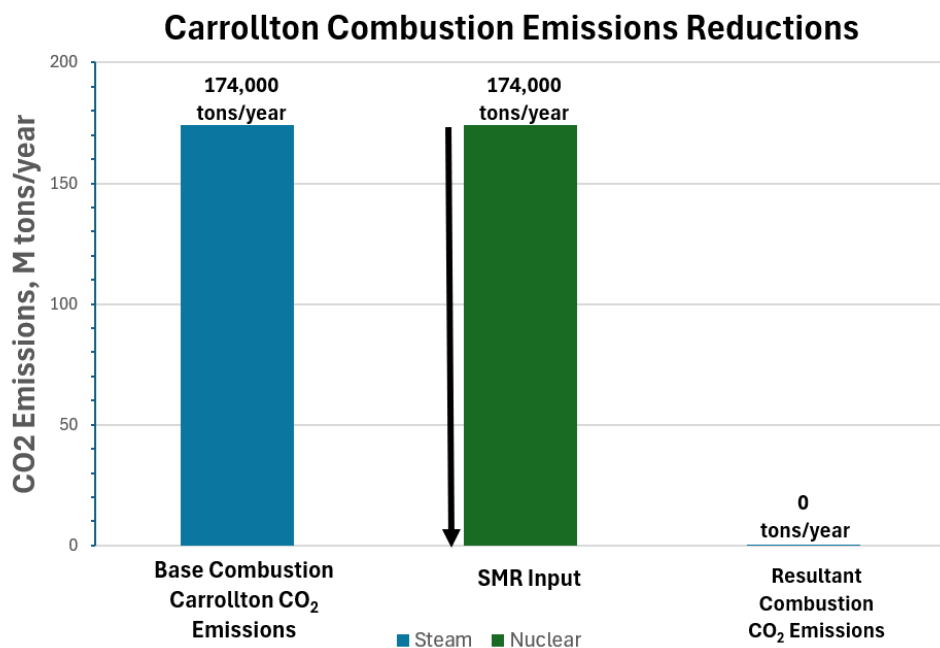


Figure 81. DSC's Carrollton site combustion CO₂ emissions, and the reduction by introducing μ Rxs.

5.5 Siting Hazard Analysis

The area around the SCO plant presents multiple kinds of hazards in potentially siting additional nuclear power in the immediate area. This section evaluates the following six criteria in terms of their potential impact to having the SMR sited near to the SCO plant: seismic potential, flooding area, local transportation, population density, current utility layout, and concussive force scenarios stemming from both the SCO plant and local chemical transportation systems on rail cars.

Facility data for the Carrollton site were not as detailed, and so the analysis in this section focuses squarely on the SCO facility. Furthermore, the specific siting criteria needed in order to evaluate μ Rxs are less certain than for SMRs, meaning that some of the siting aspects investigated herein may be inapplicable at Carrollton.

5.5.1 Seismic Possibility

All nuclear designs consider seismic activity in both their general system design and in specific site structure designs. The SCO area does not experience much seismic activity, with just three earthquakes having been reported within a 150 km radius of St. Charles Parish, LA, in the time since 1950. The reported earthquakes are tabulated in Table 13. The strongest earthquake in the area measured magnitude 3 on the Richter scale, at a depth of 0.4 km [101]. The probability of an earthquake corresponding to a Mercalli intensity V, in which moderate shaking occurs, is felt by nearly everyone (with many people being awakened), and generally leads to minimal damage (some windows and dishes broken, unstable objects overturned) is only around 2% in the SCO area [102]. No tectonic fault lines exist in the area, and so no challenges have been identified in the region with respect to earthquakes.

Table 13 Earthquakes reported near St. Charles Parish since 1950.

Date	Epicenter (Coordinates)	Distance from the Site	Magnitude (Richter Scale)	Depth
08/02/2010	30.815, -90.854	62.3 mile	3	0.4 km
12/20/2005	30.258, -90.708	24.6 mile	3	5 km
09/09/1975	30.662, -89.248	85.2 mile	2.9	5 km

5.5.2 Flooding

The SCO plant borders the Mississippi River on one of its sides, and is located in a generally low-lying area adjacent to swamp land. The Flood Insurance Rate Map, shown in Figure 82, highlights an area that has at least a 1% chance per annum of becoming a Flood Hazard Area. The Federal Emergency Management Agency considers flood levels in the area to be 4 feet of water. Precautionary measures implemented in the area have actively reduced the flooding potential of the SCO site, as well as of some of the immediately surrounding area.

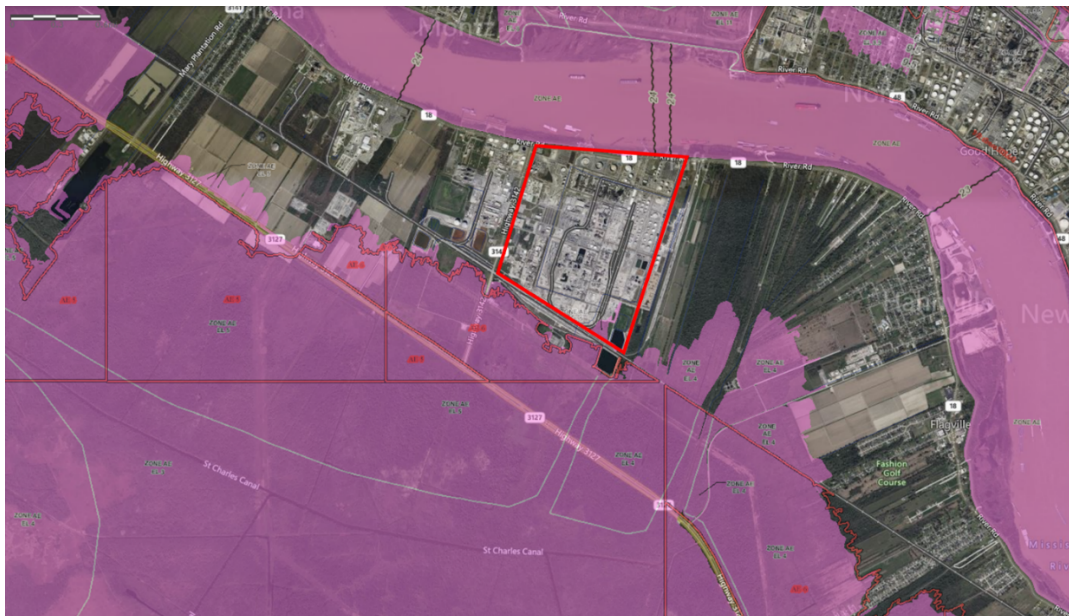


Figure 82. Flood Insurance Rate Map near the SCO site [103]. The red area indicates the general location of the SCO facility.

5.5.3 Road Traffic and Railroad Information

Figure 83 shows the road traffic load near the SCO site. The values presented in Figure 83 are annually averaged daily road traffic values. The busiest portion of road near the SCO site is Highway 3127, located on the south side of the site. Approximately 9,000 cars pass over it daily. About half this traffic is associated with the SCO facility itself.



Figure 83. Annually averaged road traffic near the SCO plant site. The red area indicates the general location of the SCO facility.

Figure 84 is the railroad map of the area near the SCO facility. Union Pacific, Canadian National Railway, and Kansas City Southern operate near the SCO site, with Union Pacific servicing the Dow site itself. Typically, NPPs are not sited immediately adjacent to busy railway, due to potential transport of explosive chemicals. In this case, however, it is a necessary consideration.

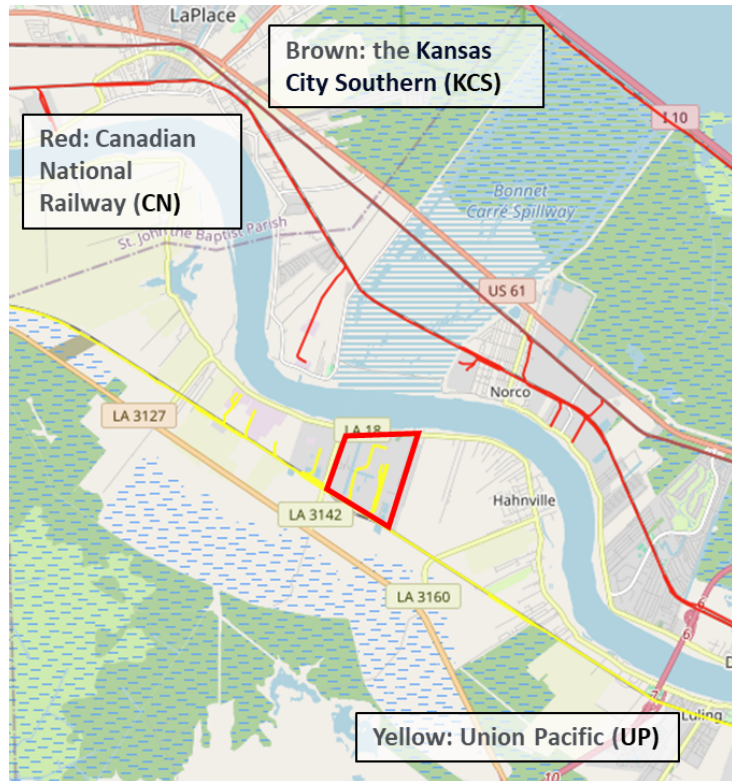


Figure 84. Map of railroads located near the SCO site. The red area indicates the approximate location of the SCO facility.

5.5.4 Population

Figure 85 shows the local daytime (Figure 85a) and nighttime (Figure 85b) population, both on and around the SCO site, based on 2021 data from LandScan [104]. The nighttime population, indicating residential areas, is low—with population densities of fewer than 1,000 people per square mile for the local municipalities. During the day, the working populations of the large industrial facilities and power plants lead to population increases. While there is no strict population density requirements, these towns do not appear to represent significant challenges to siting an NPP [105]. Furthermore, one of the daytime crowded locations is the Waterford 3 NPP, which would have a significantly larger emergency planning zone (likely extending 10 miles than any SMR installations, which would have a 500 m (0.31 miles) emergency planning zone at most [106]. The Siting Tool for Advanced Nuclear Development tool was used to map areas where the population is greater than 500 people per square mile; this mapping is shown in Figure 86.



Figure 85. Population density during the (a) daytime and (b) nighttime in the area surrounding the SCO facility. The red area indicates the approximate location of the SCO facility.

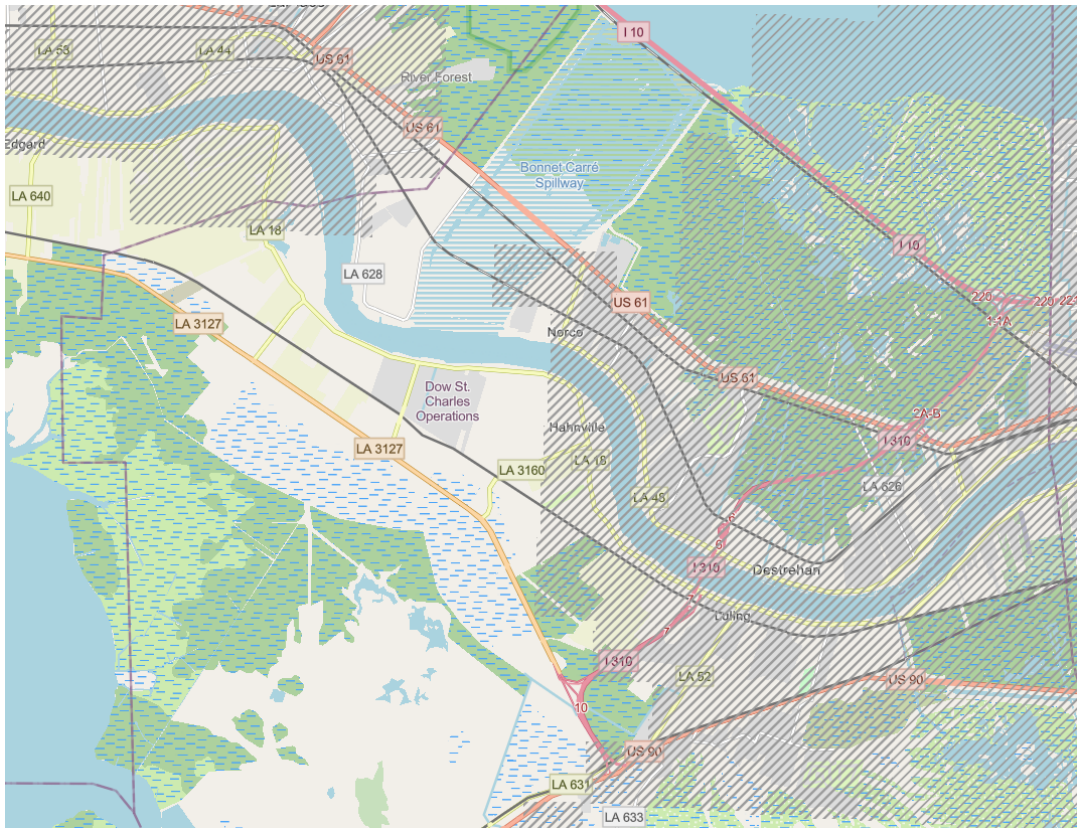


Figure 86. Population density results from Siting Tool for Advanced Nuclear Deployment [107]; the shaded regions represent areas with a population density over 500 people per square mile.

5.5.5 Utility and Chemical Facility

The elements of the local utility configuration—including other power plants, transmission lines, substations, chemical plants, pipelines, and landfill sites—are tracked due to their potential to interact with an operating NPP. Figure 87 shows various aspects of the local utility configuration near the SCO site. Gray lines indicate transmission lines, and the dots represent towers. Transmission icons show substations. The orange line is a natural gas pipeline, with a presumed 8-in.-diameter transmission pipe. The dark blue line is an ammonia pipeline, also with a presumed diameter of 4–8 in. The green line in the figure is an ethylene pipeline, and an industrial waste facility is represented by the trash icon.

The numbered labels on Figure 87 reflect different electrical generation facilities located in the immediate area, including SCO itself. These values correspond to systems listed in Table 14. The power facilities labeled 1–5 are all natural gas facilities, with facility 6 being the Waterford 3 NPP.

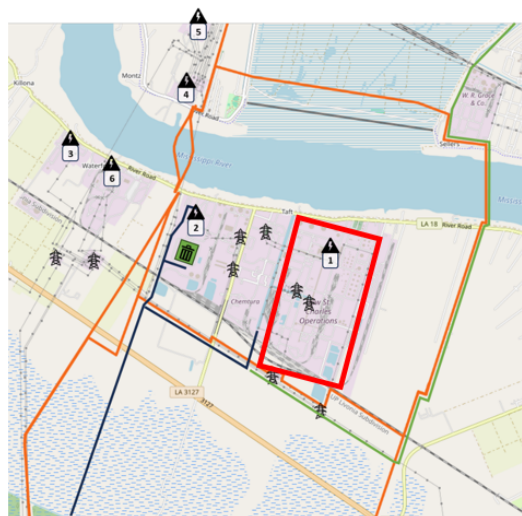


Figure 87. Utility map of the area near the SCO site. The red area indicates the approximate location of the SCO facility.

Table 14. Power plants near the SCO site.

#	Name	Unit Name	Fuel(s)	Capacity (MW)	Technology	CHP	Commissioned	Retired Year
1	Dow SCO power station	Unit CC1	gas, other gas	324	combined cycle	yes	2002	—
2	Taft cogeneration facility	Unit CC1	gas, other gas	894	combined cycle	yes	2002	—
3	Waterford 1 & 2 power station	Unit 1	gas, fuel oil	446	steam turbine	no	1975	—
		Unit 2	gas, fuel oil	446	steam turbine	no	1975	2024 planned
4	Little Gypsy power station	Unit 2	gas, fuel oil	421	steam turbine	no	1966	2026 planned
		Unit 3	gas, fuel oil	582	steam turbine	no	1969	2029 planned

#	Name	Unit Name	Fuel(s)	Capacity (MW)	Technology	CHP	Commissioned	Retired Year
5	St. Charles power station (LA)	PB01	gas	1,000	combined cycle	no	2019	—
6	Waterford NPP	3	1250 MW	PWR	CE 2LP (DRYAMB)	1985	N/A	

5.5.6 Land Ownership

Land ownership may prove a critical issue with regard to nuclear siting. Historically, land ownership laws have led to interesting land ownership shapes, as owners typically own the land in strips perpendicular to the Mississippi River, thus guaranteeing access. The two most likely land owners for NPPs integrated at SCO are Dow and Entergy; both companies own sufficient land in the area on which to potentially site a NPP. Figure 88 shows the land owners local to the SCO site.



Figure 88. Map of land ownership for the immediate area surrounding the SCO facility.

5.5.7 Combined Hazards Map

Figure 89 combines the analyzed impacts of population density and flood hazard zones onto a single overlayed plot. Primarily residential areas are marked where the population density exceeds 500 people per square mile, indicating that a SMR should not be located in those precise spots. The green and purple shaded areas are locations made hazardous due to potential flooding. The black outlined area shows the approximate location of the SCO plant. There are areas both on the east and west edges of the boxed area within Figure 89 that should be considered candidate nuclear locations.

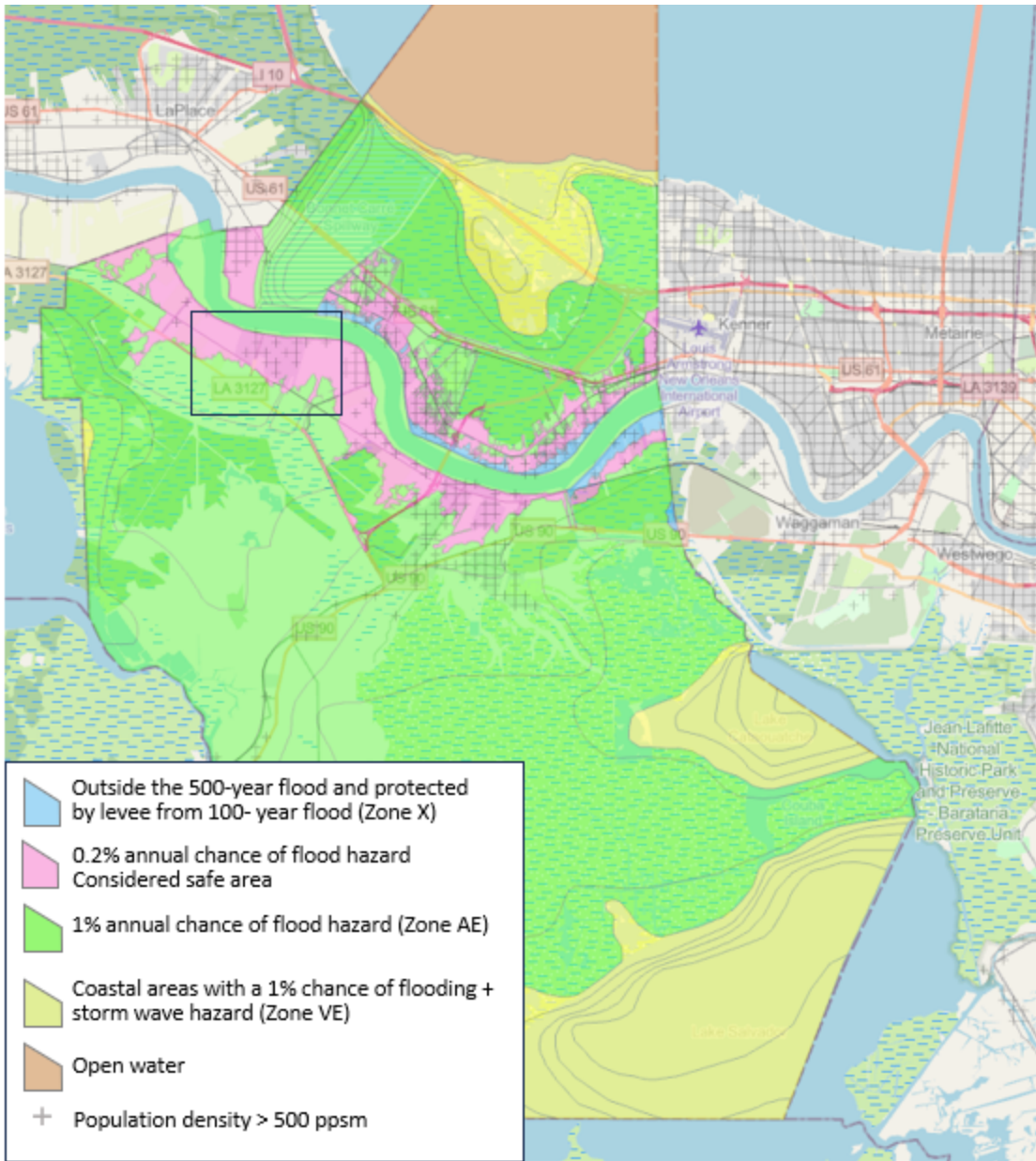


Figure 89. Multi-layered map presenting potential consideration for NPP site selection at SCO area. Dow facility is within boxed area.

6. CONCLUSIONS

Viable solutions are made possible by using advanced reactors to leverage nuclear power at the SCO and Carrollton facilities. Four or five SMRs at St. Charles should enable around a 30% reduction in site emissions relative to the 2021 values. And introducing around 167.3 MWth of μ Rx capacity at Carrollton should allow for near-complete decarbonization onsite. Given the current deployment timelines for advanced reactor systems, these solutions likely will not be deployable until the mid-2030s at the earliest—not necessarily an immediate solution, but still available to be included as part of Dow's 2050 decarbonization goals.

The present study investigated the thermodynamic and engineering challenges of introducing nuclear power as a complete clean energy solution at two Dow facilities. This document shows nuclear power to generally be a good fit for these industrial cases, as it is clean, dispatchable, reliable, power dense, and modularly deployable to meet demands as needed. The largest hurdle appears to be cost, which remains uncertain and could potentially be quite high—especially in terms of capital—for industrial applications. A broad portfolio of decarbonization solutions is likely needed before 2050, and all potential systems should be compared. Power-to-heat solutions that leverage clean electricity, electrification, and other clean thermal sources (e.g., biomass) remain uninvestigated by this analysis. All solutions will require new-generation assets as current systems go offline and energy requirements change or expand to accommodate different energy sources.

The FORCE tools leveraged by INL within this analysis are either open-source or substitutable (in the case of thermodynamic calculations), but expert support is recommended due to their complexity and the expert engineering judgments used throughout. The conclusions and recommendations reached over the course of this work are based on current thermal and electrical consumption profiles at St. Charles and Carrollton. It is not recommended to extrapolate these results to other sites, and the analysis of these two sites may be invalidated by significant changes to the system configuration in terms of increased electrification or operational expansion/reduction. It is well known that nuclear costs are presently uncertain, and as values become more concrete after first-of-a-kind deployments, the tools used herein should be reapplied with updated values to ensure that the recommendations remain unchanged.

7. ACKNOWLEDGEMENTS

This work was supported by the IES program at INL under DOE Operations contract no. DE-AC07-05ID14517. This research made use of INL computing resources, which are supported by the DOE Office of Nuclear Energy and the Nuclear Science User Facilities under contract No. DE-AC07-05ID14517.

8. REFERENCES

- [1] Kentucky Office of Energy Policy, "Report to the Kentucky Legislative Research Commission Pursuant to 2023RS SJR 79." November 17, 2023.
https://eec.ky.gov/Energy/Documents/Final%20Report%20SJR79_11.17.23.pdf.
- [2] Cornell University. n.d. "advanced nuclear reactor." U.S. Code Definition. Accessed May 4, 2024.
[https://www.law.cornell.edu/definitions/uscode.php?width=840&height=800&iframe=true&def_id=42-USC-1970775658-1412714348&term_occur=999&term_src=#:-:text=\(1\)%20Advanced%20nuclear%20reactor%20The,operating%20on%20December%202027%2C%202020](https://www.law.cornell.edu/definitions/uscode.php?width=840&height=800&iframe=true&def_id=42-USC-1970775658-1412714348&term_occur=999&term_src=#:-:text=(1)%20Advanced%20nuclear%20reactor%20The,operating%20on%20December%202027%2C%202020).
- [3] GAIN. 2024. "Advanced Nuclear Directory: Developers, Suppliers, and National Laboratories." Gateway for Accelerated Innovation in Nuclear. Accessed April 23, 2024.
https://gain.inl.gov/content/uploads/4/2023/02/GAINAdvancedNuclearDirectory-EighthEdition_01Feb2023.pdf.

[4] International Atomic Energy Agency. n.d. "Advanced Reactors Information System." Data Catalog. Accessed May 2, 2024. <https://aris.iaea.org/>.

[5] Ibarra, Jr., V. 2023. "Advanced Nuclear Reactor Technology: A Primer." Nuclear Innovation Alliance. Accessed: January 17, 2024. <https://www.nuclearinnovationalliance.org/sites/default/files/2023-07/ANRT-APrimer-27July2023.pdf>.

[6] Spilling Project Partner. n.d. "Steam Compression." Fact sheet. Accessed 22 April, 2024. <https://www.spilling.de/applications-steam/steam-compression.html>.

[7] Office of Nuclear Energy. 2023. "NRC Certifies First U.S. Small Modular Reactor Design." Press release. Accessed May 7, 2024. <https://www.energy.gov/ne/articles/nrc-certifies-first-us-small-modular-reactor-design>.

[8] NuScale Power, LLC. 2023. "NuScale Power Enhances Case for Small Modular Reactor Applications in Major Industrial Processes with New Steam Production Estimates." Press release. Accessed May 20, 2024. <https://www.nuscalepower.com/en/news/press-releases/2023/nuscale-enhances-case-for-small-modular-reactor-applications-in-major-industrial-processes>.

[9] NuScale Power, LLC. 2023. "Utah Associated Municipal Power Systems (UAMPS) and NuScale Power Agree to Terminate the Carbon Free Power Project (CFPP)." Press release. Accessed May 19, 2024. <https://www.nuscalepower.com/en/news/press-releases/2023/uamps-and-nuscale-power-agree-to-terminate-the-carbon-free-power-project>.

[10] Gardner, Timothy. 2023. "NuScale CEO defends modular nuclear plants after project cancellation." Reuters. News article. Accessed May 23, 2024. <https://www.reuters.com/business/energy/nuscale-ceo-defends-modular-nuclear-plants-after-project-cancellation-2023-11-14/#:~:text=NuScale%20and%20the%20Utah%20Associated,was%20upbeat%20despite%20the%20cancellation>.

[11] Schlissel, David. 2023. "Eye-popping new cost estimates released for NuScale small modular reactor." Institute for Energy Economics and Financial Analysis. Accessed May 23, 2024. <https://iefa.org/resources/eye-popping-new-cost-estimates-released-nuscale-small-modular-reactor>.

[12] NRC. 2024a. "SMR-300." Accessed May 18, 2024. <https://www.nrc.gov/reactors/new-reactors/smr/licensing-activities/pre-application-activities/holtec.html>.

[13] GE Vernova. n.d. "BWRX-300 small modular reactor." GE-Hitachi Nuclear Energy. Fact sheet. Accessed May 18, 2024. <https://www.gevernova.com/nuclear/carbon-free-power/bwrx-300-small-modular-reactor>.

[14] International Atomic Energy Agency. 2019. "Status Report - BWRX-300 (GE Hitachi and Hitachi GE Nuclear Energy)." Accessed 30 May, 2024. https://aris.iaea.org/PDF/BWRX-300_2020.pdf.

[15] NRC. 2024b. "GEH BWRX-300." Accessed May 28, 2024. <https://www.nrc.gov/reactors/new-reactors/smr/licensing-activities/pre-application-activities/bwrx-300.html>.

[16] Wald, Matt. 2024. "2024: The State of Advanced Reactors." Nuclear News. Accessed May 22, 2024. <https://www.ans.org/news/article-5634/2024-the-state-of-advanced-reactors/>.

[17] NRC. 2011. "10. Steam and Power Conversion System." AP1000 Design Control Document, Revision 19. Accessed May 23, 2024. <https://www.nrc.gov/docs/ML1117/ML11171A341.pdf>.

[18] NRC. 2024c. "Westinghouse AP300." Accessed May 6, 2024. <https://www.nrc.gov/reactors/new-reactors/smr/licensing-activities/pre-application-activities/westinghouse.html>.

[19] Westinghouse. 2023. "AP300 SMR; Most advanced, proven & readily deployable smr solution." Fact sheet. Accessed May 6, 2024.

https://www.westinghousenuclear.com/media/1vwbzcj1/ap300_smr-brochure_04-23-2023.pdf

[20] X Energy, LLC. 2023. "Submittal of X Energy, LLC (X-energy) White Paper: Xe-100 Plant Control and Data Acquisition System, Revision 3." Project No. 99902071, Accessed April 12, 2024. <https://www.nrc.gov/docs/ML2304/ML23048A309.pdf>.

[21] NRC. 2024d. "Xe-100." Accessed May 12, 2024. <https://www.nrc.gov/reactors/new-reactors/advanced/who-were-working-with/licensing-activities/pre-application-activities/xe-100.html>.

[22] Office of Nuclear Energy. 2020a. "U.S. Department of Energy Announces \$160 Million in First Awards under Advanced Reactor Demonstration Program." Accessed May 12, 2024. <https://www.energy.gov/ne/articles/us-department-energy-announces-160-million-first-awards-under-advanced-reactor>.

[23] Fu, C., H. Choi, and J. Bolin. 2021. "The Fast Modular Reactor (FMR) Pre-Application Regulatory Engagement Plan." In Transactions of the American Nuclear Society, 2021 ANS Winter Meeting, November 30–December 3, Washington, DC. <https://www.osti.gov/biblio/1862044>.

[24] Fu, C. 2022. "Fast Modular Reactor Principal Design Criteria." General Atomics, EMS-0194, Rev E, Accessed January 18, 2024. <https://www.nrc.gov/docs/ML2215/ML22154A556.pdf>.

[25] Choi, H., et al. 2021. "The Fast Modular Reactor (FMR) - Development Plan of a New 50 MWe Gas-cooled Fast Reactor." In proceedings of the 2021 ANS Virtual Annual Meeting, June 14-16. <https://www.osti.gov/biblio/1862041>.

[26] NRC. 2024c. "Fast Modular Reactor." Accessed May 6, 2024. <https://www.nrc.gov/reactors/new-reactors/advanced/who-were-working-with/licensing-activities/pre-application-activities/general-atomics.html>.

[27] General Atomics. n.d. "Advanced Reactors." Accessed May 7, 2024. <https://www.ga.com/nuclear-fission/advanced-reactors>.

[28] General Atomics. 2024. "General Atomics Signs a Memorandum of Understanding with Emirates Nuclear Energy Corporation." Accessed May 28, 2024. <https://www.ga.com/ga-signs-a-memorandum-of-understanding-with-emirates-nuclear-energy-corporation>.

[29] NRC. 2023a. "Energy Multiplier Module (EM2)." Accessed May 19, 2024. <https://www.nrc.gov/reactors/new-reactors/advanced/who-were-working-with/licensing-activities/pre-application-activities/genatom.html>.

[30] NRC. 2024d. "Natrium." Accessed May 20, 2024. <https://www.nrc.gov/reactors/new-reactors/advanced/who-were-working-with/licensing-activities/pre-application-activities/natrium.html>.

[31] TerraPower. 2023. "TerraPower and Uranium Energy Corp Announce MOU to Collaborate on Domestic Uranium Fuel Supply for the Natrium Reactor." Accessed May 20, 2024. <https://www.terrapower.com/terrapower-and-uranium-energy-corp-announce-mou-to-collaborate-on-domestic-uranium-fuel-supply-for-the-natrium-reactor/>.

[32] TerraPower. 2022. "Global Nuclear Fuel and TerraPower Announce Natrium Fuel Facility." Accessed May 20, 2024. <https://www.terrapower.com/global-nuclear-fuel-and-terrapower-announce-natrium-fuel-facility/>.

[33] Westinghouse. n.d. "Versatility of Application." Accessed May 23, 2024. <https://www.westinghousenuclear.com/energy-systems/lead-cooled-fast-reactor/versatility-of-application/>.

[34] Lee, S. J. et al. 2024. "Westinghouse Test Facilities for Lead Fast Reactor Development." *Nuclear Technology* 210(4): 666–680. <https://doi.org/10.1080/00295450.2023.2197667>.

[35] Nuclear Engineering International. 2023. "Initial tests completed for Westinghouse LFR design." Accessed May 23, 2024. <https://www.neimagazine.com/news/initial-tests-completed-for-westinghouse-lfr-design-10878673/>.

[36] ARC Clean Technology. 2023. "ARC-100 Technical Summary." Accessed May 28, 2024. https://www.arc-cleantech.com/uploads/ARC-100%20Technical%20Overview%20August%202023_FINAL.pdf.

[37] Government of Canada. 2023. "Proposed nuclear facility - NB Power's ARC-100 Project at the Point Lepreau Nuclear Generating Station site." Accessed May 8, 2024. <https://www.cnsccsn.gc.ca/eng/resources/status-of-new-nuclear-projects/nbpower/>.

[38] NRC. 2024e. "ARC-100." Accessed May 6, 2024. <https://www.nrc.gov/reactors/new-reactors/advanced/who-were-working-with/licensing-activities/pre-application-activities/arc-100.html>.

[39] NRC. 2024f. "Kairos." Accessed May 2, 2024. <https://www.nrc.gov/reactors/new-reactors/advanced/who-were-working-with/licensing-activities/pre-application-activities/kairos.html>.

[40] Kairos Power. n.d. "Technology." Web page. Accessed May 2, 2024. <https://kairospower.com/technology/>.

[41] NRC. 2023b. "Hermes - Kairos Application." Accessed May 2, 2024. <https://www.nrc.gov/reactors/non-power/new-facility-licensing/hermes-kairos.html>.

[42] NRC. 2024f. "Hermes 2 - Kairos Application." Accessed May 2, 2024. <https://www.nrc.gov/reactors/non-power/new-facility-licensing/hermes2-kairos.html>.

[43] Terrestrial Energy. n.d. "Commercial advantages." Accessed May 20, 2024. <https://www.terrestrialenergy.com/applications/commercial-advantages/>.

[44] Nuclear Engineering International. 2024. "Terrestrial Energy and Schneider Electric to collaborate on advanced reactor deployment." Accessed May 20, 2024. <https://www.neimagazine.com/news/terrestrial-energy-and-schneider-electric-to-collaborate-on-advanced-reactor-deployment-11726303/>.

[45] Terrestrial Energy. n.d. "Path to market." Accessed May 20, 2024. <https://www.terrestrialenergy.com/technology/leading-the-way/>.

[46] BWX Technologies, Inc. n.d. "Terrestrial Micro RX." Accessed May 18, 2024. <https://www.bwxt.com/what-we-do/advanced-technologies/terrestrial-micro-rx>.

[47] Nygaard, Erik. 2021. "BWXT's Advanced Nuclear Reactor (BANR)." Presentation. Accessed May 18, 2024. <https://www.nationalacademies.org/documents/embed/link/LF2255DA3DD1C41C0A42D3BEF0989ACAEC3053A6A9B/file/DD7F72C500641846CD3FC86C8D19F97B8889C926B7DE?noSaveAs=1>.

[48] Nuclear Newswire. 2024. "Wyoming as a hub for new nuclear manufacturing and microreactor deployment?" American Nuclear Society. Accessed May 18, 2024. <https://www.ans.org/news/article-5995/wyoming-as-a-hub-for-new-nuclear-manufacturing-and-microreactor-deployment/>.

[49] Governor's Energy Matching Funds Initiative. 2023. "BWXT AT Executive Summary." Accessed May 18, 2024. https://wyoenergy.org/wp-content/uploads/2023/08/BWXT-AT-Executive-Summary-08_07_23.pdf.

[50] Nuclear Newswire. 2023a. "Project Pele in context: An update on the DOD's microreactor plans." Accessed May 18, 2024. <https://www.ans.org/news/article-5308/project-pele-in-context-an-update-on-the-dods-microreactor-plans/>.

[51] Ultra Safe Nuclear. n.d. "MMR Energy System." Accessed May 9, 2024. <https://www.usnc.com/mmr/>.

[52] Global First Power. 2019. "Project Description for the Micro Modular Reactor Project at Chalk River." Accessed May 1, 2024. <https://www.usnc.com/assets/media-kit/01%20CRP-LIC-01-001%20Rev%202%20Project%20Description.pdf?v=177cbcb665>.

[53] Ultra Safe Nuclear. 2023. "USNC Selects Gadsden, Alabama for Advanced Microreactor Assembly Plant." Accessed May 1, 2024. <https://www.usnc.com/usnc-selects-gadsden-alabama-for-advanced-microreactor-assembly-plant/>.

[54] Gougar, H. et al 2022. "Market-driven Optimization of the XENITH Microreactor." Office of Nuclear Energy. Accessed May 18, 2024. <https://www.energy.gov/sites/default/files/2023-05/ne-abstract-ARD-22-28734.pdf>.

[55] Nuclear Newswire. 2023b. "Oklo to deploy two Aurora plants in Ohio." Accessed May 9, 2024. <https://www.ans.org/news/article-5031/oklo-to-deploy-two-aurora-plants-in-ohio/>.

[56] Oklo. n.d. "FAQs." Accessed May 9, 2024. <https://oklo.com/investor-faqs/default.aspx>.

[57] NRC. 2024g. "Oklo Aurora Powerhouse." Accessed May 6, 2024. <https://www.nrc.gov/reactors/new-reactors/advanced/who-were-working-with/licensing-activities/pre-application-activities/oklo-aurora-powerhouse.html>.

[58] Westinghouse. n.d. "eVinci™ Microreactor." Accessed April 26, 2024. <https://www.westinghousenuclear.com/energy-systems/evinci-microreactor/>.

[59] Office of Nuclear Energy. 2020b. "Energy Department's Advanced Reactor Demonstration Program Awards \$30 Million in Initial funding for Risk Reduction Projects." Accessed April 11, 2024. <https://www.energy.gov/ne/articles/energy-departments-advanced-reactor-demonstration-program-awards-30-million-initial>.

[60] Westinghouse Electric Company. 2023. "First Canadian eVinci Microreactor Targeted for Saskatchewan." Accessed April 26, 2024. <https://info.westinghousenuclear.com/news/first-canadian-evinci-microreactor-targeted-for-saskatchewan>.

[61] NRC. 2023c. "eVinci." Accessed April 26, 2024. <https://www.nrc.gov/reactors/new-reactors/advanced/who-were-working-with/licensing-activities/pre-application-activities/evinci.html>.

[62] Environmental Protection Agency. n.d. "St Charles Operations (Taft/Star) Union Carbide Corp" Facility Information. Accessed May 22, 2024. <https://ghgdata.epa.gov/ghgp/service/facilityDetail/2021?id=1007031&ds=E&et=&popup=true>.

[63] Energy Information Agency. 2023a. "Louisiana State Profile and Energy Estimates." Accessed May 18, 2024. <https://www.eia.gov/state/analysis.php?sid=LA>.

[64] National Conference of State Legislatures. 2020. "State Approaches to Wind Facility Siting." Accessed May 15, 2024. <https://www.ncsl.org/energy/state-approaches-to-wind-facility-siting>.

[65] Department of Energy. 2021. "State of Louisiana Energy Sector Risk Profile." Accessed May 15, 2024. <https://www.energy.gov/sites/default/files/2021-09/Louisiana%20Energy%20Sector%20Risk%20Profile.pdf>.

[66] Department of Energy. 2007. "Dow Chemical Company: Assessment Leads to Steam System Energy Savings in a Petrochemical Plant." Accessed May 15, 2024. <https://cdn2.hubspot.net/hub/297110/file-300136228-pdf/docs/42009.pdf?t=1502892574327>.

[67] Entergy. n.d. "About Entergy." Accessed May 18, 2024. <https://www.entropy.com/about/>.

[68] Environmental Protection Agency. n.d. "Dow Silicones Corporation" Facility Information. Accessed May 22, 2024. <https://ghgdata.epa.gov/ghgp/service/facilityDetail/2021?id=1002548&ds=E&et=&popup=true>.

[69] LG&E and KU Energy. n.d. "Ghent Generating Station." Accessed May 2, 2024. <https://lge-ku.com/our-company/community/neighbor-neighbor/ghent-generating-station>.

[70] Middlesboro News. 2023. "PSC to retire several coal, natural gas plants." Accessed May 2, 2024. <https://www.middlesboronews.com/2023/07/24/psc-to-retire-several-coal-natural-gas-plants/>.

[71] Hansen, J, Jenson, W, Wrobel, A, Stauff, N, Biegel, K, Kim, T, Belles, R, Omitaomu, F. 2022. "Investigating Benefits and Challenges of converting Retiring Coal Plants into Nuclear Plants." Idaho National Laboratory. Idaho Falls, ID. INL/RPT-22-67964 Rev 2. doi: <https://doi.org/10.2172/1886660>.

[72] Kentucky General Assembly. 2024. "Senate Bill 198." Accessed May 2, 2024. <https://apps.legislature.ky.gov/record/24rs/sb198.html>.

[73] Kentucky Public Service Commission. 2024. "Electric Service Areas." Accessed May 2, 2024. https://psc.ky.gov/agencies/psc/images/Electric_Service_Areas_Legal_Size_Map.pdf.

[74] LG&E and KU Energy. n.d. "Large commercial & industrial Green Energy calculator." Accessed May 2, 2024. <https://lge-ku.com/environment/green-energy-program/green-energy-calculator/commercial-green-energy-calculator>

[75] LG&E and KU Energy. n.d. "Green Energy Program." Accessed May 2, 2024. <https://lge-ku.com/environment/green-energy-program>.

[76] LG&E and KU Energy. 2008. "Development of Guidelines for Interconnection and Net Metering for Certain Generators with Capacity up to Thirty Kilowatts." Accessed May 13, 2024. Appendix A p. 2. https://lge-ku.com/sites/default/files/media/files/downloads/KPSC_Net_Metering_Interconnection_Guidelines.pdf.

[77] LG&E and KU Energy. n.d. "Net metering for your home or business." Requirements. Accessed May 13, 2024. <https://lge-ku.com/net-metering>.

[78] LG&E and KU Energy. 2020. "Interconnection Requirements." Accessed May 13, 2024. <https://lge-ku.com/node/23706>.

[79] Mulder, Eben J. 2021. "Overview of X-Energy's 200 MWth Xe-100 Reactor." Accessed May 1, 2024. <https://www.nationalacademies.org/documents/embed/link/LF2255DA3DD1C41C0A42D3BEF0989ACAEC3053A6A9B/file/DCB77DCC95AEF75D0CA6FE9C717CAA34436F7817D15A>.

[80] Office of Technology, NuScale Power. 2023. "A Preliminary Assessment of NuScale Steam Production Rates for Industrial Applications." NuScale Power. Portland, Oregon, USA. WP-139434, Rev. 3.

[81] Siemens Energy. 2021. "Efficiency: More value to your facility – Industrial steam turbines from 2 to 250 MW." Accessed May 1, 2024. <https://assets.new.siemens.com/siemens/assets/api/uuid:6ff783f7-dc10-41ab-83b7-c42817643306/siemens-steam-turbine-portfolio.pdf>.

[82] Spilling Project Partner. n.d. "Steam Compressors – The Spilling Steam Compressor: A Unique Specialist." Accessed May 1, 2024. <https://www.spilling.de/products/steam-compressors.html>.

[83] G-Team. "G-Team: Steam Turbines." Accessed May 1, 2024. <http://www.g-team.cz/steam-turbines.html>.

[84] Chart Industries. "Steam Turbines – Howden steam turbines provide a power output up to 40 MW." Accessed May 1, 2024. <https://www.chartindustries.com/Products/Steam-Turbines>.

[85] Edwards, J, and H. Bindra. 2017. "An experimental study on storing thermal energy in packed beds with saturated steam as heat transfer fluid." *Solar Energy* 157. Pp. 456-461.

[86] Saeed, R. et al. "Multilevel Analysis, Design, and Modeling of Coupling Advanced Nuclear Reactors and Thermal Energy Storage in an Integrated Energy System." Idaho National Laboratory. Idaho Falls, ID, USA. INL/RPT-22-69214. doi: 10.2172/1890160.

[87] Box, G.E.P. and G.M. Jenkins, and G. Ljung. 1976. *Time Series Analysis: Forecasting and Control*. Holden-Day, San Francisco.

[88] Abou-Jaoude, A., L. Lin, C. Bolisetti, E. Worsham, L. Larsen, and A. Epiney. 2023. "Literature Review of Advanced Reactor Cost Estimates." Idaho National Laboratory. Idaho Falls, ID, USA. INL/RPT-23-72972. doi:10.2172/1986466

[89] Gautam, K. R., G.B. Andresen, and M. Victoria. 2022. "Review and Techno-Economic Analysis of Emerging Thermo-Mechanical Energy Storage Technologies." *Energies* 15 (17), 6328. doi: 10.3390/en15176328

[90] Charkas, Hasan. 2020. "Separating Nuclear Heat Island from Balance of Plant." Electric Power Research Institute. Accessed May 20, 2024. https://infuse.ornl.gov/wp-content/uploads/2020/12/EPRI_SeparatingBOP_Charkas.pdf.

[91] Moe, W. L. and T. E. Hicks. 2020. "Establishing Jurisdictional Boundaries at Collocated Advanced Reactor Facilities." Idaho National Laboratory. Idaho Falls, ID, USA. INL/EXT-20-57762. <https://www.osti.gov/biblio/1668676>.

[92] NRC. 2014. "Regulatory Guide 4.7: general site suitability criteria for nuclear power stations." Washington, D.C. USA. Accessed May 20, 2024. <https://www.nrc.gov/docs/ML1218/ML12188A053.pdf>.

[93] Worsham, E. C. Bolisetti, G. Griffith, and D. Mikkelsen. 2023. "Siting Requirements for Colocating Nuclear Power Plants with Industrial Facilities." Idaho National Laboratory. Idaho Falls, ID, USA. INL/RPT-23-74311.

[94] Glover, A., A. Baird, and D. Brooks. 2020. "Final Report on Hydrogen Plant Hazards and Risk Analysis Supporting Hydrogen Plant Siting near Nuclear Power Plants." Sandia National Laboratories. Albuquerque, NM, USA. SAND2020-10828. <https://www.osti.gov/biblio/1678837/1000>.

[95] Lobato, J. et al. 2009. "Consequence analysis of an explosion by simple models: Texas refinery gasoline explosion case." *Afinidad* 66 (543), pp 372-379. <https://raco.cat/index.php/afinidad/article/view/279547>.

[96] Vedros, K. G., R. Christian, and C. Otani. 2022. "Probabilistic Risk Assessment of a Light-Water Reactor Coupled with a High-Temperature Electrolysis Hydrogen Production Plant." Idaho National Laboratory. Idaho Falls, ID, USA. INL/EXT-20-60104. doi: 10.2172/1691486.

[97] Fu, X., H. Li, and G. Li. 2016. "Fragility analysis and estimation of collapse status for transmission tower subjected to wind and rain loads." *Structural Safety* 58. pp 1-10. doi: 10.1016/j.strusafe.2015.08.002

[98] Energy Information Agency. 2022-2024. "Electric Power Monthly, Capacity Factors for Utility Scale Generators Primarily Using Non-Fossil Fuels." Accessed March 26, 2024. https://www.eia.gov/electricity/monthly/epm_table_grapher.php?t=epmt_6_07_b.

[99] Mikkelsen, D. and K. Frick. 2022. "Analysis of controls for integrated energy storage system in energy arbitrage configuration with concrete thermal energy storage." *Applied Energy* 313 (118800).

doi: 10.1016/j.apenergy.2022.118800

- [100] Environmental Protection Agency. n.d. "Scope 1 and Scope 2 Inventory Guidance." Accessed May 21, 2024. <https://www.epa.gov/climateleadership/scope-1-and-scope-2-inventory-guidance>.
- [101] Database.earth. n.d. "Latest Earthquakes Near Saint Charles Parish, Louisiana in United States." Accessed May 7, 2024. <https://database.earth/earthquakes/united-states/louisiana/saint-charles-parish>.
- [102] Petersen, M. D. et al. 2023. "The 2023 US 50-State National Seismic Hazard Model: Overview and implications." *Earthquake Spectra*. 40(1):5-88. doi: 10.1177/87552930231215428.
- [103] Federal Emergency Management Agency. n.d. "FEMA Flood Map Service Center." <https://msc.fema.gov/portal/advanceSearch#searchresultsanchor>.
- [104] Weber, E., J. Moehl, S. Weston, A. Rose, C. Brelsford, and T. Hauser. 2022. "LandScan USA 2021." Data set. Oak Ridge National Laboratory. doi: 10.48690/1527701.
- [105] NRC. 2023d. "50.33 Contents of applications; general information." Accessed May 21, 2024. <https://www.nrc.gov/reading-rm/doc-collections/cfr/part050/part050-0033.html>.
- [106] Kelk, R., A. Murad, R. de Oliveira, and M. Jeltsov. 2020. "Emergency planning zones for small modular reactors." National Institute of Chemical Physics and Biophysics, Nuclear Science and Engineering. Accessed May 21, 2024. <https://fermi.ee/wp-content/uploads/2021/03/epz-report-kbfi-20210211.pdf>.
- [107] National Reactor Innovation Center. n.d. "Siting Tool for Advanced Nuclear Development (STAND)." <https://nric.inl.gov/stand-tool/>